Rational Drug-design of Compounds Targeting Protein Kinase Related Diseases

Pedro Miguel Miranda Araújo
Mestrado em Bioquímica
Departamento de Química e Bioquímica
2014

Advisor
Professor Doutor Joaquim C.G. Esteves da Silva, Associated Professor with Aggregation, Faculdade de Ciências da Universidade do Porto

Co-Advisor
Master Luís Pinto da Silva, Phd Student, Faculdade de Ciências da Universidade do Porto

U.PORTO
FACULDADE DE CIÊNCIAS
UNIVERSIDADE DO PORTO

All the corrections determined by the Jury, and only those, were made.

The Jury President,

Porto, _____/_____/_____

Abstract

Protein phosphorylation is one of the most important mechanisms within living cells, having a central role in the cellular signalling pathways. One of the most important functions of protein kinases is the control of checkpoints during cell cycle. The outcome of checkpoints activation depends on the DNA damage severity. If it is possible to repair the cell cycle is arrested giving the cellular repair mechanism the needed time to act but if the damage is too extended the result is apoptosis. The three most relevant checkpoints are located in late G1 (start checkpoint), before entering mitosis (G2/M checkpoint) and during mitosis (M checkpoint). Protein p53 is an essential factor in the G1 checkpoint. However, it is absent in many tumors leading to the loss of this checkpoint. The inhibition of G2/M checkpoint in p53-deficient cells conjugated with common radio or chemotherapy would create and increase DNA damage leading to a catastrophic mitotic event that would result in apoptosis. Through this mechanism inhibition of G2/M checkpoint was proposed as a sensitization therapy in p53-dificient cells. G2/M checkpoint is regulated by ATM and ATR pathways with the downstream effectors Checkpoint kinase 1 and 2. More recently the role of MK2 in the regulation of G2/M checkpoints was also revealed.

Aiming the reduction of time and costs in drug development computational tools started to be employed in this field, being the processes in which they took part commonly called Computer aided drug design (CADD). These methods can be separated in two different types of approaches, structure based (SBDD) and ligand based (LBDD). In this work SBDD methods were used. Starting from x-ray crystallography structures semi-empirical energy calculation were performed to study the binding sites of protein kinases Chk1 and MK2.

In the first stage of this work the binding between Checkpoint kinase 1 and two molecules with known inhibitory potential, C39 and C40 was studied. Similarly to the experimental data C39 showed the best binding potential towards Chk1, being this inhibition mode highly dependent on the interactions with the residues Lys38 and Glu91. In C40 binding mode residue Glu91 was also very important. Using this knowledge 10 novel molecules were designed based on C39, Modified molecule 1 to 10 (MD1-10). When compared to C39, MD8 and MD9 showed significant improvements in the binding energy. MD9 achieved the best improvement (21%) and MD8 the second best (19%).

Due to difficulties in the study of MK2 a closely related protein from the same family, MK3, was suggested as a model structure. Thus the binding characteristics of two potential inhibitors, P4O and 05B, to MK2 and MK3 was studied. This work revealed the importance of binding site water molecules and the similarity in the binding profile of both enzymes with the same central characteristics.

From the work present in this thesis two oral communications were performed, one book chapter and two papers in peer-reviewed journals were published, while other paper is currently submitted:

- P. Araújo, L. Pinto da Silva and J.C.G. Esteves da Silva, Molecular Design of Potential Chk1-targeting Anti-Cancer Drugs, IJUP 14 - Encontro de Jovens Investigadores da Universidade do Porto (2014);
- P. Araújo, L. Pinto da Silva and J.C.G. Esteves da Silva, Computational Study of G2 Checkpoint Protein Kinases-Inhibitor Complexes, 4º PYCheM - 4th Portuguese Young Chemists Meeting (2014);
- Pedro M. M. Araújo, Luís Pinto da Silva and Joaquim C. G. Esteves da Silva, Computational Chemistry Theories, Methods and Applications, Chapter 1: Protein Kinase-targeting drug Discovery and Design: Computational Chemistry as an Indispensable Tool, Nova Publishers (2014) 1-22;
- Pedro M.M. Araújo, Luís Pinto da Silva, Joaquim C.G. Esteves da Silva, Comparative theoretical study of the binding of potential cancer-treatment drugs to Checkpoint kinase 1 Chemical Physics Letters 591 (2014) 273–276;
- Pedro M.M. Araújo, Luís Pinto da Silva, Joaquim C.G. Esteves da Silva, Theoretical Modelling of Potential Chk1 Inhibitors, Letters in Drug Design & Discovery, 2015.

Resumo

A fosforilação proteica é um dos mecanismos mais relevantes nas células vivas, tendo um papel fulcral nas vias de sinalização celulares. Um das funções mais importantes das proteínas cinases é a de controlo dos checkpoints durante o ciclo celular. O resultado da ativação dos checkpoints depende da severidade do dano do ADN. Se for possível o seu reparo o ciclo celular é parado criando o tempo necessário para os mecanismos de reparo do ADN atuarem no entanto se os danos forem muito extensos o resultado é apoptose. Os três checkpoint mais relevantes estão localizados em G1 (checkpoint de inicio), antes de entrar em mitose (G2/M checkpoint) e durante a mitose (M checkpoint). A proteína p53 é uma fator essencial do checkpoint G1. No entanto, está ausente em muitos tumores levando a perda deste checkpoint. A inibição do checkpoint G2/M em células sem p53 funcional conjugada com a radio ou quimioterapia comum iria criar e aumentar danos no ADN levando a um evento mitótico catastrófico que resultaria na apoptose. Através deste mecanismo a inibição do checkpoint G2/M foi proposta como uma terapia de sensibilização para células deficientes em p53. O checkpoint G2/M é regulado pelas vias de sinalização ATM e ATR tendo como efetores downstream a Checkpoint kinase 1 e 2. Mais recentemente foi descrito o papel da MK2 na regulação do checkpoint G2/M.

Tendo como objetivo a redução do tempo e custos no desenvolvimento de novos fármacos as ferramentas computacionais começaram a ser aplicadas nesta área, sendo os processos nos quais estão envolvidas chamados Computer aided drug design (CADD). Estes métodos podem ser divididos em dois tipos diferentes de abordagens, baseadas na estrutura (SBDD) ou baseadas no ligando (LBDD). No presente trabalho métodos de SBDD foram usados, começando a partir de estruturas de cristalografia raio-x cálculos semi-empíricos de energia foram feitos para estudar os locais de ligação das cinases Chk1 e MK2.

Na primeira fase deste trabalho a ligação à Chk1 de duas moléculas com potencial inibitório conhecido, C39 e C40, foi estudada. Similarmente aos resultados experimentais C39 mostrou o melhor potencial de inibição da Chk1, sendo o seu modo de inibição é altamente dependente das interações com os resíduos Lys38 e Glu91. De forma semelhante no modo de ligação da C40 o resíduo Glu91 também foi muito importante. Usando o conhecimento obtido foram criadas 10 novas moléculas baseadas na C39, Modified molecule 1 a 10 (MD1-10). Quando comparadas com a C39 as moléculas MD8 e MD9 mostraram melhorias significantes na energia de ligação. MD9 atingiu o melhor resultado (21% de melhoria) enquanto a MD8 o segundo melhor (19% de melhoria).

Devido a dificuldades no estudo da MK2 uma proteína semelhante da mesma família, MK3, foi sugerida como modelo. Desta forma foram estudas as características da ligação de dois potenciais inibidores, P4O e 05B, a MK2 e MK3. Este estudo revelou a importância das moléculas de água presentes nos locais ligação e a semelhança entre os perfis de ligação das duas enzimas, que apresentaram as mesmas características centrais.

A partir do trabalho presente nesta tese duas comunicações orais foram realizadas, um capítulo de livro e dois artigos em revistas com revisão por pares foram publicados, enquanto um outro artigo se encontra submetido:

- P. Araújo, L. Pinto da Silva and J.C.G. Esteves da Silva, Molecular Design of Potential Chk1-targeting Anti-Cancer Drugs, IJUP 14 - Encontro de Jovens Investigadores da Universidade do Porto (2014);
- P. Araújo, L. Pinto da Silva and J.C.G. Esteves da Silva, Computational Study of G2 Checkpoint Protein Kinases-Inhibitor Complexes, 4º PYCheM - 4th Portuguese Young Chemists Meeting (2014);
- Pedro M. M. Araújo, Luís Pinto da Silva and Joaquim C. G. Esteves da Silva, Computational Chemistry Theories, Methods and Applications, Chapter 1: Protein Kinase-targeting drug Discovery and Design: Computational Chemistry as an Indispensable Tool, Nova Publishers (2014) 1-22;
- Pedro M.M. Araújo, Luís Pinto da Silva, Joaquim C.G. Esteves da Silva, Comparative theoretical study of the binding of potential cancer-treatment drugs to Checkpoint kinase 1 Chemical Physics Letters 591 (2014) 273–276;
- Pedro M.M. Araújo, Luís Pinto da Silva, Joaquim C.G. Esteves da Silva, Theoretical Modelling of Potential Chk1 Inhibitors, Letters in Drug Design & Discovery, 2015.

Acknowledgments

To my family for all the love and support.

To Sara Vaz for always being there when I needed most.

To my colleagues Celso, Daniel and Inês for the support and help during the two years of my master degree.

To Bruno, Diana, Dilson, Joel, Margarida, Mariana, Paulo and Teresa for the good environment created in group, the good times, the laughs and the amazing lunch times.

To my co-advisor Master Luís Pinto Silva for all the patience, knowledge transferred, good laughs and for the assistance in all the work performed during this year, I could only do this with your help.

To my advisor Professor Doctor Joaquim C.G. Esteves da Silva for the opportunity to participate in this work and join this group and for all the advising and help.

Contents

List of Abbreviations

Ala	Alanine
Arg	Arginine
Asn	Asparagine
Asp	Aspartic acid
ATM	Ataxia telangiectasia mutated
ATP	Adenosine triphosphate
ATR	Ataxia telangiectasia and Rad3 related
C39	Compound 39
C40	Compound 40
CADD	Computer aided drug design
Cdc25	Cell division cycle
Cdk1	Cyclin-dependent kinase 1
Cdk2	Cyclin-dependent kinase 2
Chk1	Checkpoint kinase 1
Chk2	Checkpoint kinase 2
CK2	Casein kinase 2
CML	Chronic myeloid leukemia
CYS	Cysteine
DDR	DNA damage response
DNA	Deoxyribonucleic acid
G1	Gap 1 (cell cycle)
G2	Gap 2 (cell cycle)
Gadd45α	Growth arrest and DNA-damage-inducible protein GADD45 alpha
GIST	Gastrointestinal stromal Tumor
Gln	Glutamine
Gly	Glycine
Glu	Glutamic acid
GPU	Graphics processing unit
GSK	Glycogen synthase kinase
GTP	Guanine triphosphate
H-bond	Hydrogen Bound
His	Histidine
HIV	Human immunodeficiency virus
HPV	Human Papilloma Virus
HTS	High throughput screening
IC50	Half maximal inhibitory concentration
Ile	Isoleucine
IUPAC	International Union of Pure and Applied Chemistry
JAK	Janus kinase
LBDD	Ligand based drug design
LBVS	Ligand based virtual screening
Leu	Leucine
LHS	Left Hand Side
Lys	Lysine
M phase	Mitosis (cell cycle)
MAPK	Mitogen-activated protein kinases
MD	Molecular dynamics
MD1 - MD10	Modified molecule 1 to 10
MET	Methionine
MK2/MAPKAPK2	MAP kinase-activated protein kinase 2

MK3	MAP kinase-activated protein kinase 3
mRNA	Messenger Ribonucleic acid
NMR	Nuclear magnetic resonance spectroscopy
NSCLC	Non-small-cell lung carcinoma
p38	P38 mitogen-activated protein kinases
p53	Tumor protein p53
PDB	Protein data bank
Phe	Phenylalanine
PM6	Parameterization Method 6
Pro	Proline
PTK	Protein tyrosine kinase
RHS	Right Hand Side
RMSD	Root-mean-square deviation
S	Synthesis (cell cycle)
SBDD	Structure based drug design
SBVS	Structure based virtual screening
Ser	Serine
STPK	Serine/threonine protein kinase
TIP53	Tumor protein p53 gene
THR	Threonine
TNFα	Tumor necrosis factor alpha
TRP	Tryptophan
TYR	Tyrosine
Val	Valine
vHTS	Virtual throughput screening
VS	Virtual screening

Chapter 1- Introduction

1.1. - Kinases

Kinases are a subclass within the enzymes family with the capacity to covalently attach a phosphate group to diverse molecular targets as proteins, lipids and nucleotides. The most abundant subgroup is the one that targets amino acid substrates, the protein kinases with more than 500 constituents. This process consists in the transfer of a phosphate group, mainly from ATP but also from GTP, that when attached to the target originates conformational changes that might lead to functional alterations in proteins. Phosphorylation is the most common process of post-translational protein reversible modification [1–6].

Protein phosphorylation can be seen as an on/off mechanism, promoting or stopping the cellular function of the targets according to the active signal pathways. It was proposed that at any given period of time one third of all the proteins within the cell are phosphorylated, representing the abundance of signal pathways affected by this process [2,3].

Protein kinases are substrate specific, meaning they can be differentiated according to the amino acid they phosphorylate. There are 3 typical groups, the largest being protein serine/threonine kinases (STPKs), followed by protein tyrosine kinases (PTKs) and unspecific protein kinases [2,6,7]. STPKs have a conserved domain with about 300 residues able to bind to ATP (or GTP), and after that to bind to the protein target, resulting in the transfer of a phosphate to the hydroxyl group of a serine or threonine residue [1].

1.2. – Cell Cycle Checkpoints

One of the most important functions of protein kinases is the control of the cell cycle, especially the checkpoints. Different endogenous/metabolic or exogenous/environmental factors may originate damage in the DNA. The checkpoints are activated during the cell cycle in order to keep the integrity of the genetic information [8]. The outcome of these mechanisms activation depends on the DNA damage severity. If it is possible to repair, the cell cycle is arrested giving the cellular repair mechanism time to act but if the damage is too extended the result is apoptosis [9]. For this reason checkpoints have a central role in the DNA damage response (DDR) [8]. The three most relevant checkpoints are located in late G1 (start checkpoint), before entering mitosis (G2/M checkpoint) and before anaphase (metaphase-to-anaphase) or M checkpoint [10].

1.3. – G1 Checkpoint and p53-deficient cells

Protein p53 (or only p53) is an essential factor in the G1 checkpoint. However, many tumor cells lack in p53 function due to mutations in its gene or inactivation through the HPV (human papillomavirus) infection, especially oncoproteins E6 and E7. The percentage of tumor cells without functional p53 is high, with some authors pointing values above 50% [9,11,12].

The absence of p53 function leads to the loss of G1 checkpoint, increasing the relevance of G2/M checkpoint in the protection of the DNA stability. Thus, through the inhibition of G2/M checkpoint in p53-deficient cells both checkpoint would be lost. With the absence of those control mechanisms the p53-deficient tumor cells would be more susceptibility for common cancer treatment therapies, accumulating DNA alteration in a large scale that ultimately would create a catastrophic mitotic event leading to apoptosis. Therefore, G2/M checkpoint inhibition was hypothesized as a sensitization therapy in cancer treatment [9,11–14].

1.4. – DNA Damage Response mechanism

DNA damage response related to checkpoints G1 and G2/M is controlled by ATM (ataxia telangiectasia mutated) and ATR (ataxia telangiectasia and Rad3 related), members of the phosphadylinositol 3-kinase family. Their pathways have the downstream effectors Checkpoint kinase 1 (Chk1) and 2 (Chk2) [11,12]. More recently Mitogen activated protein kinase-activated protein kinase 2 (MAPKAPK2 or MK2) was also proposed as a downstream member of this pathway with influence in G2/M checkpoint in p53-deficient cells [9,15]. The process in which MK2 takes part is delayed from the common G2/M nuclear checkpoint and also has a different location, the cytoplasm [16,17].

Although Chk1 and Chk2 possess similar functions in the control of the checkpoint mechanism this two serine/threonine kinases respond to different stimulus. Chk1 acts in response to single-strand DNA lesions and failures in replication forks, being activated through ATR phosphorylation. Active Chk1 has the ability to inactivate Cdc25 phosphatase avoiding the activation of Cdk1 and Cdk2 (cyclin-dependent kinase 1 and 2) by this phosphatase. Cdk2 and Cdk1 take part in the cell cycle processes to enter in S and M phase respectively, being inactive the cycle is arrested in G1 and G2/M checkpoints. However, facing large DNA lesions Chk1 allows the progression of the cell cycle to mitosis where the abnormal DNA does not allow a regular chromosome segregation leading to mitotic catastrophe followed by programed cell death.

Chk2 is activated from double-strand DNA brakes. Its mechanism of action its less studied than the Chk1 however it is accepted that its ability to arrest the cell cycle also comes from Cdc25 inactivation [15,18,19].

As previously referred MK2 checkpoint mechanism takes place in the cytoplasm so in response to DNA damage the first step is the relocalization of the p38/MK2 from the nucleus to cytoplasm. Similar to Chk1 the arrest of the cycle caused by MK2 is also derived by Cdc25 inactivation. In the cytoplasm MK2 will phosphorylate several molecules resulting in the stabilization of Gadd45α mRNA and also avoiding its degradation. Then the Cdc25 sequestration by MK2 is maintained in a positive feedback loop due to Gadd45α mRNA, this allows the prolonged inhibition of the cell cycle [20].

1.5. - Objectives

The central focus of this work is the usage of computational tools to study the binding mode of potential inhibitors to protein kinases. Checkpoint kinase 1 was the first target, due to its relevance in sensitization of p53-deficient tumour cells. As referred in the previous chapter more recently the role of MK2 in this topic was reported, turning this protein kinase in the second focus of this thesis. The inclusion of MK3 in this work aims the improvement in the understanding of MK2 binding site, creating more data from crystallography structures with better resolution.

Thus, the objectives can be summarized in the following topics:

- Bibliographic review on the topic of computational methods in protein kinase studies;
- Understand the binding mode of potential inhibitors to Chk1;
    - Uncovering the most relevant residues for those bindings;
- Improve the binding energy of potential Chk1 inhibitors;
- Observe the main characteristics of the binding of potential inhibitors to MK2 and MK3;
    - Expose the most relevant residues in those bindings;
    - Infer the contribution of the water molecules in the binding sites of both kinases.

1.6. - References

[1] A. Zorina, N. Stepanchenko, G. V Novikova, M. Sinetova, V.B. Panichkin, I.E. Moshkov, et al., Eukaryotic-like Ser/Thr protein kinases SpkC/F/K are involved in phosphorylation of GroES in the Cyanobacterium synechocystis., DNA Res. 18 (2011) 137–51.

[2] K. Balakrishnan, V. Gandhi, Protein kinases: emerging therapeutic targets in chronic lymphocytic leukemia., Expert Opin. Investig. Drugs. 21 (2012) 409–23.

[3] J.M. Arencibia, D. Pastor-Flores, A.F. Bauer, J.O. Schulze, R.M. Biondi, AGC protein kinases: from structural mechanism of regulation to allosteric drug development for the treatment of human diseases., Biochim. Biophys. Acta. 1834 (2013) 1302–21.

[4] S.M. Yarmoluk, a. Y. Nyporko, V.G. Bdzhola, Rational design of protein kinase inhibitors, Biopolym. Cell. 29 (2013) 339–347.

[5] J. Martin, K. Anamika, N. Srinivasan, Classification of protein kinases on the basis of both kinase and non-kinase regions., PLoS One. 5 (2010) e12460.

[6] J.M. Kyriakis, In the beginning, there was protein phosphorylation., J. Biol. Chem. 289 (2014) 9460–2.

[7] Q. Liu, Y. Sabnis, Z. Zhao, T. Zhang, S.J. Buhrlage, L.H. Jones, et al., Developing irreversible inhibitors of the protein kinase cysteinome., Chem. Biol. 20 (2013) 146–59.

[8] Y. Dai, S. Grant, New insights into checkpoint kinase 1 in the DNA damage response signaling network., Clin. Cancer Res. 16 (2010) 376–83.

[9] Z. Meng, J.P. Ciavarri, A. McRiner, Y. Zhao, L. Zhao, P.A. Reddy, et al., Potency switch between CHK1 and MK2: discovery of imidazo[1,2-a]pyrazine- and imidazo[1,2-c]pyrimidine-based kinase inhibitors., Bioorg. Med. Chem. Lett. 23 (2013) 2863–7.

[10] B. Alberts, Molecular Biology of the cell, Fifth Edit, Garland Science, 2008.

[11] J.B. Mitchell, R. Choudhuri, K. Fabre, A.L. Sowers, D. Citrin, S.D. Zabludoff, et al., In vitro and in vivo radiation sensitization of human tumor cells by a novel checkpoint kinase inhibitor, AZD7762., Clin. Cancer Res. 16 (2010) 2076–84.

[12] C.-J. Busch, M. Kriegs, S. Laban, S. Tribius, R. Knecht, C. Petersen, et al., HPV-positive HNSCC cell lines but not primary human fibroblasts are radiosensitized by the inhibition of Chk1., Radiother. Oncol. 108 (2013) 495–9.

[13] G.R. Borst, M. McLaughlin, J.N. Kyula, S. Neijenhuis, A. Khan, J. Good, et al., Targeted radiosensitization by the Chk1 inhibitor SAR-020106., Int. J. Radiat. Oncol. Biol. Phys. 85 (2013) 1110–8.

[14] C. Ma, S. Cai, S. Li, C. Ryan, Targeting Chk1 in p53-deficient triple-negative breast cancer is therapeutically beneficial in human-in-mouse tumor models, J. Clin. Invest. 122 (2012) 1541–1552.

[15] D.A. Canton, J.D. Scott, Chk-ing in and Chk-ing out: Kinase compartmentalization comes to checkpoint control, Mol. Cell. 40 (2010) 1–2.

[16] H.C. Reinhardt, A.S. Aslanian, J. a Lees, M.B. Yaffe, p53-deficient cells rely on ATM- and ATR-mediated checkpoint signaling through the p38MAPK/MK2 pathway for survival after DNA damage., Cancer Cell. 11 (2007) 175–89.

[17] I. a Manke, A. Nguyen, D. Lim, M.Q. Stewart, A.E.H. Elia, M.B. Yaffe, MAPKAP kinase-2 is a cell cycle checkpoint kinase that regulates the G2/M transition and S phase progression in response to UV irradiation., Mol. Cell. 17 (2005) 37–48.

[18] C. King, H. Diaz, D. Barnard, D. Barda, D. Clawson, W. Blosser, et al., Characterization and preclinical development of LY2603618: a selective and potent Chk1 inhibitor., Invest. New Drugs. (2013).

[19] T.H. Stracker, T. Usui, J.H.J. Petrini, Taking the time to make important decisions: the checkpoint effector kinases Chk1 and Chk2 and the DNA damage response., DNA Repair (Amst). 8 (2009) 1047–54.

[20] H.C. Reinhardt, P. Hasskamp, I. Schmedding, S. Morandell, M.A.T.M. van Vugt, X. Wang, et al., DNA damage activates a spatially distinct late cytoplasmic cell-cycle checkpoint network controlled by MK2-mediated RNA stabilization, Mol. Cell. 40 (2010) 34–49.

[21] S.P. Davies, H. Reddy, M. Caivano, P. Cohen, Specificity and mechanism of action of some commonly used protein kinase inhibitors., Biochem. J. 351 (2000) 95–105.

[22] J.C. Lee, J.L. Adams, Inhibitors of serine/threonine kinases., Curr. Opin. Biotechnol. 6 (1995) 657–61.

[23] P. Cohen, D.R. Alessi, Kinase drug discovery--what's next in the field?, ACS Chem. Biol. 8 (2013) 96–104.

[24] K. Tian, R. Rajendran, M. Doddananjaiah, M. Krstic-Demonacos, J.-M. Schwartz, Dynamics of DNA damage induced pathways to cancer., PLoS One. 8 (2013) e72303.

[25] S. Grabauskiene, E.J. Bergeron, G. Chen, A.C. Chang, J. Lin, D.G. Thomas, et al., CHK1 levels correlate with sensitization to pemetrexed by CHK1 inhibitors in non-small cell lung cancer cells., Lung Cancer. 82 (2013) 477–484.

[26] M.I. Walton, P.D. Eve, A. Hayes, M. Valenti, A. De Haven Brandon, G. Box, et al., The preclinical pharmacology and therapeutic activity of the novel CHK1 inhibitor SAR-020106., Mol. Cancer Ther. 9 (2010) 89–100.

[27] R. Thompson, A. Eastman, The cancer therapeutic potential of Chk1 inhibitors: how mechanistic studies impact on clinical trial design., Br. J. Clin. Pharmacol. 76 (2013) 358–69.

[28] X. Huang, C.C. Cheng, T.O. Fischmann, J.S. Duca, M. Richards, P.K. Tadikonda, et al., Structure-based design and optimization of 2-aminothiazole-4-carboxamide as a new class of CHK1 inhibitors., Bioorg. Med. Chem. Lett. 23 (2013) 2590–4.

[29] P.M.M. Araújo, L. Pinto da Silva, J.C.G. Esteves da Silva, Comparative theoretical study of the binding of potential cancer-treatment drugs to Checkpoint kinase 1, Chem. Phys. Lett. 591 (2014) 273–276.

[30] D.A. Case, T.E. Cheatham, T. Darden, H. Gohlke, R. Luo, K.M. Merz, et al., The Amber biomolecular simulation programs., J. Comput. Chem. 26 (2005) 1668–1688.

[31] Y. Duan, C. Wu, S. Chowdhury, M.C. Lee, G. Xiong, W. Zhang, et al., A point-charge force field for molecular mechanics simulations of proteins based on condensed-phase quantum mechanical calculations., J. Comput. Chem. 24 (2003) 1999–2012.

[32] T. Yanai, D.P. Tew, N.C. Handy, A new hybrid exchange?correlation functional using the Coulomb-attenuating method (CAM-B3LYP), Chem. Phys. Lett. 393 (2004) 51–57.

[33] M.J. Frisch, G.W. Trucks, H.B. Schlegel, G.E. Scuseria, M.A. Robb, J.R. Cheeseman, et al., Gaussian 09, Revision A.02, Gaussian Inc Wallingford CT. 34 (2009) Wallingford CT.

[34] J. Wang, R.M. Wolf, J.W. Caldwell, P.A. Kollman, D.A. Case, Development and testing of a general amber force field., J. Comput. Chem. 25 (2004) 1157–1174.

[35] J.C. Phillips, R. Braun, W. Wang, J. Gumbart, E. Tajkhorshid, E. Villa, et al., Scalable molecular dynamics with NAMD., J. Comput. Chem. 26 (2005) 1781–802.

[36] U. Essmann, L. Perera, M.L. Berkowitz, T. Darden, H. Lee, L.G. Pedersen, A smooth particle mesh Ewald method, J. Chem. Phys. 103 (1995) 8577–8593.

[37] J.J.P. Stewart, Optimization of parameters for semiempirical methods V: Modification of NDDO approximations and application to 70 elements, J. Mol. Model. 13 (2007) 1173–1213.

[38] V.M. Anisimov, C.N. Cavasotto, Quantum Mechanical Binding Free Energy Calculation for Phosphopeptide Inhibitors of the Lck SH2 Domain, J. Comput. Chem. 1 (2011) 1–8.

[39] K.D. Dubey, R.P. Ojha, Binding free energy calculation with QM/MM hybrid methods for Abl-Kinase inhibitor., J. Biol. Phys. 37 (2011) 69–78.

[40] N. Nunthaboot, F. Tanaka, S. Kokpol, H. Chosrowjan, S. Taniguchi, N. Mataga, Quantum mechanical study of photoinduced charge transfer in FMN binding protein., J. Phys. Chem. B. 112 (2008) 15837–15843.

[41] Y.-Z. Xiong, P.-Y. Chen, ONIOM DFT/PM3 calculation on the interaction between STI-571 and abelson tyrosine kinase., J. Mol. Model. 14 (2008) 1083–1086.

[42] L. Pinto da Silva, J. Vieira, J.C.G. Esteves da Silva, Comparative theoretical study of the binding of luciferyl-adenylate and dehydroluciferyl-adenylate to firefly luciferase, Chem. Phys. Lett. 543 (2012) 137–141.

Chapter 2 - Protein Kinase-Targeting Drug Discovery and Design: Computational Chemistry as an Indispensable Tool

The following chapter was written in response to the invitation from Nova Publishers to the group of Professor Joaquim C.G. Esteves da Silva. The design of the structure and the selection of the topics covered was conducted by the three authors of the publication according to the publisher suggestion to address the topic of “computational drug design”. The text was written by the author Pedro Araújo. The supervision, revisions and suggestions of improvement were added by Luis Pinto da Silva and Professor Joaquim Esteves da Silva.

In: Computational Chemistry
Editor: Daria Bove
ISBN: 978-1-63321-354-8
© 2014 Nova Science Publishers, Inc.

Chapter 1

PROTEIN KINASE-TARGETING DRUG DISCOVERY AND DESIGN: COMPUTATIONAL CHEMISTRY AS AN INDISPENSABLE TOOL

Pedro M. M. Araújo, Luís Pinto da Silva and Joaquim C. G. Esteves da Silva*
Centro de Investigação em Química, Departamento de Química e Bioquímica, Faculdade de Ciências da Universidade do Porto, Porto, Portugal

ABSTRACT

The development of new drugs always was time consuming and costly. With the development in experimental methods was possible to scan small-compounds libraries in order to find potentially suitable molecules. Nevertheless, these methods are able to so with a very low rate. Protein kinases are a class of enzymes involved in the great majority of cellular process. Due to its presence in many signal pathways, cell cycle and gene expression control mechanisms, this class is one of the major targets for pharmaceutical industries today. Aiming the reduction of time and costs in drug development computational tools started to be used, and commonly called Computer aided drug design (CADD). These methods can be separated in two different types of approaches, structure

* Corresponding author: Joaquim C.G. Esteves da Silva, e-mail: jcsilva@fc.up.pt; Tel: (+351) 220-402-569; Fax: (+351) 220-402-659.

based (SBDD) and ligand based (LBDD). In order to use structure based methods, information about the 3D structure of the target is needed, normally obtained through x-ray crystallography or NMR. Ligand based methods are preferred when this information is not available. The focus of the present chapter is the structure based methods used in the computer drug discovery and design process targeting kinases. Starting with the visual and energetic analysis of the binding site, it is obtained enough information for the creation of a Pharmacophore model and the application of Virtual Screening process. The results of the screening can then be analysed through Molecular Docking process followed by Molecular Dynamics in order to better simulate the real binding conditions. The obtained complexes can be analysed using energy calculations, in order to better understand the binding process. Within the described procedures, computational tools originate a great amount of useful information since hit discovery from lead optimization. The data obtained can save time and reduce costs in the process of drug design and discovery in a large scale.

1. INTRODUCTION

The procedure to develop and uncover new drugs was always time consuming. Before the automation of the processes, the manual synthesis followed by the test of small groups of compounds was extremely inefficient. With the advances in chemistry linked to the emergence of new techniques as combinatorial chemistry and high-throughput screening (HTS) was finally possible to synthesized and analyse a large number of compounds within relatively small periods of time. With the progress in the number of chemical compounds screened was expected an increase in the number of new drugs obtained. However, even with the growth in new drug research funding, the results were not proportionally. From 1993 to 2007 the investment in this area almost quadrupled. However, in the same period of time, the number of new approved drugs did not suffer a significant improvement. That is mainly a consequence of the high failure rate verified, as in 10 000 tested molecules only 1 or 2 have the potential to reach the market. The cost from a drug discovery and development program from the start to the implementation of the product in the market can take up to 14 years with a cost near 1 billion USD (United states dollar) [1–3].

In the post-genome era the amount of available information increased exponentially. Combining that with the high cost of experimental procedures created the need for a more efficient approach to the topic. Since it is

impossible to treat efficiently huge quantities of data manually, automated analysis procedures naturally emerged as an answer to the challenge (Figure 1). These methods are known by Computational tools or more commonly as Bioinformatics tools [4].

Virtual high-throughput screening (vHTS) or only Virtual screening (VS), can be classified as the class of computer tools able to automatically evaluate very large libraries of compounds [5]. Doman et al. performed a project to identify novel inhibitors for the enzyme protein tyrosine phosphatase 1B (PTP1B), pointed as a key factor in type II diabetes [6]. In this study both HTS and VS were used. The experimental HTS was performed in a library of 4,000,000 compounds while VS was applied to 235,000 molecules using the X-ray structure of PTP1B. The hit rate of the experimentally method was 0.021% with only 85 compounds showing IC50 values inferior to 100 µM. On the other side, the computational method obtained 365 high-scoring molecules of which 127 (34.8%) had IC50 value inferior to 100 µM in the *in vitro* tests. The best IC50 result was obtained using the vHTS methodology with the value of 1.7 µM, when the best result for classic HTS was 4.2µM. This work gives us a rare comparison between HTS and VS and elucidates the potential of the computational tools.

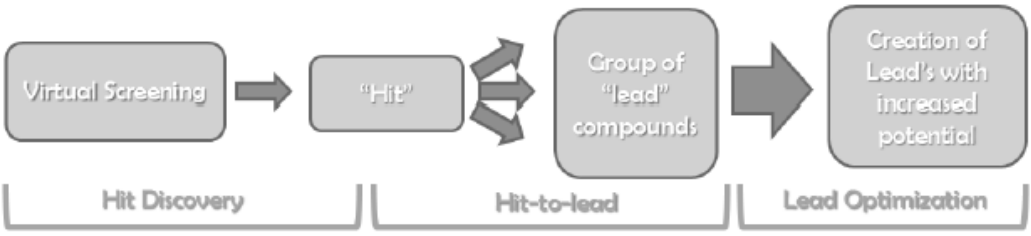

Figure 1. Schematic representation of the Hit discovery to lead optimization process.

Computational methods rapidly became core tools in the novel drug discovery and development, being commonly called Computer aided drug design (CADD) [7]. It is impossible to deny the contribution of these methods in drug development programs. Computational methods can simulate almost all the aspects in the drug discovery and design process [3]. However, they cannot stand alone in the creation of novel drugs [8]. CADD is especially useful in reducing the number of compounds needed to be experimentally tested. The activity prediction allows the exclusion of the some molecules while focusing on those forecasted to be active, resulting in a more time efficient "hit identification". A hit is a compound with specificity and potency to bind to the desired target [9]. The next step is the so called "hit-to-lead"

phase, where a lead series is created based on the interesting characteristics of the most promising hit [10]. The selected molecules undergo an improvement process called "lead optimization". Due to the high costs of this phase the usage of computational tools in it show a big economic impact. CADD is able to point the way that lead optimization should take, and also to save time and money that will be needed to explore several options. Computational aided drug design enclosures two big subgroups of methods. Structure-based (SBDD) and Ligand-Based (LBDD). SBDD is highly dependent on the 3D information of the target, normally obtained through x-ray crystallography or NMR. Structure based methods aim the creation of specific molecules to the binding site of the target. LBDD focus on the information available on the active molecules known to bind to the target, searching for compound with chemical similarities. Ligand based methods are preferred when the available information on the structure of the target is not enough to perform SBDD [2, 11].

Kinases have the ability to transfer a phosphate groups manly from ATP or GTP to cellular targets as proteins, nucleotides and lipids. Protein kinases are able to phosphorylate proteins at Ser, Thr or Tyr residues, being the most significant subgroup of kinases. Protein phosphorylation is abundant within the Eukaryotic cell, being estimated that at a given time one third of all the cellular proteins are phosphorylated. As a consequence of its abundance, kinases can be found in almost all cellular mechanisms but especially in the regulation of signal transduction pathways [12–14]. In recent years kinases have become the central target in cancer drug design. This attention is manly a result of the success of Imatinib, also known as Gleevs. With the ability to inhibit a variety of tyrosine kinases this small molecule has been used in the treatment of diverse types of cancer. However, Imatinib had more relevance in the treatment of chronic myelogenous leukemia (CML) and gastrointestinal tumours (GIST). The effect of this compound was tremendous in transforming these two extremely fatal cancers in "possible to control" conditions. Nevertheless, protein kinase inhibitors have more therapeutic targets that cancer treatments, having already been approved kinase inhibitors in the treatment of inflammatory diseases [15].

During the present chapter we aim to show the common approach to a rational drug design pipeline using structure-based methods while providing some examples of application in the study of protein kinases.

2. BINDING SITE IDENTIFICATION

Ideally a CADD program begins with the existing 3D structure of the target protein bound to a ligand, obtained through x-ray crystallography or NMR. However, the 3D structure of the target alone also represents a good starting point. When the data is not available it is possible to use Homology modelling processes, based on the belief that similar amino acid sequences originate similar three dimensional protein structures [16]. When a bonded ligand is absent and the binding site is unknown the first challenge is to define the binding site. The ligand binding site is generally a depression in the protein surface. The binding process occurs when in a defined site there are specific interactions between the protein and the ligand, generally non-covalent, and those are superior in strength to the repulsive contributions. The non-covalent interactions can be placed in four categories: hydrogen bonds, Van der Waals forces, π-effects and ionic interactions [17]. Computational approaches can be used to identify and characterize high-affinity or new binding sites. These methods are usually divided in several distinct classes: geometric methods, energetic based methods, combination of the previous two, pocket matching and molecular dynamics (MD) based detection.

Geometric methods use grids to identify cavities or to define the 3D structure of a protein. Examples of programs using this strategy are POCKET [18], LIGSIET [19] and its extension LIGSITEcsc [20], SURFNET [21], ConCavity [22], APROPOS [23] and DEPTH [24]. Energetic-based methods are more sensitive and specific that geometric methods using the same amount of time. These methods use a probe system to identify favourable interactions in the protein surface, and collections of positive points represent possible binding sites. Programs using energetic calculations to evaluate binding sites are Q-Site Finder [25], SITEHOUND [26], POCKETPICKER [27], one developed by Morita el al [28] and FLASPSITE [29]. The downside of these two classes of methods result from the large number of false-positive results originated [30]. Pocket matching uses data from known binding sites to evaluate the existence of these regions in other proteins. This method follows the principle that binding sites have unique characteristics when compared to the other protein regions. There are some methods based on this idea like Catalytic Site Atlas [31], AFT [32], Pocket-surfer [33] and Patch-surfer [34]. Proteins are not fixed molecules. They present some fluctuation between conformations. Sometimes the available molecular conformation is not the ideal to the binding of other molecules due to the shape of the binding site. In these cases a molecular dynamic step needs to be added to the process in order

to obtain a set of multiple conformations of the target. It is more likely to find the ideal conformation of a binding site in a group or conformations that in only one static structure. For more information on molecular dynamics see the respective topic (further on this chapter).

The previously presented methods can identify correctly the binding site in 70-90% of the cases when the protein is in the ideal binding conformation (holo) but only in 50-70% if the protein is not in this conformation (apo) [11, 35]. The obtained binding sites results can them be used to guide a Virtual screening process (VS) in order to find new possible ligands.

3. VIRTUAL SCREENING

Virtual screening (VS) is the computational analogue of the high throughput screening (HTS), and therefore can also be named virtual high throughput screening (VHTS). To avoid misunderstandings on this chapter we refer to this technique only as Virtual screening (VS). It can be used to evaluate libraries that contain a vast number of compounds in an automatically and consequently fast mode. The purpose of this method is not to obtain a high number of molecules but otherwise achieve novel structures with the desired pharmacological profiles, called virtual screening hits [5, 36].

VS is undoubtedly a core technique in rational drug discovery and design programs, both for academic research and pharmaceutical companies [37]. Its value raised with the constant growth in the number and size of compounds databases, especially virtual databases [5, 36]. Virtual screening can evaluate a large number of compounds more efficiently in a less time consuming and less expensive manner then HTS, being preferred for the study of bigger databases. *In silico* methods consume computational time in order to decrease the costs of the experimental phase of the study. Nevertheless, VS does not exclude HTS. In fact the use of both methods together resulted in the prompt identification of novel compounds [36]. VS can be seen as a method to restrict the number of residues in the study before HTS, decreasing expenses and saving time.

In Structure Based VS (SBVS), also called Receptor Based VS, the search aims specific features observed in the receptor-ligand interaction [38], such as hydrogen bound acceptors or donors, polar or apolar regions and particular conformations. Its objective is to differentiate ligands that bind strongly to the target from those who not. However, the search can be focused in characteristics independent of the target as drug-likeness [36]. Methods based in ligands characteristics are commonly called Ligand based Virtual Screening

(LBVS). Thus, VS can be divided in Structure based (SBVS) and Ligand based (LBVS) methods.

Structure based methods can be further divided in two different classes, active site derived pharmacophore methods and molecular docking.

3.1. Pharmacophore

The concept of Pharmacophore was describe by IUPAC [39] as "an ensemble of steric and electronic features that is necessary to ensure the optimal supramolecular interactions with a specific biological target and to trigger (or block) its biological response" [40].

The creation of a pharmacophoric model can be achieved with the inclusion of the relevant binding characteristics observed in the 3D structure of the receptor, specially focusing the points that are already known to create interactions to molecular targets. Hydrogen bond acceptors or donors and charged groups are the main features to look for. Pharmacophore methods focus exclusively in the binding site and its features, a simplification that decreases the computational demand in its usage.

Pharmacophore models can be applied in different stages of the novel drug discovery and design process, as de novo design and lead optimization but excelling in virtual screening [11, 38]. The usage of pharmocophore models for virtual screening of compounds databases sometimes face the limitation in the number of features that can be used in the process, with the maximum of seven, although more than these were found in the target analysis. More screening parameters mean more computational time spent. In order to study one target it is ideal to study more than one 3D structure of it. However this is not always possible due to the lack of 3D representations [40, 41].

It is possible to create pharmocophore models from the 3D structure of the target alone. However, the usage of the complex target-ligand is the most common and the ideal starting point. Naturally structure based pharmocophore methods are divided in complex (with ligand) based and macromolecular (without ligand) based.

In the complex based approach the binding site is already known and the challenge is to find the central interactions between the target and the existing ligands. Without available 3D structures of the target-ligand complex this approach is unavailable. Ligand Scout [42] and Pocket v.2 [43] are two examples of programs that perform this type of analysis.

In the absence of the 3D structure of the complex but with existing structure of the target, macromolecular based methods can be applied. If the binding site is known its study can begin, if not it needs to be defined (see section Binding site identification). HS-Pharm [44] and the protocol developed by Tintori et al. [45] are examples of programs that use macromolecular structure based pharmocophore approaches.

3.2. Molecular Docking

Docking tries to preview the position and orientation of two different molecules at the time they interact. When a small molecule is docked in a target protein the process is commonly named protein-ligand docking [46, 47]. These methodologies rely on the docking protocol (Figure 2) and in the quality of the used structures to obtain high value hits, a model independent of any human subjective evaluation [48]. Protein-ligand docking is the "number one" choice in virtual screening protocols, as it generally creates extra and more detailed information that than the other structure based or ligand based methods. It is also computationally more expensive [38].

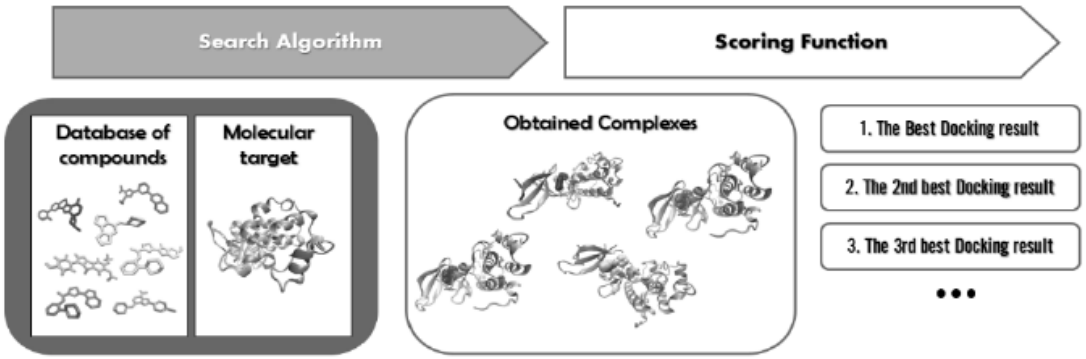

Figure 2. Schematic representation of the Molecular Docking protocol.

There are currently many docking software packages, and due to the relevance of these types of programs they are in constant update with new versions being released within short periods of time. AutoDock4 [49] is the most recent version of this family of programs and allows ligand flexibly and at the same time limited receptor flexibility. Its release was made together with the suit of programs AutoDockTools4, a user friendly interface for the usage of AutoDock. AutoDock Vina is another docking program package similar to AutoDock but with improvements in the speed and accuracy of the calculation

thanks to the parallelism using multithreading on multicore machines [50]. Genetic Optimisation for Ligand Docking (GOLD), uses a genetic algorithm that allows the complete flexibly of the ligand and partially of the receptor while being able to displace water molecules on the binding site [51]. Any docking protocol has two main components: the search algorithm and the scoring function.

3.2.1. Search Algorithm

The search algorithm, sometimes also called docking algorithm, explores the possible positions and orientations of the ligand within the target. In order to perform the docking in a fast pace and being able to rapidly dock large libraries of compounds, the searching algorithms cannot be too exigent in computational power. However, the needed degrees of freedom to find the true binding mode must be included. Thus, the docking algorithm always tries to create the best ratio between the effectiveness in screening the binding site and the speed of the process [38]. Flexibility of both, the ligand and the protein, needs to be taken into account. The available 3D structures of the target do not necessarily represent the binding state of the target or the conformation of its binding site when occupied, as proteins are dynamic molecules in constant motion specially when interacting with other structures. Although in some rigid proteins there is a dominant conformation, in the majority of the cases it does not happen [46, 52].

Flexibility is accepted as one of the major challenges in docking. To simulate structures flexibility, more degrees of freedom must be included in the calculation making it more time consuming. In the beginning of protein-ligand docking, flexibility was not taken into account, and both the ligand and the protein were treated as rigid structures. This is the most basic approach and consequently the faster. Consequently the rate of false negatives created was high with the loss of many hit compounds that failed to bind to the single conformation of the available binding site [38]. The ideal protocol would always consider ligand and target flexibility, however due to the computational demand of it, today the most common approach considers only the flexibility of the ligand. In order to bypass this issue some approaches have been delineated like the "hierarchical docking" in which the faster method is used previously to decrease the amount of compounds in the study, and afterwards the more accurate method could be applied for a smaller pool of compounds [38, 53]. Still, the usage of protocols like this need to give special attention to the creation of false negative results from methods used early like

rigid protein-ligand docking that would exclude potential interesting residues prematurely.

3.2.2. Scoring Functions

After the screening of the target binding site the obtained conformations need to be evaluated by the scoring function. Is not enough to find the proper posing, it is crucial to successfully identify it. Scoring functions need to be able to recognize the active compounds and distinguish the true binding posing from the others. The usage of an extremely rigorous scoring function would have increased computational time, turning the virtual screening of larger compound databases impracticable. In order to decrease the cost of the scoring function, part of its accuracy is sacrificed applying simplifications to the functions.

The ratio between accuracy and speed for the scoring functions is another of the major problems of docking [38]. The success rate of both the scoring functions and the search algorithm are highly dependent of the protein and the ligand in the study. It is expected that the same pair of scoring function and search algorithm achieve different accuracy rates by studying different targets, since both these functions are highly dependent on the molecular characteristics of the targets. There is not such a thing as a universal best pair of search function and scoring algorithm but there are in fact best pairs for different situation.

Generally the scoring functions can be classified according to the used method into three different classes: the force-field-based, the empirical-based and the knowledge-based. In the first class, force-field-based is used to assess the protein-ligand binding. These methods are computationally challenging since they do not enclose any experimental parameters to simplify the calculation. Nevertheless, it has known limitations like the inexact treatment of long range effects.

Empirical methodologies are scoring functions design to mimic experimental binding energy data. As a consequence these methods are highly dependent in the availability of experimental data and its accuracy. The last class, in contrast to the previously exposed scoring functions, focus on the structures instead of the binding energies. This is the less computational demanding class. Due to its dependence in existing data even knowledge-based methods can face limitations [38].

4. MOLECULAR DYNAMICS

As previously said biomolecules, especially proteins, are dynamic entities. Each molecule can roam between a group of different conformations, of which some are more prevalent than others. However, the most common position for a protein alone can be different from the bound state and even differ for complexes with different ligands. In order to better understand the binding of molecules to protein targets Molecular dynamics (MD) simulations are usually applied, creating an ensemble of conformations available to study [11].

MD uses Newtonian physics to simulate atomic motions of desired molecular targets. Without this simplification the calculations of the quantum-mechanical motions of molecules like protein would be unreal to perform due to the exigency in computational time. The first step in this process is to estimate the forces acting in each atom of the system, which is normally accomplish using Equation 1 [54]. The forces in this equation are generally translated into a force-field that describes the molecular motions resulting from the forces applied in each atom of the system. When the forces applied in each atom of the system are calculated, Newton's laws of motion are applied changing the positioning of the atoms. Then the simulation time progress in a time step defined by the user and the process repeats itself until the desired simulation time is achieved [11, 55]. Molecular dynamics still faces some limitation mainly due to the high amount of computation power required to large dynamics and due to limitations in some of the force fields available. The progress in other fields of study is of major relevance to the improvement of MD [55].

GPUs (graphics-processing-units) are an example of recent developed technology that can be used to speed up Molecular dynamics calculations [55–57]. DE Shaw group created processor units specific for MD calculations, thus obtaining a super computer able to perform microseconds of simulations per day and making it possible to observe events as protein folding and unfolding and drug-binding [55, 58, 59].

The Molecular dynamics simulation program packages more popular are the AMBER [60, 61], CHARMM [62] and NAMD [63, 64]. These platforms are sometimes mistaken by the force-fields they apply since they usually have the same name [55].

$$E_{total} = \sum_{bonds} K_r\,(r - r_{eq})^2 + \sum_{angles} K_\theta(\theta - \theta_{eq})^2 + \sum_{dihedrals} \frac{V_n}{2}[1 + \cos(n\phi - \gamma)] + \sum_{i<j}\left[\frac{A_{ij}}{{R_{ij}}^{12}} - \frac{B_{ij}}{{R_{ij}}^{6}} + \frac{q_i q_j}{\epsilon R_{ij}}\right]$$

Equation 1. Atomic forces that generate molecular motion. Can be divided in covalent, bonds, angles and dihedrals angles energy's and non-covalent caused by Vander wall interactions and electronic charges.

5. Examples of Success

In October of 2007 researchers at Merck Pharmaceutical Company successfully obtained Isentress™ (raltegravir) the first clinical-approved HIV Integrase inhibitor, which was only possible due to the previously computational work of McCammon et al. [65]. This case is considered by many the first explicit example of the structure based methods application in the discovery of a new drug.

Thenceforth many other drug discovery programs benefited from computational tools, being this field in constant growth. The Kinases are one of the largest families of human proteins, representing 1.7% of the total of this class [66]. The phosphorylation process can be seen as a molecular "on-off" mechanism, able to activate or inactive cellular effectors. The transfer of a phosphate group to an aminoacid of a protein can be enough to trigger a signal pathway resulting in a huge variety of cellular events since cell cycle abrogation/progression, from transcription of specific DNA regions to cellular apoptosis or survival mechanisms [66]. Alterations in protein kinases regulation has been related to many pathological events as diabetes, inappropriate inflammatory response, oncological diseases and others [66, 67]. Protein kinases gained special attention from the pharmaceutical industry in the search for cancer treatment drugs after the success of Imatinib (Glivec), a "blockbuster" drug that transformed Chronic Myelogenous Leukemia (CML) and Gastrointestinal Tumors (GIST) from fatal conditions with very bad prognostics into treatable situations. Is interesting to notice that in this particular case the low specificity of kinase inhibitors (affecting many protein kinases) was a positive factor that allowed these drugs to be so effective and at the same time treat more than one pathology. At the end of 2013 there was only 26 approved protein kinase inhibitors for clinical use, being 23 of them related to cancer treatment [15].

Table 1. Approved protein kinase inhibitors for clinical use [15]

Name	Target	Year of approval
Imatinib	CML	2001
Getitinib	Lung cancer	2005
Erlotinib	Lung, pancreatic and others cancers	2005
Sorafenib	Renal cancer	2005
Desatinib	CML	2005
Sunitinib	Renal cancer and GIST	2006
Temsirolimus	Renal cell carcinoma	2007
Nilotinib	CML	2007
Everolimus	Several cancers	2009
Lapatinib	Renal cancer	2009
Toceranib	Canine mastocytma	2009
Pazopanib	Renal cancer	2009
Cabozantinib	Canine thyroid cancer	2010
Masivet Kinavet	Canine mastocytoma	2010
Ruxolitinib	Myelofibrosis	2011
Crizotinib	NSCLC	2011
Vemurafenib	Melanoma	2011
Vadetinib	Thyroid cancer	2012
Axitinib	Renal cell carcinoma	2012
Bosutinib	CML	2012
Tivozanib	Kidney cancer	2012
Regorafenib	Thyroid cancer	2012
Lenvatinib	Thyroid cancer	2012

Depending on the site and mechanism of interaction protein kinases inhibitors can be classified in three different types. The first type contains the compounds that bind to the ATP binding site of the target, a conserved region along protein kinases. This is the standard class with a variable specificity that can go from low to high. Type II interact with the "extended ATP binding site", a region less conserved than the ATP binding site making this class more target specific. Type III inhibitors don't compete with ATP having particular binding sites in order regions of the target kinase, being the class more distant from the others [66].

Due to the high number of kinases that the human genome codes is sometimes difficult to define which effector is responsible to the phosphorylation of a particular target. To overcome this matter several

computational tools have been created, and in 2014 at least two new features have been created, PKIS [68] and PSEA [69]. PKIS is a free web service reported as capable to outperform already exiting tools in the identification of protein kinases associated with phosphorylated targets as KinasePhos 2.0 [70], Musite [71], and GPS2.1 [72]. The comparison study between the different methods was made using data from Phospho.ELM [73], a database of serine, threonine and tyrosine phosphorylation sites. The authors of PSEA focused their attention in disease related phosphorylation subtracts, trying to preview which kinases are more likely to create abnormal phosphorylation events and which kinases can be related to known pathology. Remarkably, using this new method they were able to observe a correlation between MAPK (Mitogen-activated protein kinase) and GSK (Glycogen synthase kinase) families overexpression in diseases related to phosphorylation [69].

Casein kinase 2 (CK2) has a large pool of molecular targets, over 400, with distinct functions. Due to the high number of targets affected by this enzyme its overexpression can be related with pathologies as oncological diseases, deregulation of inflammatory response and others. The creation of inhibitors to CK2 was a must and it was only possible using virtual screening in the early stages of the process, followed by biochemical trials and chemical optimization. This process resulted in the creation of the first patent of inhibitors to CK2 by IMBG medicinal chemistry [66, 74, 75].

Janus kinase 2 and 3 (JAK2/3) are involved in lymphoid derivate diseases and have recently receiving attention from virtual screening structure based pharmocophore studies. The work of Rajeswari et al. [76] and Jsuja et al. [77] show some similarities in the used methods. Both authors created pharmocophoric profiles, followed by virtual screening and evaluation by molecular docking and other techniques. The purpose of both studies was also alike: create information to better understand the binding site of these two enzymes and identify novel molecules with inhibitory potential to these targets.

In a different approach Srinivasan et al. [78] studied Nek6, a NIMA (never in mitosis, gene A) related kinase and an important factor to the start of the cell cycle. This group performed a virtual screening study starting from a homology structure of the enzyme obtained by them. After the docking validation they reported the identification of two novel Nek6 inhibitors.

Focusing on the cell cycle study, especially related to the G2 checkpoint, our group studied Chk1 (Checkpoint kinase 1) [79]. This enzyme has a key role in the cell cycle control. To better understand the binding of potential inhibitors to this enzyme we started from already published structures of two

compounds bond to Chk1, compound 39 (C39) and compound 40 (C40) [80], and we performed semi-empirical calculations [81] to obtain the free energy differences from the unbound state (Chk1 without ligand) to the complex state (Chk1 with ligand) and infer the energy contributions of 18 residues of the target binding site. We successfully identified the key factors in the binding of small molecules to Chk1 and simultaneously we showed that C39 had the best inhibitory potential in the study. This type of results can be further used in improvement programs targeting this protein kinase.

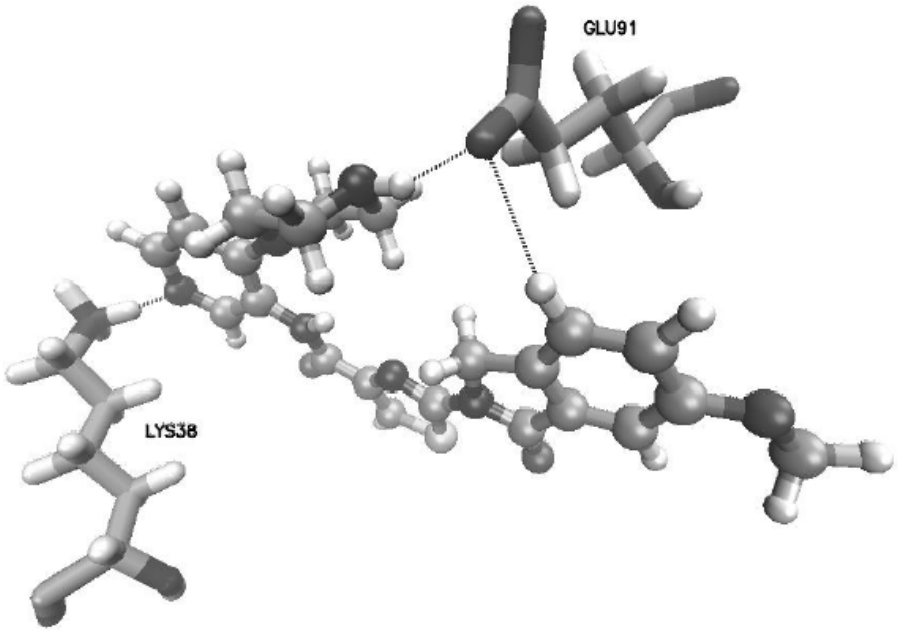

Figure 3. Representation of the interaction between Compound 39 and the two most favourable residues to its binding to Checkpoint kinase 1.

CONCLUSION

The usage of computational tools in the discovery and improvement of novel drugs is undoubtedly necessary. New drug discovery pipelines require high amounts of monetary investment and time. As such any method that is able to maintain the accuracy rate of the process, and at the same time make it faster and less costly must be embraced.

Structure-based methods are already well developed, and in a post-genomic era the number of available 3D structures of molecular targets will only grow, increasing the need for more efficient methods. Computational tools are always dependent on the developments related to hardware.

Nevertheless, more potent equipments will always require more advanced programs. This field of study will continue its growth and hopefully the challenges that we face today due to their computational exigency will be surpassed tomorrow and new objectives will rise.

The better understanding of protein kinases binding sites, its inhibitors and their functions is necessary to treat a high number of pathologies. Creating or finding molecules that bind to kinases in a specific way is still a challenge today but as it was reported in this chapter the efforts of researchers worldwide are creating small advances daily to a higher end.

REFERENCES

[1] Lobanov V. Using artificial neural networks to drive virtual screening of combinatorial libraries. *Drug Discov Today BIOSILICO* 2004;2:149–56.

[2] Ou-Yang S, Lu J, Kong X, Liang Z, Luo C, Jiang H. Computational drug discovery. *Acta Pharmacol Sin* 2012;33:1131–40.

[3] Shekhar C. In silico pharmacology: computer-aided methods could transform drug development. *Chem Biol* 2008;15:413–4.

[4] Yu U, Lee SH, Kim YJ, Kim S. Bioinformatics in the post-genome era. *J Biochem Mol Biol* 2004;37:75–82.

[5] Walters WP, Stahl MT, Murcko M a. Virtual screening—an overview. *Drug Discov Today* 1998;3:160–78.

[6] Doman TN, McGovern SL, Witherbee BJ, Kasten TP, Kurumbail R, Stallings WC, et al. Molecular Docking and High-Throughput Screening for Novel Inhibitors of Protein Tyrosine Phosphatase-1B. *J Med Chem* 2002;45:2213–21.

[7] Durrant JD, McCammon JA. Computer-aided drug-discovery techniques that account for receptor flexibility. *Curr Opin Pharmacol* 2010;10:770–4.

[8] Richards WG. Computer-aided drug design. *Pure Appl Chem* 1994;66:1589–96.

[9] Kalyaanamoorthy S, Chen Y-PP. Structure-based drug design to augment hit discovery. *Drug Discov Today* 2011;16:831–9.

[10] Keseru GM, Makara GM. Hit discovery and hit-to-lead approaches. *Drug Discov Today* 2006;11:741–8.

[11] Sliwoski G, Kothiwale S, Meiler J, Lowe EW. Computational Methods in Drug Discovery. *Pharmacol Rev* 2014;66:334–95.

[12] Zorina A, Stepanchenko N, Novikova G V, Sinetova M, Panichkin VB, Moshkov IE, et al. Eukaryotic-like Ser/Thr protein kinases SpkC/F/K are involved in phosphorylation of GroES in the Cyanobacterium synechocystis. *DNA Res* 2011;18:137–51.

[13] Martin J, Anamika K, Srinivasan N. Classification of protein kinases on the basis of both kinase and non-kinase regions. *PLoS One* 2010;5:e12460.

[14] Arencibia JM, Pastor-Flores D, Bauer AF, Schulze JO, Biondi RM. AGC protein kinases: from structural mechanism of regulation to allosteric drug development for the treatment of human diseases. *Biochim Biophys Acta* 2013;1834:1302–21.

[15] Cohen P, Alessi DR. Kinase drug discovery--what's next in the field? *ACS Chem Biol* 2013;8:96–104.

[16] Chen L, K. Morrow J, T. Tran H, S. Phatak S, Du-Cuny L, Zhang S. From Laptop to Benchtop to Bedside: Structure-based Drug Design on Protein Targets. *Curr Drug Metab* 2012;18:1217–39.

[17] Sotriffer C, Klebe G. Identification and mapping of small-molecule binding sites in proteins: computational tools for structure-based drug design. *Farmaco* 2002;57:243–51.

[18] Levitt DG, Banaszak LJ. POCKET: A computer graphics method for identifying and displaying protein cavities and their surrounding amino acids. *J Mol Graph* 1992;10:229–34.

[19] Hendlich M, Rippmann F, Barnickel G. LIGSITE: Automatic and efficient detection of potential small molecule-binding sites in proteins. *J Mol Graph Model* 1997;15:359–63.

[20] Huang B, Schroeder M. LIGSITEcsc: predicting ligand binding sites using the Connolly surface and degree of conservation. *BMC Struct Biol* 2006;6:19.

[21] Laskowski RA. SURFNET: A program for visualizing molecular surfaces, cavities, and intermolecular interactions. *J Mol Graph* 1995;13:323–30.

[22] Capra JA, Laskowski RA, Thornton JM, Singh M, Funkhouser TA. Predicting protein ligand binding sites by combining evolutionary sequence conservation and 3D structure. *PLoS Comput Biol* 2009;5.

[23] Peters KP, Fauck J, Frömmel C. The automatic search for ligand binding sites in proteins of known three-dimensional structure using only geometric criteria. *J Mol Biol* 1996;256:201–13.

[24] Tan KP, Varadarajan R, Madhusudhan MS. DEPTH: a web server to compute depth and predict small-molecule binding cavities in proteins. *Nucleic Acids Res* 2011;39:W242–W248.

[25] Laurie ATR, Jackson RM. Q-SiteFinder: an energy-based method for the prediction of protein-ligand binding sites. *Bioinformatics* 2005;21:1908–16.

[26] Hernandez M, Ghersi D, Sanchez R. SITEHOUND-web: a server for ligand binding site identification in protein structures. *Nucleic Acids Res* 2009;37:W413–6.

[27] Weisel M, Proschak E, Schneider G. PocketPicker: analysis of ligand binding-sites with shape descriptors. *Chem Cent* J 2007;1:7.

[28] Morita M, Nakamura S, Shimizu K. Highly accurate method for ligand-binding site prediction in unbound state (apo) protein structures. *Proteins* 2008;73:468–79.

[29] Henrich S, Salo-Ahen OMH, Huang B, Rippmann FF, Cruciani G, Wade RC. Computational approaches to identifying and characterizing protein binding sites for ligand design. *J Mol Recognit* 2009;23:209–19.

[30] Laurie ATR, Jackson RM. Methods for the prediction of protein-ligand binding sites for structure-based drug design and virtual ligand screening. *Curr Protein Pept Sci* 2006;7:395–406.

[31] Porter CT, Bartlett GJ, Thornton JM. The Catalytic Site Atlas: a resource of catalytic sites and residues identified in enzymes using structural data. *Nucleic Acids Res* 2004;32:D129–33.

[32] Arakaki AK, Zhang Y, Skolnick J. Large-scale assessment of the utility of low-resolution protein structures for biochemical function assignment. *Bioinformatics* 2004;20:1087–96.

[33] Chikhi R, Sael L, Kihara D. Real-time ligand binding pocket database search using local surface descriptors. *Proteins* 2010;78:2007–28.

[34] Sael L, Kihara D. Detecting local ligand-binding site similarity in nonhomologous proteins by surface patch comparison. *Proteins* 2012;80:1177–95.

[35] Bianchi V, Gherardini PF, Helmer-Citterich M, Ausiello G. Identification of binding pockets in protein structures using a knowledge-based potential derived from local structural similarities. BMC *Bioinformatics 2012;13 Suppl 4:S17.*

[36] Muegge I, Oloff S. Advances in virtual screening. *Drug Discov Today Technol* 2006;3:405–11.

[37] Yuriev E. Challenges and advances in structure-based virtual screening. *Future Med Chem* 2014;6:5–7.

[38] Sousa SF, Cerqueira NMFS a, Fernandes P a, Ramos MJ. Virtual screening in drug design and development. *Comb Chem High Throughput Screen* 2010;13:442–53.
[39] Wermuth CG, Ganellin CR, Lindberg P, Mitscher LA. Glossary of terms used in medicinal chemistry. *Pure Appl Chem* 1998;70:1129–43.
[40] Yang S-Y. Pharmacophore modeling and applications in drug discovery: challenges and recent advances. *Drug Discov Today* 2010;15:444–50.
[41] Zou J, Xie HZ, Yang SY, Chen JJ, Ren JX, Wei YQ. Towards more accurate pharmacophore modeling: Multicomplex-based comprehensive pharmacophore map and most-frequent-feature pharmacophore model of CDK2. *J Mol Graph Model* 2008;27:430–8.
[42] Wolber G, Langer T. LigandScout: 3-D pharmacophores derived from protein-bound ligands and their use as virtual screening filters. *J Chem Inf Model* 2005;45:160–9.
[43] Chen J, Lai L. Pocket v.2: further developments on receptor-based pharmacophore modeling. *J Chem Inf Model* 2006;46:2684–91.
[44] Barillari C, Marcou G, Rognan D. Hot-spots-guided receptor-based pharmacophores (HS-Pharm): a knowledge-based approach to identify ligand-anchoring atoms in protein cavities and prioritize structure-based pharmacophores. *J Chem Inf Model* 2008;48:1396–410.
[45] Tintori C, Corradi V, Magnani M, Manetti F, Botta M. Targets looking for drugs: a multistep computational protocol for the development of structure-based pharmacophores and their applications for hit discovery. *J Chem Inf Model* 2008;48:2166–79.
[46] Sousa SF, Fernandes PA, Ramos MJ. Protein-ligand docking: current status and future challenges. *Proteins* 2006;65:15–26.
[47] Kitchen DB, Decornez H, Furr JR, Bajorath J. Docking and scoring in virtual screening for drug discovery: methods and applications. *Nat Rev Drug Discov* 2004;3:935–49.
[48] Waszkowycz B, Perkins TDJ, Sykes RA, Li J. Large-scale virtual screening for discovering leads in the postgenomic era. *IBM Syst J* 2001;40:360–76.
[49] Morris GM, Huey R, Lindstrom W, Sanner MF, Belew RK, Goodsell DS, et al. AutoDock4 and AutoDockTools4: Automated docking with selective receptor flexibility. *J Comput Chem* 2009;30:2785–91.
[50] Trott O, Olson AJ. AutoDock Vina: improving the speed and accuracy of docking with a new scoring function, efficient optimization, and multithreading. *J Comput Chem 2010*;31:455–61.

[51] Jones G, Willett P, Glen RC, Leach AR, Taylor R. Development and validation of a genetic algorithm for flexible docking. *J Mol Biol* 1997;267:727–48.

[52] Carlson H a. Protein flexibility and drug design: how to hit a moving target. *Curr Opin Chem Biol* 2002;6:447–52.

[53] Cerqueira NMFS a, Bras NF, Fernandes P a, Ramos MJ. MADAMM: a multistaged docking with an automated molecular modeling protocol. *Proteins* 2009;74:192–206.

[54] Cornell WD, Cieplak P, Bayly CI, Gould IR, Merz KM, Ferguson DM, et al. A Second Generation Force Field for the Simulation of Proteins, Nucleic Acids, and Organic Molecules. *J Am Chem Soc* 1995;117:5179–97.

[55] Durrant JD, McCammon JA. Molecular dynamics simulations and drug discovery. *BMC Biol* 2011;9:71.

[56] Yang J, Wang Y, Chen Y. GPU accelerated molecular dynamics simulation of thermal conductivities. *J Comput Phys* 2007;221:799–804.

[57] Liu W, Schmidt B, Voss G, Müller-Wittig W. Accelerating molecular dynamics simulations using Graphics Processing Units with CUDA. *Comput Phys Commun* 2008;179:634–41.

[58] Shan Y, Kim ET, Eastwood MP, Dror RO, Seeliger MA, Shaw DE. How does a drug molecule find its target binding site? *J Am Chem Soc* 2011;133:9181–3.

[59] Shaw DE, Maragakis P, Lindorff-Larsen K, Piana S, Dror RO, Eastwood MP, et al. Atomic-level characterization of the structural dynamics of proteins. *Science* 2010;330:341–6.

[60] Case DA, Cheatham TE, Darden T, Gohlke H, Luo R, Merz KM, et al. The Amber biomolecular simulation programs. *J Comput Chem* 2005;26:1668–88.

[61] Wang J, Wolf RM, Caldwell JW, Kollman PA, Case DA. Development and testing of a general amber force field. *J Comput Chem* 2004;25:1157–74.

[62] Brooks B, Bruccoleri R. CHARMM: A program for macromolecular energy, minimization, and dynamics calculations. *J Comput Chem* 1983;4:187–217.

[63] Kalé L, Skeel R, Bhandarkar M, Brunner R, Gursoy A, Krawetz N, et al. NAMD2: Greater Scalability for Parallel Molecular Dynamics. *J. Comput Phys* 1999;151:283–312.

[64] Phillips JC, Braun R, Wang W, Gumbart J, Tajkhorshid E, Villa E, et al. Scalable molecular dynamics with NAMD. *J Comput Chem* 2005;26:1781–802.

[65] Schames JR, Henchman RH, Siegel JS, Sotriffer C a, Ni H, McCammon JA. Discovery of a novel binding trench in HIV integrase. *J Med Chem* 2004;47:1879–81.

[66] Yarmoluk SM, Nyporko a. Y, Bdzhola VG. Rational design of protein kinase inhibitors. *Biopolym Cell* 2013;29:339–47.

[67] Badrinarayan P, Sastry GN. Rational approaches towards lead optimization of kinase inhibitors: the issue of specificity. *Curr Pharm Des* 2013;19:4714–38.

[68] Zou L, Wang M, Shen Y, Liao J, Li A, Wang M. PKIS: computational identification of protein Kinases for experimentally discovered protein Phosphorylation sites. *BMC Bioinformatics* 2013;14:247.

[69] Suo S-B, Qiu J-D, Shi S-P, Chen X, Liang R-P. PSEA: Kinase-specific prediction and analysis of human phosphorylation substrates. *Sci Rep* 2014;4:4524.

[70] Wong Y-H, Lee T-Y, Liang H-K, Huang C-M, Wang T-Y, Yang Y-H, et al. KinasePhos 2.0: a web server for identifying protein kinase-specific phosphorylation sites based on sequences and coupling patterns. *Nucleic Acids Res* 2007;35:W588–94.

[71] Gao J, Thelen JJ, Dunker a K, Xu D. Musite, a tool for global prediction of general and kinase-specific phosphorylation sites. *Mol Cell Proteomics* 2010;9:2586–600.

[72] Xue Y, Ren J, Gao X, Jin C, Wen L, Yao X. GPS 2.0, a tool to predict kinase-specific phosphorylation sites in hierarchy. *Mol Cell Proteomics* 2008;7:1598–608.

[73] Dinkel H, Chica C, Via A, Gould CM, Jensen LJ, Gibson TJ, et al. Phospho.ELM: a database of phosphorylation sites--update 2011. *Nucleic Acids Res* 2011;39:D261–D267.

[74] Singh NN, Ramji DP. Protein kinase CK2, an important regulator of the inflammatory response? *J Mol Med (Berl)* 2008;86:887–97.

[75] Faust RA, Gapany M, Tristani P, Davis A, Adams GL, Ahmed K. Elevated protein kinase CK2 activity in chromatin of head and neck tumors: Association with malignant transformation. *Cancer Lett* 1996;101:31–5.

[76] Rajeswari M, Santhi N, Bhuvaneswari V. Pharmacophore and Virtual Screening of JAK3 inhibitors. *Bioinformation* 2014;10:157–63.

[77] Jasuja H, Chadha N, Kaur M, Silakari O. Dual inhibitors of Janus kinase 2 and 3 (JAK2/3): designing by pharmacophore- and docking-based virtual screening approach. *Mol Divers* 2014;3:253–67.

[78] Srinivasan P, Chella Perumal P, Sudha a. Discovery of novel inhibitors for Nek6 protein through homology model assisted structure based virtual screening and molecular docking approaches. *Scientific World Journal* 2014;2014:967873.

[79] Araújo PMM, Pinto da Silva L, Esteves da Silva JCG. Comparative theoretical study of the binding of potential cancer-treatment drugs to Checkpoint kinase 1. *Chem Phys Lett* 2014;591:273–6.

[80] Huang X, Cheng CC, Fischmann TO, Duca JS, Richards M, Tadikonda PK, et al. Structure-based design and optimization of 2-aminothiazole-4-carboxamide as a new class of CHK1 inhibitors. *Bioorg Med Chem Lett* 2013;23:2590–4.

[81] Moreira IS, Fernandes PA, Ramos MJ. Accuracy of the numerical solution of the Poisson-Boltzmann equation. *J. Mol. Struct. THEOCHEM,* vol. 729, 2005, p. 11–8.

Chapter 3 – Checkpoint kinase 1 binding site and inhibition model

3.1. - Comparative theoretical study of the binding of potential cancer-treatment drugs to Checkpoint kinase 1

The following article published in Chemical Physics Letters was outlined by the authors Luis Silva Pinto and Professor Joaquim Esteves da Silva. The bibliographic research was performed by Luis Pinto Silva and Pedro Araújo. The theoretical calculations were executed by Luís Pinto Silva and Pedro Araújo. The text writing of Theoretical Methods section was performed by Luís Pinto Silva and the remaining document by Pedro Araújo. Revision of the manuscript, suggestions of improvement and correction were added by Luis Pinto Silva and Professor Joaquim Esteves da Silva. The supplementary information of this document can be seen in Appendix 1.

The succeeding paper reports our initial studies regarding the Chk1 ATP binding site.

Chemical Physics Letters 591 (2014) 273–276

Contents lists available at ScienceDirect

Chemical Physics Letters

journal homepage: www.elsevier.com/locate/cplett

Comparative theoretical study of the binding of potential cancer-treatment drugs to Checkpoint kinase 1

Pedro M.M. Araújo, Luís Pinto da Silva, Joaquim C.G. Esteves da Silva *

Centro de Investigação em Química, Departamento de Química e Bioquímica, Faculdade de Ciências da Universidade do Porto , R. Campo Alegre 687, 4169-007 Porto, Portugal

ARTICLE INFO

Article history:
Received 10 October 2013
In final form 20 October 2013
Available online 27 November 2013

ABSTRACT

This Letter focuses the binding between Checkpoint kinase 1 and two molecules with known inhibition potential, C39 and C40. In order to find the most relevant residues the structures were submitted to an optimization process. As expected C39 presented the highest inhibitory power towards Chk1, being this inhibition mode highly dependent on the interactions with Lys38 and Glu91. Glu55 and Asp148 exhibit unfavorable interactions to C39. Glu91 was the most important residues in the binding of C40 to Chk1, while interaction with Lys38, Glu55 and Gly90 resulted in repulsion.

© 2013 Elsevier B.V. All rights reserved.

1. Introduction

Kinases are a family of proteins able to transfer phosphate from ATP to a determined molecular target such as lipids, carbohydrates and proteins. The kinase-catalyzed process is called phosphorylation, which produce a variety of modifications in the target that may lead to its activation or inactivation. The human genome encodes more that 500 kinases of which 420 are serine/threonine kinases [1]. This family of proteins is involved in the majority of cellular process being of most relevance in cell signaling and cell cycle control [2].

In eukaryotes, the cell cycle is highly controlled. If an event did not occur as it should, the cycle can be arrested in three specific points called Checkpoints. These are located in late G1 (start Checkpoint), before mitotic event (G2/M) and before sister-chromatid separation (metaphase-to-anaphase). The start Checkpoint, in G1, has the ability to prolong this phase if the conditions are not the ideal to replicate the DNA, which can occur after DNA damage. However if the damage is too severe, the apoptotic process can be triggered.

One of the most relevant proteins in this mechanisms is p53 [3]. Tumor protein p53 is encoded by the gene TP53, and somatic mutations in it can be found in 25% of breast cancers and are associated with poor prognosis [4–6]. Breast cancer is the most common type of cancer in woman worldwide and the second most common, after lung cancer, for both sexes.

Nevertheless, in p53-deficient tumor cells the DNA stability is ensured by G2 Checkpoint, in a process dependent of Checkpoint kinase 1 (Chk1) [7]. As a result of Chk1 action cell cycle arrest, giving the necessary time that DNA repair mechanism needs to act [8]. Although G2 elongation is the most well recognized function of Chk1, this enzyme also has a relevant role in stabilization and control of replication forks progression [9] and in the control of replication origin site [10].

When Chk1 is inhibited or downregulated in p53-deficient tumor cell lines with DNA damage, these cells undergo a catastrophic mitotic process resulting in apoptosis. Thus, inhibition of Chk1 emerged as a possible therapy to sensitize p53-deficient cells to the usual DNA damaging agents such as chemotherapy and radiation used in cancer treatment, especially in breast cancer [11]. Due to this therapeutic window, the need for specific and cell active Chk1 inhibitors significantly increased.

Huang et al. (2013) [11] held a structure based design and optimization of Chk1 inhibitors after obtaining a hit compound using Automated Ligand Identification (ALIS) reaching significant biochemical improvements. In the end of this Letter two compounds, 39 and 40, emerged as very promising Chk1 inhibitors with high selectivity (CDK2/Chk1) and promising IC50 values (1nM and 3nM respectively). The crystallography structure of this two molecules was also obtained (4HYH and 4HYI respectively).

In the present Letter we aimed to study Chk1 inhibition by the two compounds aforementioned in a computational approach. This method allowed us to infer what residues played the most relevant role in this inhibitor-enzyme interaction. In order to accomplish this end a molecular mechanic approach was used. Semi-empirical calculations were applied to determine the energetic contribution of several active site residues in the binding to compounds 39 and 40.

2. Theoretical methods

The PDB structures 4HYH (Checkpoint kinase 1 complexed with compound 39) and 4HYI (Checkpoint kinase 1 complexed with compound 40) were used as starting structure [11]. The hydrogen atoms, the missing atoms, and TIP3P water molecules

* Corresponding author. Fax: +351 22608259.
E-mail address: jcsilva@fc.up.pt (J.C.G. Esteves da Silva).

0009-2614/$ - see front matter © 2013 Elsevier B.V. All rights reserved.
http://dx.doi.org/10.1016/j.cplett.2013.11.049

up to 10 Å were added by the LEAP module of the AMBER suite of programs [12]. The ff03 force field was used for intramolecular interactions [13]. The geometries of Compounds 39 and 40 were obtained with the CAM-B3LYP/6-31G method, due to the very high number of atoms present in the molecule [14]. These geometry optimizations were made with the GAUSSIAN09 software package [15]. The CAM-B3LYP/6-31G obtained geometries were used in the parameterization of the ligands with the ANTECHAMBER module of AMBER and the general AMBER force field [16]. The parameterization was made by performing a CAM-B3LYP/6-311G (d,p) single point energy calculation, at the CAM-B3LYP/6-31G geometries.

One phase of 30 000 steps of energy minimizations was performed for each enzyme–ligand complex, by using the Not (just) Another Molecular Dynamics program (NAMD) molecule dynamic code with AMBER potential functions, parameters, and the file formats [17]. In this process, the Particle Mesh Ewald method was used to include the long-range interactions [18]. All the minimizations steps were performed in a NVT ensemble, with a temperature of 298.15 K, with the cutoff value of 14 Å.

In the end of the molecular mechanics simulations, one selection of binding site residues were withdrawn from the complexes Chk1-C39 and Chk1-C40. The selected residues for both compounds were: Leu15, Gly16, Try20, Val23, Lys38, Glu55, Leu84, Glu85, Try86, Cys87, Ser88, Gly90, Glu91, Glu134, Asn135, Leu137, Ser147 and Asp148. These selections were made taking into account the results observed by us after energy minimizations and discussion of results made by Huang et al. (2013) [11].

The energies of association of the two ligands with Chk1 were estimated through single point energy calculations with the semi-empirical method PM6 [19]. To assess the energy of association for each ligand (ΔE_{ass}), three calculations were performed (Eq. (1)): PM6 single point energy calculations on the model composed by the ligand and all the chosen active site residues ($E_{complex}$); PM6 single point energy calculations on a model including only the chosen active site molecules ($E_{active\ site}$); PM6 single point calculations on the ligand (E_{ligand}). After the calculation of ΔE_{ass} for each ligand, the energetic contribution to the ΔE_{ass} of each active site molecule was evaluated. For an active site molecule X, its contribution was estimated by removing it from the respective model and by calculation of the corresponding energy of association as already described. By comparing the ΔE_{ass} obtained for the model in the absence of that molecule, with the results obtained with all the active site molecules present, it is possible to get a quantitative picture of the contribution of each molecule to the associating energy of the ligands ($\Delta\Delta E_{ass}$, Eq. (2)). The removal of the molecules that contribute favorably to the interaction of the ligands with the active site will lead to less stable complexes and consequently to more positive $\Delta\Delta E_{ass}$. The family of PMx methods was used due to the very high number of atoms present in these models, and due to its use in previous studies where interaction/binding energies were calculated [20–24]. The single point energy calculations were performed with the GAUSSIAN 09 program package [15].

$$\Delta E_{ass} = E_{complex} - (E_{enzyme} + E_{ligand}) \quad (1)$$

$$\Delta\Delta E_{ass}(\text{Molecule}X) = \Delta E_{ass}(\text{Without Mol}X) - \Delta E_{ass}(\text{With All Mol}) \quad (2)$$

3. Results and discussion

As expected, the compounds 39 (C39) and 40 (C40) interact with a similar pool of residues but with some variations. In this Letter 18 residues were selected for the energetic analysis of the two ligands (Table 1).

Within the 18 residues analyzed for C39 two of them showed negative interactions, repelling the compound, Glu55 and Asp148 (Figure 1A). Asp148 contribution is due to its negative charge that interacts with the closest ring in C39, also negatively charged, originating repulsion (−2 kcal mol^{-1}). After the energy minimization process Glu55 showed to be too far from the compound to be favorable to the creation of complex.

Although the repulsion observed, was also detected some strong positive interactions with Lys38 and Glu91 (Figure 1B). One of the oxygen atoms in the negative charged region of Glu91 seems to create an H-bond with one of the nitrogens in the outer

Table 1
Energetic contributions (in kcal mol^{-1}) of the selected residues to the binding of compounds C39 and C40 to Chk1.

	Leu 15	Gly 16	Try 20	Val 23	Lys 38	Glu 55	Leu 84	Glu 85	Tyr 86	Cys 87	Ser 88	Gly 90	Glu 91	Glu 134	Asn 135	Leu 137	Ser 147	Asp 148
C39	4	0	0	1	14	−14	0	1	5	5	1	0	17	5	1	0	4	−2
C40	4	0	0	1	−1	−4	1	2	2	3	0	−1	14	3	0	0	4	4

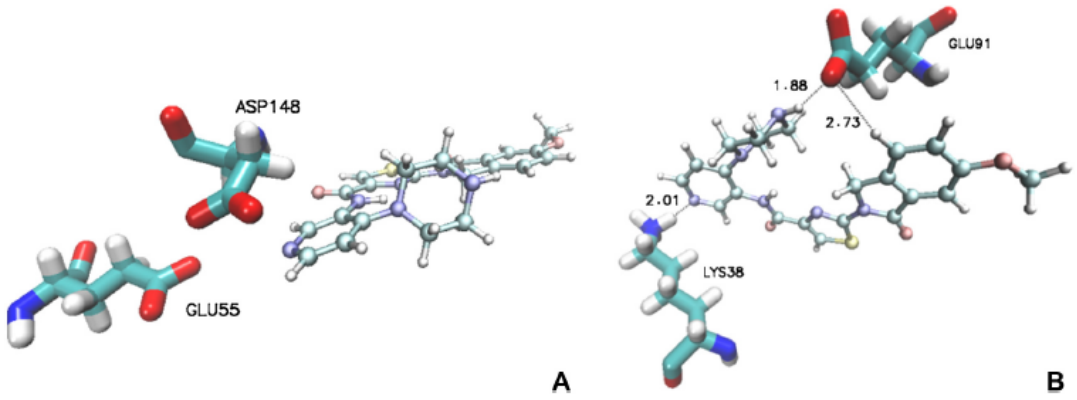

Figure 1. Interactions between most significant residues and compound 39, (A) negative interactions; (B) positive interactions (distance in Angstroms).

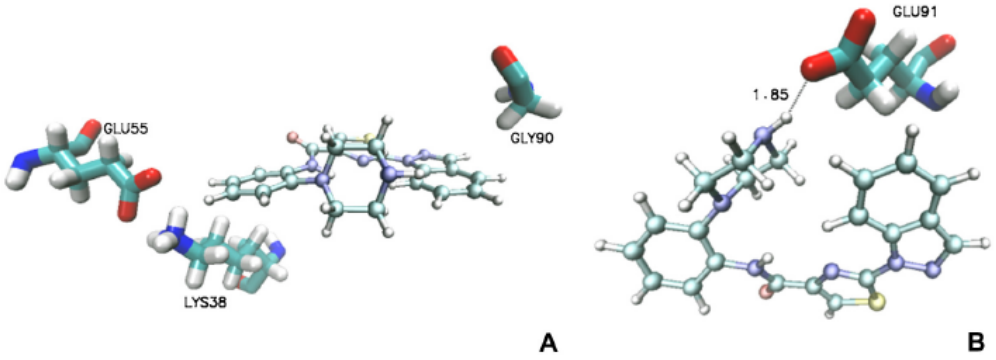

Figure 2. Interactions between most significant residues and compound 40, (A) negative interactions; (B) positive interactions (distance in Angstroms).

ring of the RHS (right hand side) in C39. Also, the negative charge of this residue may create some attraction towards the aromatic ring on the LHS (left hand side) of C39, a weak H-Bond may exist in this site. These results indicate that Glu91 interacts with both RHS and LHS of C39 (14 kcal mol^{-1}). Lys38 takes part in an H-bond with an NH group as donor and an N of C39 as acceptor. This is the stronger H-bond in this complex, which justifies the strong attraction of this residue towards C39 (17 kcal mol^{-1}).

The interactions with C40 showed to be energetically distinct for those observed with C39. For C40, negative interactions were weaker. Only Glu55 (−4 kcal mol^{-1}) was present in a non-negligible unfavorable interaction with C40. This repulsion doesn't results directly from the interaction of this residue with C40 but with its interaction with Lys38, as discussed forward. The repulsions originated by Gly90 and Lys38 have low or none significance. Both probably occur due to charge interactions (Figure 2A).

According to our results there is only one strong attractive residues in the C40-kinase complex, Glu91. This interaction is similar to what was previously stated in this work for the interaction between this residue and C39. Here the H-bond towards RHS seems to be stronger, because the distance is shorter (1.88 Å for C39 and 1.85 Å for C40). However, here the existence of an H-bond towards the LHS seems unlikely (Figure 2B).

Although the residues that interact with both compounds are overall the same, they have different relevance in the two cases. The most similar results come from Leu15, Gly16, Tyr20, Val23, Leu137 and Ser147, which have a small positive or null contribution, but also from Glu91 one of the most important residues. For C39 the Lys38 is the most relevant residue to the binding, but in C40 this residue is insignificant. The conclusion is different when the most significant residue for C40 interaction, Glu91 is observed in C39, which is the second most important.

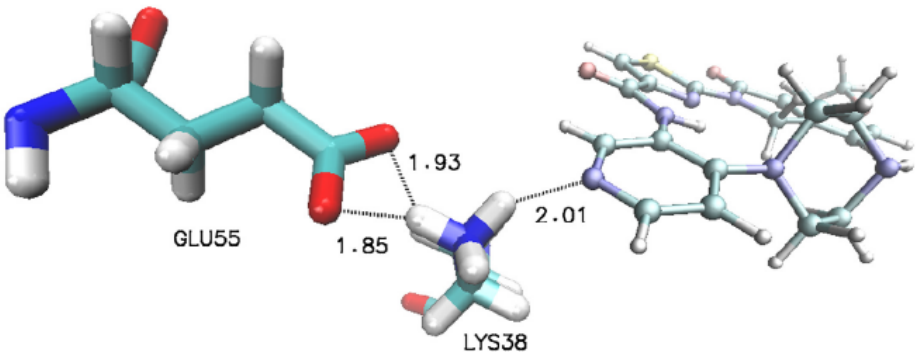

Figure 3. Interactions between Glu55, Lys38 and Compound 39 (distance in Angstroms).

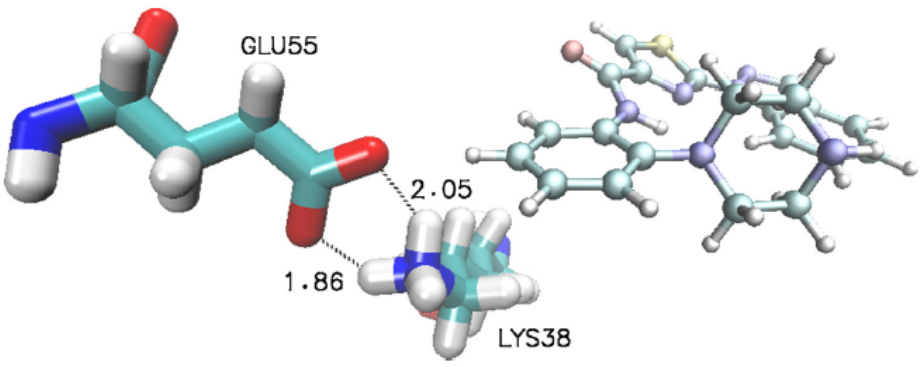

Figure 4. Interactions between Glu55, Lys38 and Compound 40 (distance in Angstroms).

As it was previously said in this text, residues Lys38 and Glu55 interact with one another in both complexes, Chk1 complexed with C39 and C40. In C39 the closest ring to Lys38 have one added nitrogen that C40 doesn't have. This atom turns this ring charge negative. Also the added nitrogen allows the creating of the H-bond previously reported between Lys38 and C39. Since Lys38 is a positive residue and the ring has negative charge they should attract each other. Glu55 also attracts Lys38, due to charge interaction, but to the opposite direction of C39. Also an hydrogen of Lys38 seems to interact with both the oxygens in Glu55 charged site. All this interactions result in a complex scheme where Glu55 harms the positive interaction of Lys38 towards C39 (on the H-bond) (Figure 3). In C40 since it doesn't have the added nitrogen the closest ring to Lys38 has positive charge, repelling this residue. In this case the action of Glu55 is favorable to the complex (C40-Chk1) since this residue attracts Lys38 (due to charge interactions) keeping this lysine away from C40, decreasing its repulsive effect (Figure 4).

Huang et al. (2013) [11] observed that the addition of one nitrogen in the RHS improved the biochemical potency of the compounds, and they hypothesized that this improvement was due to a hydrogen-bond to Lys38. Our results support this idea. However we also showed that this change created a weaker repulsion towards Asp148 [11].

The calculation of the ΔE_{ass} value (Eq. (1)) for each compound demonstrated, as expected, that the interaction with C39 was stronger (-45 kcal mol^{-1}) than the interaction with C40 (-34 kcal mol^{-1}). Thus, this outcome meets the experimental results already reported [11].

4. Conclusions

The binding of the two compounds, C39 and C40, to the ATP binding site of Checkpoint kinase 1 was studied using a semi-empirical/molecular mechanics methodology. During this Letter was possible to infer the contribution of the different residues to the establishment of the enzyme-inhibitor complex.

As expected, compound 39 proved to be the best molecule to inhibit Chk1 in this Letter. Nevertheless, this compound presented some negative interactions towards the enzyme. In order to improve the compound specificity to Chk1 the repulsive interactions involving Glu85 and Asp148, should be eliminated and the interactions to Glu91 and Lys38 need to be maintained and, if possible, reinforced. The insertion of a nitrogen in the RHS did create an improvement in the inhibition potential of the compound C39, due to a complex game of charges with Lys38 and Glu55.

As the compound 40 did not show strong repulsive interactions to the enzyme, it also have some potential for improvement specially aiming the creation of positive interactions with Lys38. The maintenance of interactions of C40 with Glu91, while deleting the interaction to Glu55 and Gly90 could be a good improvement.

Acknowledgment

A Ph.D. Grant to Luís Pinto da Silva (SFRH/BD/76612/2011), attributed by FCT, is also acknowledged.

Appendix A. Supplementary data

Supplementary data associated with this article can be found, in the online version, at http://dx.doi.org/10.1016/j.cplett.2013.11.049.

References

[1] Q. Liu, Y. Sabnis, Z. Zhao, T. Zhang, S.J. Buhrlage, L.H. Jones, N.S. Gray, Chem. Biol. 20 (2013) 146.
[2] S.P. Davies, H. Reddy, M. Caivano, P. Cohen, Biochem. J. 351 (2000) 95.
[3] B. Alberts, Molecular Biology of the Cell, Fifth ed., Garland Science, 2008.
[4] J.-C. Bourdon et al., Breast Cancer Res. 13 (2011) R7.
[5] S. Masciari et al., Breast Cancer Res. Treat. 133 (2012) 1125.
[6] M. Olivier et al., Clin. Cancer Res. 12 (2006) 1157.
[7] C.X. Ma et al., J. Clin. Invest. 122 (2012) 1541.
[8] R. Thompson, A. Eastman, Br. J. Clin. Pharmacol. 76 (2013) 358.
[9] T.H. Stracker, T. Usui, J.H.J. Petrini, DNA Repair (Amst). 8 (2009) 1047.
[10] E. Petermann, M. Woodcock, T. Helleday, Proc. Natl. Acad. Sci. U.S.A. 107 (2010) 16090.
[11] X. Huang et al., Bioorg. Med. Chem. Lett. 23 (2013) 2590.
[12] D.A. Case et al., J. Comput. Chem. 26 (2005) 1668.
[13] Y. Duan et al., J. Comput. Chem. 24 (2003) 1999.
[14] T. Yanai, D.P. Tew, N.C. Handy, Chem. Phys. Lett. 393 (2004) 51.
[15] M.J. Frisch et al., Gaussian 09, Gaussian Inc., Wallingford, CT, 2009, 34.
[16] J. Wang, R.M. Wolf, J.W. Caldwell, P.A. Kollman, D.A. Case, J. Comput. Chem. 25 (2004) 1157.
[17] J.C. Phillips et al., J. Comput. Chem. 26 (2005) 1781.
[18] U. Essmann, L. Perera, M.L. Berkowitz, T. Darden, H. Lee, L.G. Pedersen, J. Chem. Phys. 103 (1995) 8577.
[19] J.J.P. Stewart, J. Mol. Model 13 (2007) 1173.
[20] V.M. Anisimov, C.N. Cavasotto, J. Comput. Chem. 1 (2011) 1.
[21] K.D. Dubey, R.P. Ojha, J. Biol. Phys. 37 (2011) 69.
[22] N. Nunthaboot, F. Tanaka, S. Kokpol, H. Chosrowjan, S. Taniguchi, N. Mataga, J. Phys. Chem. B 112 (2008) 15837.
[23] Y.-Z. Xiong, P.-Y. Chen, J. Mol. Model 14 (2008) 1083.
[24] L. Pinto da Silva, J. Vieira, J.C.G. Esteves da Silva, Chem. Phys. Lett. 543 (2012) 137.

3.2. – Theoretical Modelling of Potential Chk1 Inhibitors

The ensuing publication in Letters in Drug Design & Discovery is based on the previously referred article Comparative theoretical study of the binding of potential cancer-treatment drugs to Checkpoint kinase 1. The design of the study was performed by the three authors. The bibliography research, all the theoretical calculation and the writing of the text was performed by the author Pedro Araújo. Revision of the document, suggestions of improvement and corrections were proposed by the authors Luis Pinto Silva and Joaquim Esteves da Silva. The document has not yet published version. The Supplementary information for this publication can be consulted in Appendix 2.

The following work consist in our attempts to improve the binding energy of a Chk1 potential inhibitor based on Compound 39.

Send Orders for Reprints to reprints@benthamscience.net

Letters in Drug Design & Discovery, **2015**, *12*, 000-000 1

Theoretical Modelling of Potential Chk1 Inhibitors

Pedro M.M. Araújo, Luís Pinto da Silva and Joaquim C.G. Esteves da Silva*

Centro de Investigação em Química, Departamento de Química e Bioquímica, Faculdade de Ciências da Universidade do Porto, R. Campo Alegre 687, 4169-007 Porto, Portugal

Abstract: In this contribution, we attempted to design novel inhibitors of the serine/threonine-protein kinase Chk1. After studying the interaction of Chk1 ATP binding site with known inhibitor C39, we created seven modified C39-based molecules in order to achieve higher binding potentials. Of those, modified molecules 2, 4, 6 and 7 (MD2, MD4, MD6 and MD7) were selected to be assembled in three new molecules, originating MD8, MD9 and MD10. When compared to C39, MD8 and MD9 showed significant improvements in the binding energy while MD10 had a smaller gain. MD9 achieved the best improvement (21%) and MD8 the second best (19%) while MD10 only reached a 6% improvement.

Keywords: Checkpoint Kinase 1, Chk1 Inhibition, Enzyme-Inhibitor Interactions, Molecular Design, Semi-empirical calculations, p53-deficient tumor.

INTRODUCTION

Phosphorylation, a process catalysed by protein kinases, is one of the most important mechanisms in living cells. It is present in the majority of the signal transduction pathways and it is one of the main mechanisms in cell cycle control.

Due to its high relevance, phosphorylation was nicknamed "molecular language" [1-5]. Today it is known that the deregulation of almost two hundred kinases is linked to different pathologies. Cancer and inflammatory diseases treatment were the fields of study where the creation of kinases inhibitors has been more stimulated [6]. In fact, more than 50% of the drug discovery programs in oncology target kinases, making this subject the most compelling for protein kinase inhibition studies [7].

The majority of protein kinases in eukaryotes belong to the serine/threonine class (STPKs) [8]. Checkpoint kinase 1 (Chk1) is an STPK of major importance in G2/M checkpoint. Checkpoints have the ability to halt the progression of the cell cycle if the conditions are not perfect to its occurrence. When there is DNA damage, G1 checkpoint extends this phase giving the needed time for DNA repair mechanisms act or, if the damage is too severe, trigger the apoptotic process [9]. Protein p53 plays an essential role in G1 checkpoint [10]. The function of this protein is essential in cell survival, however it is mutated in more than 50% of human tumours [11]. In p53-deficient tumour cells G1 checkpoint is inactivated, increasing the relevance of G2/M checkpoint in the protection of DNA integrity. The inactivation or downregulation of Chk1 in p53-deficient tumour cells originates catastrophic mitotic events that lead to apoptosis, as a consequence of the loss of G1 and G2/M checkpoints [12]. Therefore, Chk1 inhibition emerged as a potential enhance ment of classical cancer treatment methods as radio or chemotherapy, promoting the death of DNA damaged cells [13–16]. In 2013 Thompson and Eastman [17] reported a list of eleven Chk1 inhibitors that had already been in preclinical or clinical development. Some were already discontinued due to lack of specificity towards other kinases. The necessity for a specific and cellular active Chk1 inhibitor still needs to be answered.

Huang and colleagues [18] performed a structure-based design and optimization study on a new class of Chk1 inhibitors. The project started from a hit compound found using Automated Ligand Identification System (ALIS) and resulted in the obtaining of Chk1 inhibitors with good results in enzymatic and cell-based assays. Of the achieved structures the compound 39 (C39, Figure 1) was the one with the highest potential. These authors published the three-dimensional structure of C39 and C40 (compound 40), another compound obtained in their study. In our previous work [19] we studied the binding of C39 and C40 to Chk1 in a theoretical approach using semi-empirical calculations. As expected, C39 proved to be the most promising Chk1 inhibitor in the study. The binding between C39 and Chk1 showed to be highly dependent on the residues Glu91 and Lys38 while Asp148 and Glu46 repelled the inhibitor from the enzyme active site.

At the present work we aim to use the previously obtained knowledge from our study [19] and create improved Chk1 inhibitors. To achieve this objective several potential inhibitors were designed based on C39. The binding energy of Chk1 with the different molecules in this study as the individual contribution of each residue was calculated using semi-empirical methods. Improvements were found, regarding the binding of C39 to Chk1, in the order of ~20%.

MATERIALS AND METHODS

The PDB structure 4HYH (Checkpoint kinase 1 bond with compound 39) [18] was used as starting point to the creation of Modified molecules 1 to 10 (MD1 to MD10).

*Address correspondence to this author at the Centro de Investigação em Química, Departamento de Química e Bioquímica, Faculdade de Ciências da Universidade do Porto, R. Campo Alegre 687, 4169-007 Porto, Portugal; Tel.: +351 226082869; Fax: +351 226082959; E-mail: jcsilva@fc.up.pt

1570-1808/15 $58.00+.00 ©2015 Bentham Science Publishers

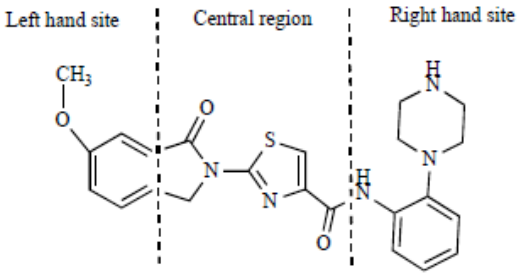

Fig. (1). Compound 39 (C39), with representation of the different molecular regions.

The modifications in the structure of C39 were first created replacing the data of original atoms for new data in the PDB files. The novel files were then used in subsequent energy minimizations calculations, with the objective to obtain stable and reliable structures. The selection of these modifications resulted from our previous observations [19]. Missing atoms (as hydrogen ones) were added by the LEAP module, present in the AMBER program package [20]. Water molecules, of the TIP3P type, were also added up to 15 Å [20]. Intramolecular interactions were modeled using the ff03 force field [21]. The geometries of C39, MD1, MD2, MD3, MD4, MD5, MD6, MD7, MD8, MD9 and MD10 were obtained at the CAM-B3LYP/6-31G level of theory [22]. The choice of the basis set was made based on the high number of atoms present in the studied compounds. Optimized structures were obtained using the GAUSSIAN09 code [23]. These structures were utilized for the ligands parameterization alongside with the general AMBER force field, within the ANTECHAMBER module [24]. The atomic charges for parameterization were obtained by performing a CAM-B3LYP/6-311G (d,p) single point energy calculation, at the CAM-B3LYP/6-31G geometries. The GAFF force field was used to acquire the force constants.

The energy minimizations consisted of 30000 steps, and were performed using the Not (just) Another Molecular Dynamics program (NAMD) molecule dynamic code [25]. The long-range interactions were modelled with the Particle Mesh Ewald method [26].

In the end of the energy minimizations process, one selection of binding site residues was withdrawn from the complexes: C39-Chk1, MD1-Chk1, MD2-Chk1, MD3-Chk1, MD4-Chk1, MD5-Chk1, MD6-Chk1 and MD7-Chk1. The selected residues were: Leu15, Gly16, Try20, Val23, Ala36, Lys38, Val68, Leu84, Try86, Cys87, Ser88, Gly90, Glu91, Glu134, Asn135, Leu137, Ser147 and Asp148. For the complexes MD8-Chk1, MD9-Chk1 and MD10-Chk1 and again C39-Chk1 a bigger selection of binding residues was withdrawn. This second selection had 25 residues: Leu15, Gly16, Glu17, Try20, Val23, Ala36, Lys38, Glu55, Val68, Leu84, Glu85, Try86, Cys87, Ser88, Gly89, Gly90, Glu91, Glu134, Asn135, Leu136, Leu137, Ser147, Asp148, Phe149 and Gly150. The selections were made taking into account results from our previous study [19] and visual observation of the complexes after energy minimizations.

The energies of association for each inhibitor C39, MD1, MD2, MD3, MD4, MD5, MD6, MD7, MD8, MD9 and MD10 with Chk1 were calculated by semi-empirical method PM6 [27]. The energy of association for each ligand (ΔE_{ass}) was estimated performing three types of calculations (Eq. (1)): single point energy calculations on the active site molecules-inhibitor complex ($E_{complex}$); energy calculations only on chosen active site molecules (E_{enzyme}); single point calculations on the bare inhibitor (E_{ligand}). After obtaining the ΔE_{ass} for each inhbitor, the energetic contribution of each active site residue was calculated. For an active site molecule X, its contribution was estimated by removing it from the respective complex and calculation the corresponding ΔE_{ass}. By comparison between the calculated ΔE_{ass} for the complex in the absence of that residue, with the results obtained with all the active site residues, we can obtain a quantitative picture of the contribution of each molecule to the associating energy of the ligands ($\Delta\Delta E_{ass}$, Eq. (2)). The removal of the molecules that contribute favourably to the interaction of the ligands with the active site will lead to less stable complexes and consequently to more positive $\Delta\Delta E_{ass}$. The PM6 method was used in this work due to the size of the presented complexes and because good results were obtained with the PMx methods in studies aiming to calculate interaction/binding energies [19,28–32]. The single point energies were calculated with the GAUSSIAN 09 code [23].

$$\Delta E_{ass} = E_{complex} - \left(E_{enzyme} + E_{ligand}\right) \quad (1)$$

$$\Delta\Delta E_{ass}\left(MoleculeX\right) = E_{ass}\left(WithoutMolX\right) - E_{ass}\left(WithAllMol\right) \quad (2)$$

RESULTS AND DISCUSSION

Phase I: Exploring Modifications.

Starting from C39 (Fig. **1**) seven modified compounds were constructed: MD1 to MD7. These molecules were separated in three groups according to the site where the modification was made (Fig. **2**). To study the binding of these new molecules to Chk1 eighteen residues were selected

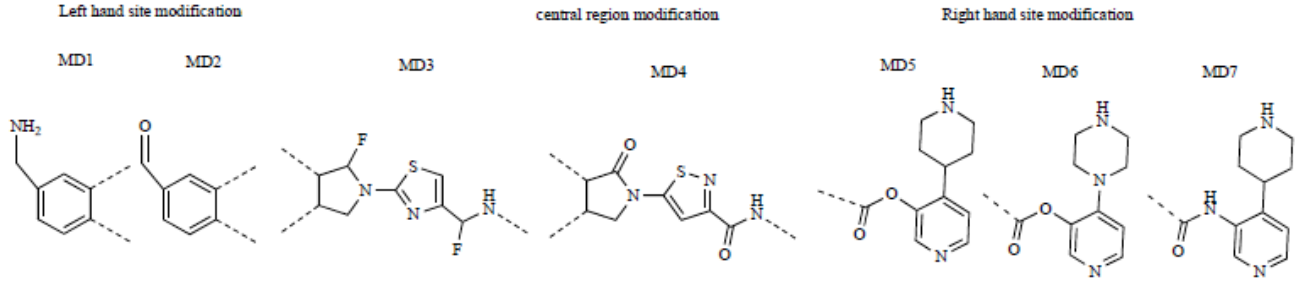

Fig. (2). Phase I modifications; Left hand site: MD1 and MD2; Central Region: MD3 and MD4; Right hand site: MD5, MD6 and MD7.

Table 1. Energetic contributions (in kcal mol^{-1}) of the selected residues to the binding of compounds MD1, MD2, MD3, MD4, MD5, MD6 and MD7 to Chk1.

	Leu 15	Gly 16	Try 20	Val 23	Ala 36	Lys 38	Val 68	Leu 84	Tyr 86	Cys 87	Ser 88	Gly 90	Glu 91	Glu 134	Asn 135	Leu 137	Ser 147	Asp 148	Com-plex
C39	4	0	-1	1	0	19	0	1	4	5	1	0	19	5	1	0	4	-5	-59
MD1	4	0	-1	1	0	18	0	0	3	3	0	1	17	5	0	-1	3	-4	-60
MD2	4	0	0	1	0	18	0	1	5	4	1	-1	20	7	1	0	5	-2	-62
MD3	4	0	-1	1	0	23	0	0	2	1	1	1	15	3	1	-1	3	-6	-45
MD4	4	0	-1	1	0	19	1	2	5	6	0	0	21	7	1	0	5	-2	-71
MD5	3	0	0	2	0	16	0	1	4	5	1	0	16	3	0	0	3	-4	-49
MD6	4	0	0	2	0	18	0	1	4	5	1	1	17	5	1	0	3	-5	-55
MD7	3	0	0	1	0	17	1	1	4	4	1	1	18	4	0	0	4	-3	-54

(Table **1**). In order to compare the obtained $\Delta\Delta E_{ass}$, calculations were also performed for C39. The selection of residues was performed based on our previous work [19] and on the observation of these complexes after energy minimizations.

MD1 modification in the Left hand site (LHS) aimed the creation of strong interactions between this region of the compound and the active site of the enzyme, something absent in C39. The overall binding power for this molecule was slightly better than the C39, but not significantly (Table **1**). The creation of the desired strong interactions was not observed and the two stronger interactions to C39, Glu91 and Lys38, lost some strength. Due to these results MD1 modification was not included in further studies.

As a result of MD1 failure in the creation of a strong interaction between the LHS and the Chk1 active site, MD2 was made by switching the position of the oxygen in this region. The binding energy had an increase of 5% (Table **1**). The repulsive interaction values decreased from -6 kcal mol^{-1} in C39 to -3kcal mol^{-1} in MD2. However, no particularly strong interaction was created or improved significantly. Due to its improvement in the general binding potential and the decreasing in repulsive forces, MD2 was maintained in the study.

Trying to maximize attractive charge effects, the two oxygen atoms in the central region of C39 were replaced by fluorine atoms, creating compound MD3. The general binding energy of the molecule decreased from -59 kcal mol^{-1} in C39 to -45 kcal mol^{-1} in MD3 (Table **1**). The individual contributions of each residue also decreased with the exception of Lys38. We believe that this increment does not outcome from an improvement in the site of Lys38 binding. It was probably the absence of other strong binding points that brought MD3 closer to Lys38.

The creation of MD4 arises from the idea to add H-bond acceptors in the central area of the compound. The alteration was the change of position of the nitrogen in the central ring, maintaining all the connection types. The binding energy of MD4 was the best in this phase of the study, with an improvement of 12 kcal mol^{-1} (Table **1**). Eight of the eighteen residues became more favourable to the binding of MD4. The repulsive energy was reduced from -6 kcal mol^{-1} in C39 to -3 kcal mol^{-1} in MD4. In this binding no new strong interaction formation was observed. Due to the positive reported results MD4 was selected for further studies.

MD5 has two modifications at the Right hand site (RHS), in order to decrease the electronegativity of this region and reduce the repulsion towards negative charged areas in the active site of the enzyme. The objective of these modifications was partly obtained since the repulsions vanished with the exception of one, towards Asp148. Nevertheless the repulsion between the inhibitor and Asp148 decreased from -5 kcal mol^{-1} to -4 kcal mol^{-1} (by comparing C39 with MD5). However, the general binding outcome was poor as the binding energy of MD5 is 17% lower than C39 (Table **1**). To better understand the individual contribution of each modification present in MD5, new molecules were created: MD6 and MD7, each one containing one of MD5 modifications.

MD6 and MD7 showed similar general outcomes with the decrease of the binding energy in less than 10%. New strong interactions were not observed in both cases. Nevertheless MD7 showed a decrease in the repulsive strength similar to MD4 and MD2. The alterations present in these two molecules did not create improvements when alone, but they may do so when conjugated with other modifications.

Phase II: Conjugation of modifications.

At the second phase of this study we created new molecules joining different modifications previously tested. In order to improve the simulation quality, the number of residues in study was increased from eighteen to twenty five (Table **2**). Using MD2, MD4, MD6 and MD7 modifications three molecules were created: MD8, MD9 and MD10 (Fig. **3**). MD8 is the assembling of MD2 and MD4 modifications, MD9 is the association of MD8 with MD6 and at last MD10 is the association of MD8 with MD7. Calculations for C39 with the new selection of residues were also performed in order to have some point of comparison between the results.

Table 2. Energetic contributions (in kcal mol-1) of the selected residues to the binding of compounds MD8, MD9 and MD10 to Chk1.

	C39	MD8	MD9	MD10
Leu 15	4	4	4	4
Gly 16	1	1	1	1
Glu 17	2	4	4	4
Try 20	0	0	0	0
Val 23	1	1	1	1
Ala 36	0	0	0	0
Lys 38	15	14	13	13
Glu 55	-14	-14	-14	-14
Val 68	0	1	1	1
Leu 84	1	2	1	2
Glu 85	-2	-5	-4	-5
Tyr 86	5	6	7	6
Cys 87	5	6	5	6
Ser 88	1	1	0	1
Gly 89	0	0	0	0
Gly 90	0	-1	-1	-1
Glu 91	17	19	23	21
Glu 134	4	7	6	5
Asn 135	1	2	2	1
Leu 136	0	1	1	1
Leu 137	0	0	0	0
Ser 147	4	5	4	4
Asp 148	-2	1	0	-1
Phe 149	1	0	1	1
Gly 150	1	0	0	1
Complex	-48	-57	-58	-51

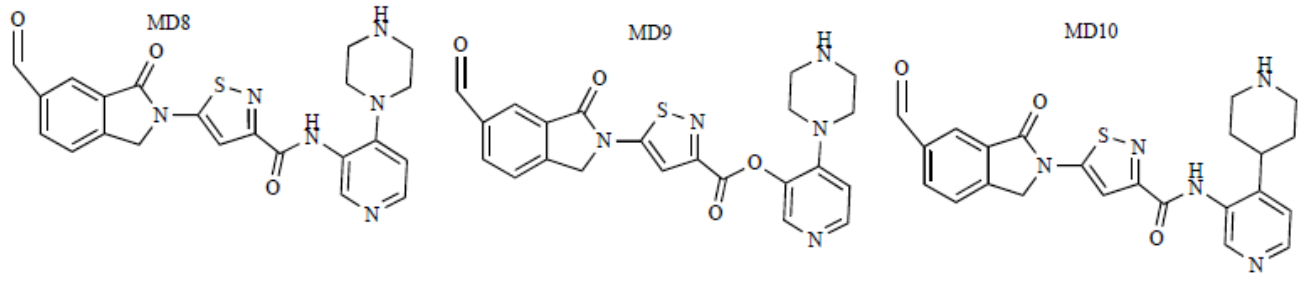

Fig. (3). Phase II modifications: MD8, MD9 and MD10.

For MD8 the binding energy obtained had an improvement of 19% compared to C39. Of the total twenty five residues eleven had an energetic improvement towards MD8. Nevertheless, two strong repulsive forces were verified, to-

wards Glu55 and Glu85 (Table **2**). Glu55 repulsion comes from electrostatic interactions with the rings in the RHS of the molecule and Lys38. The RHS of the compounds is negatively charged, which creates attraction towards Lys38, a positive residue. However Glu55, a residue negatively charged, also attracts Lys38 but for the opposite direction of MD8. Since there is a H-bond between Lys38 and one of the nitrogen atoms in the RHS, Glu55 harms that bond [19]. Glu85 repulsion was intensified in MD8 when compared to C39, what is probably a result of the MD4-based modification.

Although the previous results involving MD6 were not very promising, the conjugation of this alteration with those present in MD2 and MD4 was promising. MD9 differs from MD8 only by the inclusion of MD6 modification, which originated a small improvement in the binding energy. The strong point of this molecule is the enhancement originated in the interaction with Glu91, of 6 kcal mol^{-1}. The other individual energy alterations comparing to MD8 were small and of low significance. With 21% improvement from C39, MD9 has the best result in this study phase (Table **2**).

MD10 had the weakest result in this phase of the study. The inclusion of MD7 modification was detrimental to the binding energy. There was no residue more relevant than others in this decrease, but rather a set of small losses. Nevertheless, the binding energy of MD10 is 6% superior to C39.

CONCLUSIONS

Using a theoretical methodology the improvement potential of seven modifications in the compound 39 was studied. After semi-empirical calculations the modifications selected for further studies were MD2, MD4, MD6 and MD7. Combining these modifications three new molecules were obtained: MD8, MD9 and MD10.

MD8 and MD9 presented significant enhancements in the binding potential to Chk1, with 19% and 21% improvement respectively. Although still presenting higher affinity to Chk1 than C39, MD10 improvement was far more modest, only 6% of the binding energy. When MD8 is compared to C39, there is no big individual improvement but eleven small enhancements that justify the result. MD9 only shows eight individual enhancements but at the same time exhibits a big enhancement in Glu91 binding, of 6 $kcalmol^{-1}$.

The objective of this study was achieved, as starting from C39 was possible to create molecules with increased binding potential to Chk1. The molecules MD8 and MD9 are a valid and promising option for the inhibition of Chk1.

CONFLICT OF INTEREST

The authors confirm that this article content has no conflict of interest.

ACKNOWLEDGEMENTS

Luís Pinto da Silva acknowledges to Fundação para a Ciência e Tecnologia the attribution of a Ph.D. grant (SFRH/BD/76612/2011).

SUPPLEMENTARY MATERIAL

Table **1**: Cartesian coordinates of Checkpoint kinase 1 complexed with MD8.

Table **2**: Cartesian coordinates of Checkpoint kinase 1 complexed with MD9.

REFERENCES

[1] Balakrishnan, K.; Gandhi, V. Protein kinases: emerging therapeutic targets in chronic lymphocytic leukemia. *Expert Opin. Investig. Drugs* **2012**, *21*, 409–23.
[2] Davies, S. P.; Reddy, H.; Caivano, M.; Cohen, P. Specificity and mechanism of action of some commonly used protein kinase inhibitors. *Biochem. J.* **2000**, *351*, 95–105.
[3] Arencibia, J. M.; Pastor-Flores, D.; Bauer, A. F.; Schulze, J. O.; Biondi, R. M. AGC protein kinases: from structural mechanism of regulation to allosteric drug development for the treatment of human diseases. *Biochim. Biophys. Acta* **2013**, *1834*, 1302–21.
[4] Lee, J. C.; Adams, J. L. Inhibitors of serine/threonine kinases. *Curr. Opin. Biotechnol.* **1995**, *6*, 657–61.
[5] Martin, J.; Anamika, K.; Srinivasan, N. Classification of protein kinases on the basis of both kinase and non-kinase regions. *PLoS One* **2010**, *5*, e12460.
[6] Liu, Q.; Sabnis, Y.; Zhao, Z.; Zhang, T.; Buhrlage, S. J.; Jones, L. H.; Gray, N. S. Developing irreversible inhibitors of the protein kinase cysteinome. *Chem. Biol.* **2013**, *20*, 146–59.
[7] Cohen, P.; Alessi, D. R. Kinase drug discovery--what's next in the field? *ACS Chem. Biol.* **2013**, *8*, 96–104.
[8] Zorina, A.; Stepanchenko, N.; Novikova, G. V; Sinetova, M.; Panichkin, V. B.; Moshkov, I. E.; Zinchenko, V. V; Shestakov, S. V; Suzuki, I.; Murata, N.; Los, D. A. Eukaryotic-like Ser/Thr protein kinases SpkC/F/K are involved in phosphorylation of GroES in the Cyanobacterium synechocystis. *DNA Res.* **2011**, *18*, 137–51.
[9] Ma, C. X.; Cai, S.; Li, S.; Ryan, C. E.; Guo, Z.; Schaiff, W. T.; Lin, L.; Hoog, J.; Goiffon, R. J.; Prat, A.; Aft, R. L.; Ellis, M. J.; Piwnica-Worms, H. Targeting Chk1 in p53-deficient triple-negative breast cancer is therapeutically beneficial in human-in-mouse tumor models. *J. Clin. Invest.* **2012**, *122*, 1541–1552.
[10] Dai, Y.; Grant, S. New insights into checkpoint kinase 1 in the DNA damage response signaling network. *Clin. Cancer Res.* **2010**, *16*, 376–83.
[11] Tian, K.; Rajendran, R.; Doddananjaiah, M.; Krstic-Demonacos, M.; Schwartz, J.-M. Dynamics of DNA damage induced pathways to cancer. *PLoS One* **2013**, *8*, e72303.
[12] Grabauskiene, S.; Bergeron, E. J.; Chen, G.; Chang, A. C.; Lin, J.; Thomas, D. G.; Giordano, T. J.; Beer, D. G.; Morgan, M. A; Reddy, R. M. CHK1 levels correlate with sensitization to pemetrexed by CHK1 inhibitors in non-small cell lung cancer cells. *Lung Cancer* **2013**, *82*, 477–484.
[13] Busch, C.-J.; Kriegs, M.; Laban, S.; Tribius, S.; Knecht, R.; Petersen, C.; Dikomey, E.; Rieckmann, T. HPV-positive HNSCC cell lines but not primary human fibroblasts are radiosensitized by the inhibition of Chk1. *Radiother. Oncol.* **2013**, *108*, 495–9.
[14] Mitchell, J. B.; Choudhuri, R.; Fabre, K.; Sowers, A. L.; Citrin, D.; Zabludoff, S. D.; Cook, J. A. In vitro and in vivo radiation sensitization of human tumor cells by a novel checkpoint kinase inhibitor, AZD7762. *Clin. Cancer Res.* **2010**, *16*, 2076–84.
[15] Borst, G. R.; McLaughlin, M.; Kyula, J. N.; Neijenhuis, S.; Khan, A.; Good, J.; Zaidi, S.; Powell, N. G.; Meier, P.; Collins, I.; Garrett, M. D.; Verheij, M.; Harrington, K. J. Targeted radiosensitization by the Chk1 inhibitor SAR-020106. *Int. J. Radiat. Oncol. Biol. Phys.* **2013**, *85*, 1110–8.
[16] Walton, M. I.; Eve, P. D.; Hayes, A.; Valenti, M.; De Haven Brandon, A.; Box, G.; Boxall, K. J.; Aherne, G. W.; Eccles, S. A.; Raynaud, F. I.; Williams, D. H.; Reader, J. C.; Collins, I.; Garrett, M. D. The preclinical pharmacology and therapeutic activity of the novel CHK1 inhibitor SAR-020106. *Mol. Cancer Ther.* **2010**, *9*, 89–100.
[17] Thompson, R.; Eastman, A. The cancer therapeutic potential of Chk1 inhibitors: how mechanistic studies impact on clinical trial design. *Br. J. Clin. Pharmacol.* **2013**, *76*, 358–69.

[18] Huang, X.; Cheng, C. C.; Fischmann, T. O.; Duca, J. S.; Richards, M.; Tadikonda, P. K.; Reddy, P. A.; Zhao, L.; Siddiqui, M. A.; Parry, D.; Davis, N.; Seghezzi, W.; Wiswell, D.; Shipps, G. W. Structure-based design and optimization of 2-aminothiazole-4-carboxamide as a new class of CHK1 inhibitors. *Bioorg. Med. Chem. Lett.* **2013**, *23*, 2590–4.

[19] Araújo, P. M. M.; Pinto da Silva, L.; Esteves da Silva, J. C. G. Comparative theoretical study of the binding of potential cancer-treatment drugs to Checkpoint kinase 1. *Chem. Phys. Lett.* **2014**, *591*, 273–276.

[20] Case, D. A.; Cheatham, T. E.; Darden, T.; Gohlke, H.; Luo, R.; Merz, K. M.; Onufriev, A.; Simmerling, C.; Wang, B.; Woods, R. J. The Amber biomolecular simulation programs. *J. Comput. Chem.* **2005**, *26*, 1668–1688.

[21] Duan, Y.; Wu, C.; Chowdhury, S.; Lee, M. C.; Xiong, G.; Zhang, W.; Yang, R.; Cieplak, P.; Luo, R.; Lee, T.; Caldwell, J.; Wang, J.; Kollman, P. A point-charge force field for molecular mechanics simulations of proteins based on condensed-phase quantum mechanical calculations. *J. Comput. Chem.* **2003**, *24*, 1999–2012.

[22] Yanai, T.; Tew, D. P.; Handy, N. C. A new hybrid exchange?correlation functional using the Coulomb-attenuating method [CAM-B3LYP]. *Chem. Phys. Lett.* **2004**, *393*, 51–57.

[23] M. J. Frisch, G. W. Trucks, H. B. Schlegel, G. E. Scuseria, M. A. Robb, J. R. Cheeseman, G. Scalmani, V. Barone, B. Mennucci, G. A. Petersson, H. Nakatsuji, M. Caricato, X. Li, H. P. Hratchian, A. F. Izmaylov, J. Bloino, G. Zheng, J. L. Sonnenberg, M. Hada, M. Ehara, K. Toyota, R. Fukuda, J. Hasegawa, M. Ishida, T. Nakajima, Y. Honda, O. Kitao, H. Nakai, T. Vreven, J. A. Montgomery, Jr., J. E. Peralta, F. Ogliaro, M. Bearpark, J. J. Heyd, E. Brothers, K. N. Kudin, V. N. Staroverov, R. Kobayashi, J. Normand, K. Raghavachari, A. Rendell, J. C. Burant, S. S. Iyengar, J. Tomasi, M. Cossi, N. Rega, J. M. Millam, M. Klene, J. E. Knox, J. B. Cross, V. Bakken, C. Adamo, J. Jaramillo, R. Gomperts, R. E. Stratmann, O. Yazyev, A. J. Austin, R. Cammi, C. Pomelli, J. W. Ochterski, R. L. Martin, K. Morokuma, V. G. Zakrzewski, G. A. Voth, P. Salvador, J. J. Dannenberg, S. Dapprich, A. D. Daniels, O. Farkas, J. B. Foresman, J. V. Ortiz, J. Cioslowski, and D. J. Fox, Gaussian 09, Revision A.02. *Gaussian Inc Wallingford CT*, 2009, *34*, Wallingford CT.

[24] Wang, J.; Wolf, R. M.; Caldwell, J. W.; Kollman, P. A.; Case, D. A. Development and testing of a general amber force field. *J. Comput. Chem.* **2004**, *25*, 1157–1174.

[25] Phillips, J. C.; Braun, R.; Wang, W.; Gumbart, J.; Tajkhorshid, E.; Villa, E.; Chipot, C.; Skeel, R. D.; Kalé, L.; Schulten, K. Scalable molecular dynamics with NAMD. *J. Comput. Chem.* **2005**, *26*, 1781–802.

[26] Essmann, U.; Perera, L.; Berkowitz, M. L.; Darden, T.; Lee, H.; Pedersen, L. G. A smooth particle mesh Ewald method. *J. Chem. Phys.* **1995**, *103*, 8577–8593.

[27] Stewart, J. J. P. Optimization of parameters for semiempirical methods V: Modification of NDDO approximations and application to 70 elements. *J. Mol. Model.* **2007**, *13*, 1173–1213.

[28] Anisimov, V. M.; Cavasotto, C. N. Quantum Mechanical Binding Free Energy Calculation for Phosphopeptide Inhibitors of the Lck SH2 Domain. *J. Comput. Chem.* **2011**, *1*, 1–8.

[29] Dubey, K. D.; Ojha, R. P. Binding free energy calculation with QM/MM hybrid methods for Abl-Kinase inhibitor. *J. Biol. Phys.* **2011**, *37*, 69–78.

[30] Nunthaboot, N.; Tanaka, F.; Kokpol, S.; Chosrowjan, H.; Taniguchi, S.; Mataga, N. Quantum mechanical study of photoinduced charge transfer in FMN binding protein. *J. Phys. Chem. B* **2008**, *112*, 15837–15843.

[31] Xiong, Y.-Z.; Chen, P.-Y. ONIOM DFT/PM3 calculation on the interaction between STI-571 and abelson tyrosine kinase. *J. Mol. Model.* **2008**, *14*, 1083–1086.

[32] Pinto da Silva, L.; Vieira, J.; Esteves da Silva, J. C. G. Comparative theoretical study of the binding of luciferyl-adenylate and dehydroluciferyl-adenylate to firefly luciferase. *Chem. Phys. Lett.* **2012**, *543*, 137–141.

Received: March 20, 2014 Revised: July 14, 2014 Accepted: July 25, 2014

Chapter 4 - Theoretical Analysis of the Binding of Potential Inhibitors to Protein Kinases MK2 and MK3

In the work Theoretical Analysis of the Binding of Potential Inhibitors to Protein Kinases MK2 and MK3 the planning, the bibliographic research, all the calculations and the text writing was performed by Pedro Araújo. The supervisor, revision of the manuscript, suggestions of improvement and corrections were added by the authors Luis Pinto Silva and Professor Joaquim Esteves da Silva. The document has not yet published version. The supplementary information of this document can be seen in Appendix 3.

In this work we report our observations of the ATP binding site of MK2 and MK3.

Theoretical Analysis of the Binding of Potential Inhibitors to Protein Kinases MK2 and MK3

Pedro M.M. Araújo, Luís Pinto da Silva e Joaquim C.G. Esteves da Silva*

Centro de Investigação em Química, Departamento de Química e Bioquímica, Faculdade de Ciência da Universidade do Porto, R. Campo Alegre 687, 4169-007 Porto, Portugal.

*Corresponding author: Joaquim C.G. Esteves da Silva, E-mail: jcsilva@fc.up.pt; Tel.: 351 226082869; Fax: 351 226082959.

Abstract

MK2 (or MAPKAPK2) was already known for its role in the inflammatory response, however recent studies indicate the involvement of this protein kinase in the DNA damage response mechanism. Within its kinase family MK3 shows a high degree of similarity to MK2.

In this article we report a theoretical study of the binding of two molecules, 05B and P4O, to MK2 and MK3. The data here obtained clarifies which are the most relevant residues in the binding of potential inhibitors to these kinases and the contribution of the binding site water molecules.

Keywords

Cell cycle checkpoints; DNA damage response (DDR); Enzyme-Inhibitor Interactions; MK2; MK3; Semi-empirical calculations.

1. Introduction

The DNA damage response (DDR) can be divided into two main kinase-based-pathways, ATM (Ataxia telangiectasia mutated) and ATR (Ataxia telangiectasia and Rad3-related) with the downstream effectors Chk2 (Checkpoint kinase 2) and Chk1 (Checkpoint kinase 1) respectively. Those pathways are capable of critically influence the cell cycle checkpoints [1,2]. Checkpoints are cellular mechanisms able to respond when the conditions to the progression of the cycle are not ideal, for instance if there is DNA damage. Resulting from the activation of the checkpoints the cell cycle can be stalled in late G1 (start checkpoint), before mitosis (G2/M) or before sister-chromatid separation (M phase). This time gap gives the cell the time needed for the DNA repair mechanisms to act, or if the damage is too severe initiating the apoptotic process [1,3,4]. Protein p53 is a key factor in G1 checkpoint, however it is usually mutated or inactivated in human tumours. Without p53 G1 checkpoint is lost, increasing the importance of M and G2/M checkpoints in the protection of DNA stability.

Downstream from ATM and ATR was identified the p38/MK2 pathway as the third kinase-based mechanism to take part in DDR. The Yaffe group reported the finding of two G2/M checkpoint events in p53-deficient cells, spatially and temporally distinct. The one mediated by Chk1 occur in the nucleus while the event mediated by MK2 (or MAPKAPK2) is more delayed and took place in the cytoplasm [1]. This enzyme was already known to take part in the inflammatory response due to its presence in the synthesis of inflammatory cytokines and tumour necrosis factor α (TNFα) [3,5]. Morandell *et al.* created an animal model in which was possible to simultaneously generate MK2-expressing and MK2-deficient tumours, showing that in the absence of p53 MK2 is essential to the survival of NSCLC (non-small cell lung cancer) tumours [4]. Kooper *et al.* reported that the impairment in the DNA replication caused by gemcitabine (used in chemotherapy) and Chk1 was stopped by MK2. Making this protein in the first cellular effector whose deletion leads to the progression of DNA replication under unfavourable conditions [6].

The inhibition of G2/M checkpoint in p53-deficient tumour cells would increase the DNA instability rapidly, creating catastrophic mitotic events that would lead to the death of those cells [3]. Checkpoint kinase 1 emerged as a target to this purpose since it takes part in G2/M checkpoint. The search for Chk1 inhibitors is in an advanced state with some molecules already in clinical trials [3,7]. However, with the recent findings in this field [1,2,4,8] there is strong evidence that MK2 needs to be inhibited in order to stop G2/M checkpoint. The development of compounds targeting MK2 inhibition has been slowed due to the absence of a high resolution 3D structures of this enzyme. Since the binding domains of MK2 and MK3 have high similarity it was proposed the usage of MK3, that has published 3D structures with higher resolution, as a model to understand the binding of small molecules to MK2 [5].

In the present work we theoretically evaluated the ATP binding site characteristics of MK2 and MK3 when bond to two different ligands: 05B and P4O (Fig. 1), through semi-empirical calculations in an implicit

solvent. The purpose of our study is to obtain relevant information about the binding mode of potential inhibitors to these two kinases, which may help create novel and more specific inhibitors.

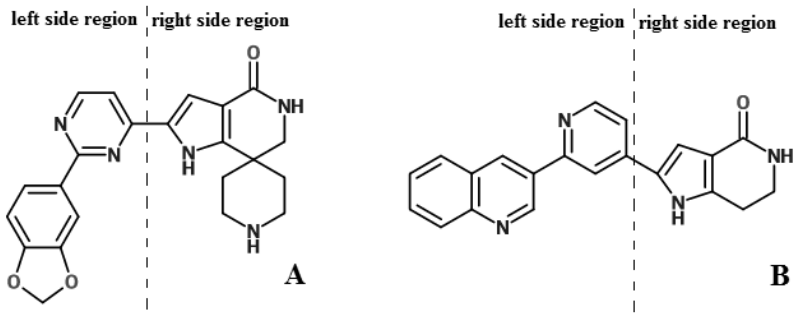

Figure 1: Two dimensional representation of A: Molecule 05B; B: Molecule P4O.

2. Theoretical Methods

The PDB ID of the 3D structures used in this study were 3R2B [9] for MK2 bond to 05B, 2JBP [10] for MK2 bond to P4O, 3R1N [9] for MK3 bond to 05B and 3FHR [5] for MK3 bond to P4O. Each complex was study with and without the water molecules from the crystallography structure, deleting the information about those molecules in the PDB file before energy minimizations.

The hydrogen atoms, the missing atoms, and TIP3P water molecules up to 15 Å were added by the LEAP module of the AMBER suite of programs [11]. The ff03 force field was used for intramolecular interactions [12]. Due to the high number of atoms present in the molecules P4O and 05B their geometries were obtained with the CAM-B3LYP/6-31G method [13]. The geometry optimizations were made with the GAUSSIAN09 software package [14]. The CAM-B3LYP/6-31G obtained geometries were used in the parameterization of the ligands with the ANTECHAMBER module of AMBER and the general AMBER force field [15]. The parameterization was made by performing a CAM-B3LYP/6-311G (d,p) single point energy calculation, at the CAM-B3LYP/6-31G geometries.

Three phases of energy minimizations were performed for each enzyme–ligand complex, using the Not (just) Another Molecular Dynamics program (NAMD) molecule dynamic code with AMBER potential functions, parameters, and the file formats. The two initial minimizations had 30 000 steps each, in the first all the non-water atoms were fixated while in the second the remaining atoms were fixated but not the water atoms. The third minimization had 45 000 steps and none atoms fixated [16]. In this process, the Particle Mesh Ewald method was used to include the long-range interactions [17].

After the energy minimizations protocol the Root-mean-square deviations (RMSD) between the atom positions of the PDB structures and the new obtained positions were calculated. The deviations values indicated that MK2 structures were more rearranged than those involving MK3. Nevertheless, the largest rearrangements occurred in regions away from the binding site not affecting its characteristics (Supplementary Information Figure 1 to 4). These results were expected since MK2 structures had a lower resolution. The RMSD values obtained were 2.17 Å for 3R2B, 1.64 Å for 2JBP, 1.18Å for 3R1N and 1.14Å for 3FHR. The deviation of each residue in the four different structures can be observed in the Supplementary Information (Graphic 1 to 4). Note that the residues numeration in the graphics does not correspond to the PDB file, residue number 1 corresponds to the first residue in the file and so on.

In the end of the energy minimizations process, one selection of binding site residues were withdrawn from the complexes bond to 05B and another for those bond to P4O. For 05B the selected residues were: Leu52, Lys69, Lys73, Met118, Met121, Glu122, Glu170, Asn171, Thr186, Asp187 and the two water molecules in the binding site for MK3 (Fig. 2A); and: Leu72, Lys89, Lys93, Met138, Leu141, Asp142, Glu190, Asn191, Thr206 and Asp207 for MK2 (Fig. 2B). For P4O the selected residues were: Leu50, Lys73, Cys120, Met121, Glu122, Glu170, Asn171, Lys177, Thr186, Asp187 and the two water molecules in the binding site for MK3 (Fig. 2C); and: Leu70, Lys93, Cys140, Leu141, Asp142, Glu190, Asn191, Lys197, Thr206, Asp207 and the water molecule in the binding site for MK2 (Fig. 2D). The selections were made based in our observation of the binding sites and based on the reports of published 3D structures of MK2 and MK3 [5,9,10].

The energies of association of the ligands with the two enzymes were estimated through single point energy calculations with the semi-empirical method PM6, with the implicit solvent diethyl ether in the SMD solvation model [18].

To assess the binding energy for each complex (ΔE_{ass}), three calculations were performed (Eq.(1)): PM6 single point energy calculations on the model composed by the ligand and all the chosen active site residues ($E_{complex}$); PM6 single point energy calculations on a model including only the chosen active site molecules (E_{enzyme}); PM6 single point calculations on the ligand (E_{ligand}). After the calculation of ΔE_{ass} for each complex, the energetic contribution to the ΔE_{ass} of each active site molecule was evaluated. To estimate the contribution of an active site residue X the energy of association was calculated without the residue X, in the same manner as previously described. By comparing the ΔE_{ass} obtained for the model in the absence of that molecule, with the results obtained with all the active site molecules present, it is possible to get a quantitative picture of the contribution of each molecule to the associating energy of the ligands ($\Delta\Delta E_{ass}$, Eq. (2)). The removal of the molecules that contribute favourably to the interaction of the ligands with the active site will lead to less stable complexes and consequently to more positive $\Delta\Delta E_{ass}$. The family of PM_x methods was used due to the very high number of atoms present in these models, and due to its use in previous studies where interaction/ binding energies were calculated [19–23]. The single point energy calculations were performed with the GAUSSIAN 09 program package [14].

$$\Delta E_{ass} = E_{complex} - (E_{enzyme} + E_{ligand})$$ (Equation 1)

$$\Delta\Delta E_{ass}(MoleculeX) = \Delta E_{ass}(Without\ MolX) - \Delta E_{ass}(With\ All\ Mol)$$ (Equation 2)

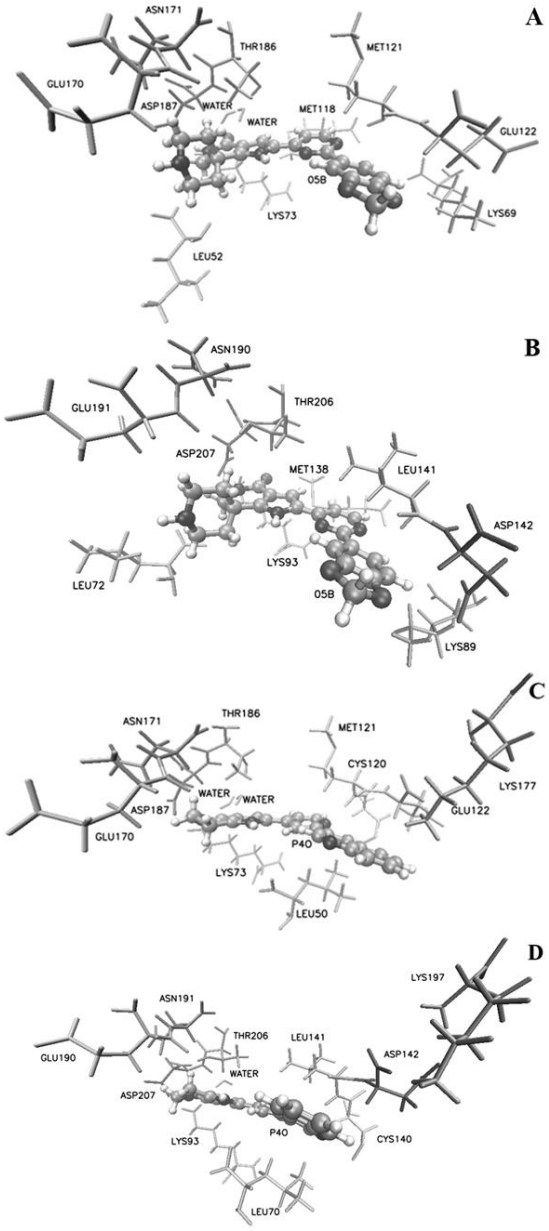

Figure 2. A: Schematic representation of 05B and the selected residues from MK3 (3R1N structure); B: Schematic representation of 05B and the selected residues from MK2 (3R2B structure); C: Schematic representation of P4O and the selected residues from MK3 (3FHR structure); D: Schematic representation of P4O and the selected residues from MK2 (2BJP structure).

3. Results and Discussion

In this study four sets of complexes were analysed, two for MK2 and two for MK3. The mentioned protein kinases were observed when bond to two different ligands, P4O and 05B. Molecule 05B was achieved in a structure-based lead identification study performed by researchers of Merck Laboratories starting from P4O, resulting in the improvement of potency and others properties as solubility and increased stability in human and rat liver [9].

In order to determine the contribution from the binding site water molecules all the complexes were studied with and without those molecules from the original crystallography data, complex 05B-MK2 was the exception since it did not have those molecules.

3.1. 05B binding mode

In order to study the binding of 05B with MK3 and MK2 ten residues from the binding site were selected. The two water molecules in the binding site of the MK3 crystallography structure were also included, which were absent in the MK2 data (Table 1).

3.1.1. MK3

In the binding of 05B to MK2 the residues Lys73 and Asp187 had a significant contribution with 7 Kcal mol^{-1} each. Was also verified a smaller but yet relevant contribution from residue Thr186 (Table 1). The Lys73 amine group creates an N-H•••O H-bond to the oxygen in the right side region of 05B, a strong interaction that justifies the $\Delta\Delta E_{ass}$ value for this residue (Fig. 3A). Asp187 interacts with 05B and the water molecule 2. The carboxyl site of this residue is the acceptor in an H-bond with the left region of 05B, while its amine group possibly creates an H-bond to the water molecule 2 (Fig. 3B). However, the results obtained in the absence of the water molecules indicate the interaction of this residue with water molecules have a low or null significance (Table 1).Thr186 does not interact directly with 05B but this residue is able to create an interaction with water molecule 2 (Fig. 3C). This idea is supported by the decrease in the binding energy of this threonine without the binding site water molecules (Table 1). As expected, in the complex without the binding site water molecules, 05B binds less effectively to MK3, which can be inferred due to increment in the ΔE_{aas} value. Note that negative values of ΔE_{aas} mean that the enzyme and the ligand are more stable when in complex than when alone (Eq.1).

3.1.2. MK2

The binding energy observed for the complex 05B-MK2 was inferior to the values observed in the binding of 05B-MK3 and 05B-MK3 without binding site water molecules. All the residues in the study showed a weaker binding energy between 05B and MK2 when compared to the previously reported results for MK3 and this molecule (Table 1). No residue excelled in the binding energy with a major contribution.

The observed binding energy decreases for this complex, which mainly result from position changes of 05B in the MK2 binding site when compared to MK3 but also from the absence of water molecules. These changes possible result from the low resolution of the crystallography data for MK2. Therefore, the binding mode observed for MK3 is probably the closest to the reality.

Table 1. Energetic contribution of each residue in the study in the binding of 05B to: MK3; MK3 without binding site water molecules; and MK2. The symbol – indicates the absence of the molecule in the structure.

		MK3	MK3 w/o water	MK2
ΔE_{ass}		-16	-11	-4
$\Delta\Delta E_{ass}$	Leu 52/72	0	1	1
	Lys 69/89	0	0	-1
	Lys 73/93	7	7	1
	Met 118/138	-1	0	0
	Met 121/Leu141	-1	-1	0
	Glu 122/Asp 142	1	1	1
	Glu 170/190	1	1	2
	Asn 171/191	1	1	1
	Thr 186/206	2	0	0
	Asp 187/207	7	6	3
	Water 1	-1	-	-
	Water 2	5	-	-

3.2. P4O Binding mode

P4O is a structure with known high affinity towards MK2, with an IC50 value of 8.5 nM. [10], increasing the interest to study this binding of this molecule to MK3.

3.2.1. MK3

Similarly to what was observed for the 05B-MK3 complex, Lys73 and Asp187 were also the most relevant residues for the binding of P4O to this kinase. Two other residues, Glu170 and Thr186, showed non negligible contributions to the creation of P4O-MK3 complex (Table 2). The interactions of Lys73, Thr186 and Asp187 with P4O are very similar to what was previously mentioned for the interaction of these residues with 05B. Although repulsive energies may act in Asp187 as suggested by other authors [5] according to our results the H-bond in which this residue takes part have a superior impact. Glu170 interacts with the same region of P4O that Lys73 but in opposite side, with a weak H-bond: C-H•••O (Fig. 3E). Our results did not indicate the existence of an H-bond to Met121 as previously reported [5], since the energetic contribution of this residue is negligible. Deleting the binding site water molecules reduced the binding energy for the complex and residues Thr186 and Asp187, similarly to what was observed for their equivalents in the 05B-MK3 complex (Table 1 and 2). Thus corroborates the hypothesis of these residues interacting with water molecules. We were unable to find evidence of a bridged water bond to Leu50 as previously proposed by the authors of the crystallography structure [5].

3.2.2. MK2

To study the interactions between MK2 and P4O the 2JBP structure was selected over 2JBO as the second contains a crystallization artefact, a phosphate group in the binding region [10]. The MK2-P4O complex showed a very distinct behaviour to what was observed for the same enzyme bond to 05B, but very similar to the complex MK3-P4O (Table 1 and 2). However, the binding of P4O to MK2 have some differences from what was described for MK3. Residue Glu190 (equivalent to Glu170 in MK3) showed a small increment in the binding energy, which results from the improvement in interaction previously reported of this residue and not from the creation of new interactions. Lys93 has a small decrease in the binding energy of low or negligible relevance.

On the other hand, after the deletion of the binding site water molecules complex P4O-MK2 showed a different behaviour from P4O-MK3 complex due to a conformational change that decreased the binding energy of residue Asp207 (equivalent to Asp187 in MK3) (Fig. 3F).

Table 2. Energetic contribution of each residue in the study in the binding of P4O to: MK3; MK3 without binding site water molecules; MK2; and MK2 without binding site water molecules. The symbol – indicates the absence of the molecule in the structure

		3FHR	3FHR w/o water	2JBP	2JBP w/o water
ΔE_{ass}		-17	-14	-17	-12
$\Delta\Delta E_{ass}$	Leu 50/70	0	0	1	1
	Lys 73/93	8	7	6	7
	CYS 120/140	0	1	0	1
	Met 121/Leu141	-1	-1	0	1
	Glu 122/Asp142	0	1	0	-1
	Glu 170/190	2	2	4	3
	Asn 171/191	1	1	1	0
	Lys 177/197	-1	-1	0	0
	Thr 186/206	2	0	2	1
	Asp 187/207	7	5	7	2
	Water 1	-1	-	0	-
	Water 2	4	-	-	-

Studying the interaction of MK2 and MK3 with 05B Barf *et al.* reported the existence of one residue that differed in the binding site of those two enzymes, with a negligible contribution to the binding. In our work we studied two distinct residues in the two enzymes binding sites, Met121/Leu141 (MK3/MK2) and Glu122/Asp142 (MK3/MK2). Through our energy calculations these two residues showed to be of low relevance in the binding of 05B (Table 1). The same authors [9] suggested the possibility of H-bonds to Met121 (MK3) and Leu141(MK2), which looks very unlikely after our analysis (Table 1). We agree with Barf and co-workers [9] in the hypothesis that the absence of binding site water molecules in MK2 structure (PDBID: 3R2B) is a consequence of limitations in the crystallography process and the binding site of MK2 is similar to MK3 in this aspect.

When studying the binding of P4O to MK2 and MK3 Cheng *et al*. [5] reported two residues that differed in the binding site of the two kinases, having low relevance for the bindings. Our results favour this idea since the binding energies of residues Met121/Leu144 (MK3/MK2) and Glu122/Asp142 (MK3/MK2) towards P4O are small (Table 2).

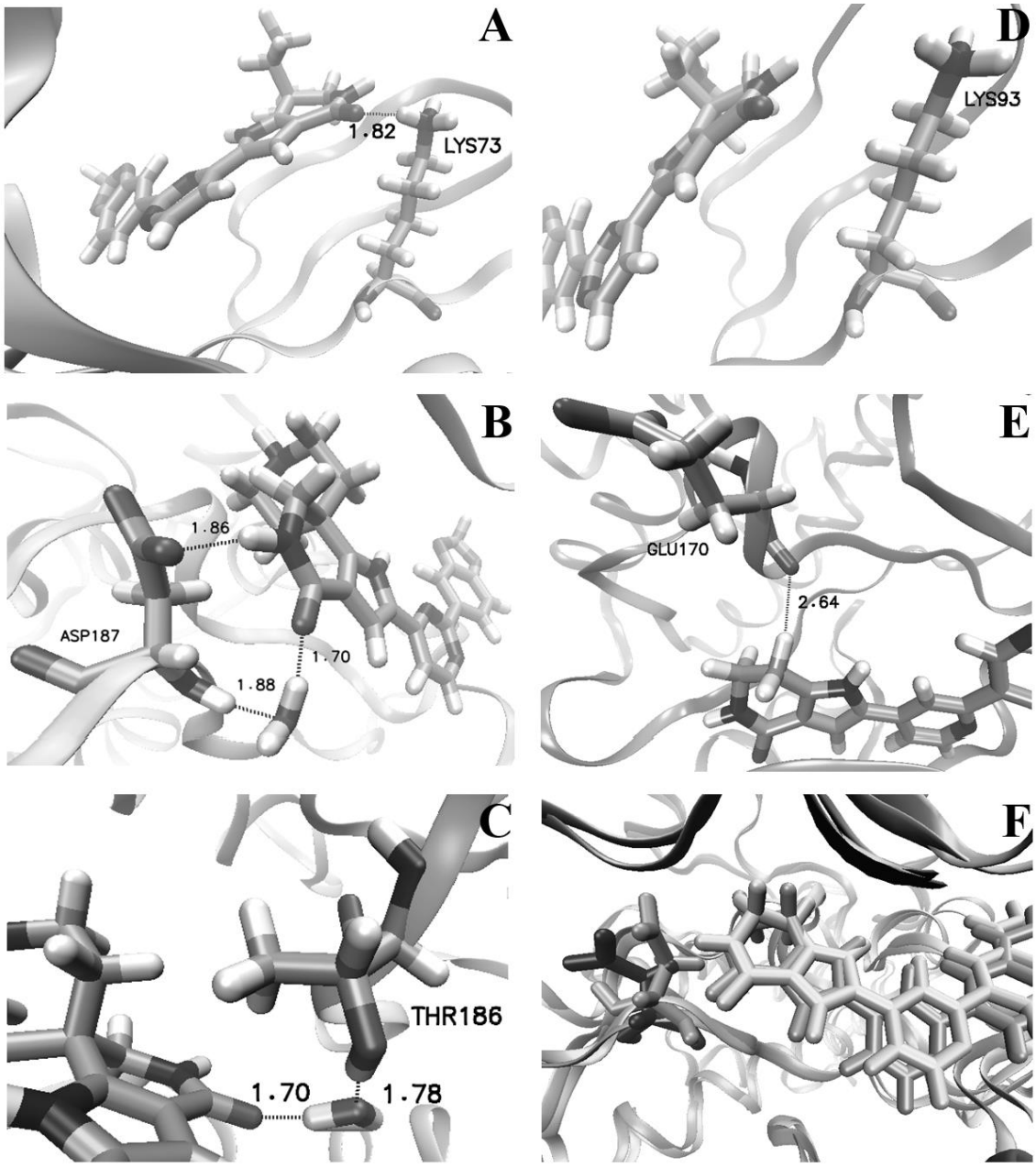

Figure 3. Three dimensional representation of key interactions; A: H-bond created between residue Lys73 and molecule 05B, enzyme MK3; B: Interactions created between residue Asp187, molecules 05B and water molecule 2, enzyme MK3; C: H-bond created between residue Thr186 and water molecule 2 and the interaction of this molecule with 05B, enzyme MK3; D: Representation demonstrating the absence of the H-bond between Lys93 and 05B in the complex with MK2; E: Interaction between Glu170 and P4O, enzyme MK3; F: Demonstration of the conformational changes of residue Asp207 verified after binding site water molecules depletion in the complex P4O-MK2, at light grey the Asp207 from the complex with binding site water molecules, at dark grey Asp207 from the complex without binding site water molecules.

4. Conclusions

From our calculations is evident that without binding site water molecules the binding potential of both molecules, 05B and P4O, decreases. This is justified by the bonds created between these potential inhibitors and the water molecules. Nevertheless, the contribution of the bonds with water molecules has low significance. The Water molecule 1 does not contribute positively to the creation of the enzyme-inhibitor complex while the Water molecule 2 does interact with several residues of both kinases. From our results it is not expected that an improvement protocol targeting the bonds to the water molecules result in a major improvement in the inhibition of MK2 and MK3.

As previously stated 05B resulted from an improvement process of P4O. However, the binding energies here obtained indicate that the complex 05B-MK3 is equally or slightly less stable than P4O-MK3. One of the main causes of that result is the contribution of the residues Glu170/Glu190 (MK3/MK2), verified in MK2 but absence in MK3. For this reason one of the possible improvements for inhibitors that target MK3 is the creation of a strong interaction with Glu170.

The residues Lys73/Lys93 (MK3/MK2) and Asp187/Asp207 (MK3/MK2) had the most significant positive contribution to the formation of all the complexes. The bonds with those residues need to be maintained or improved in order to create successful MK2/MK3 inhibitors. The residue Thr186/Thr206 (MK3/MK2) had an inferior but yet relevant positive contribution, thus becoming another potential target of improvement in the creation of inhibitors to these protein kinases.

Acknowledgment

A Ph.D. Grant to Luís Pinto da Silva (SFRH/BD/76612/2011), attributed by FCT, is also acknowledged.

Supplementary Information

Figure 1: Three dimensional representation of ligand 05B bond to MK2 before and after energy minimizations.

Figure 2: Three dimensional representation of ligand P4O bond to MK2 before and after energy minimizations.

Figure 3: Three dimensional representation of ligand 05B bond to MK3 before and after energy minimizations.

Figure 4: Three dimensional representation of ligand P4O bond to MK3 before and after energy minimizations.

Graphic 1: RMSD values for the 3R2B structure (05B bond to MK2).

Graphic 2: RMSD values for the 2JBP structure (P4O bond to MK2).

Graphic 3: RMSD values for the 3R1N structure (05B bond to MK3).

Graphic 4: RMSD values for the 3FHR structure (P4O bond to MK3).

Table 1: Cartesian coordinates of MK3 bound to 05B.

Table 2: Cartesian coordinates of MK3 bound to 05B without binding site water molecules.

Table 3: Cartesian coordinates of MK2 bound to 05B.

Table 4: Cartesian coordinates of MK3 bound to P4O.

Table 5: Cartesian coordinates of MK3 bound to P4O without binding site water molecules.

Table 6: Cartesian coordinates of MK2 bound to P4O.

Table 7: Cartesian coordinates of MK2 bound to P4O without binding site water molecules.

References

[1] Reinhardt, H. C.; Hasskamp, P.; Schmedding, I.; Morandell, S.; van Vugt, M. A. T. M.; Wang, X.; Linding, R.; Ong, S. E.; Weaver, D.; Carr, S. A.; *et al.* DNA Damage Activates a Spatially Distinct Late Cytoplasmic Cell-Cycle Checkpoint Network Controlled by MK2-Mediated RNA Stabilization. Mol. Cell, **2010**, 40, 34–49.

[2] Höpker, K.; Hagmann, H.; Khurshid, S.; Chen, S.; Schermer, B.; Benzing, T.; Reinhardt, H. C. Putting the Brakes on p53-Driven Apoptosis. Cell Cycle, **2012**, 11, 4122–4128.

[3] Meng, Z.; Ciavarri, J. P.; McRiner, A.; Zhao, Y.; Zhao, L.; Reddy, P. A.; Zhang, X.; Fischmann, T. O.; Whitehurst, C.; Arshad Siddiqui, M. Potency Switch between CHK1 and MK2: Discovery of imidazo[1,2-A]pyrazine- and imidazo[1,2-C]pyrimidine-Based Kinase Inhibitors. Bioorg. Med. Chem. Lett., **2013**, 23, 2863–2867.

[4] Morandell, S.; Reinhardt, H. C.; Cannell, I. G.; Kim, J. S.; Ruf, D. M.; Mitra, T.; Couvillon, A. D.; Jacks, T.; Yaffe, M. B. A Cre-Versible Approach Identifies Synthetic Lethal Interactions between MK2 and p53 in the DNA Damage Response in Vivo. Cell Rep., **2013**, 5, 868–877.

[5] Cheng, R.; Felicetti, B.; Palan, S.; Toogood-Johnson, I.; Scheich, C.; Barker, J.; Whittaker, M.; Hesterkamp, T. High-Resolution Crystal Structure of Human Mapkap Kinase 3 in Complex with a High Affinity Ligand. Protein Sci. , **2010**, 19, 168–173.

[6] Köpper, F.; Bierwirth, C.; Schön, M.; Kunze, M.; Elvers, I.; Kranz, D.; Saini, P.; Menon, M. B.; Walter, D.; Sørensen, C. S.; *et al.* Damage-Induced DNA Replication Stalling Relies on MAPK-Activated Protein Kinase 2 Activity. Proc. Natl. Acad. Sci. U. S. A., **201**3, 110, 16856–16861.

[7] Ma, C.; Cai, S.; Li, S.; Ryan, C. Targeting Chk1 in p53-Deficient Triple-Negative Breast Cancer Is Therapeutically Beneficial in Human-in-Mouse Tumor Models. J. Clin., **2012**, 122, 1541–1552.

[8] Reinhardt, H. C.; Aslanian, A. S.; Lees, J. a; Yaffe, M. B. p53-Deficient Cells Rely on ATM- and ATR-Mediated Checkpoint Signaling through the p38MAPK/MK2 Pathway for Survival after DNA Damage. Cancer Cell, **2007**, 11, 175–189.

[9] Barf, T.; Kaptein, A.; De Wilde, S.; Van Der Heijden, R.; Van Someren, R.; Demont, D.; Schultz-Fademrecht, C.; Versteegh, J.; Van Zeeland, M.; Seegers, N.; *et al.* Structure-Based Lead Identification of ATP-Competitive MK2 Inhibitors. Bioorganic Med. Chem. Lett., **2011**, 21, 3818–3822.

[10] Hillig, R. C.; Eberspaecher, U.; Monteclaro, F.; Huber, M.; Nguyen, D.; Mengel, A.; Muller-Tiemann, B.; Egner, U. Structural Basis for a High Affinity Inhibitor Bound to Protein Kinase MK2. J. Mol. Biol., **2007**, 369, 735–745.

[11] Case, D. A.; Cheatham, T. E.; Darden, T.; Gohlke, H.; Luo, R.; Merz, K. M.; Onufriev, A.; Simmerling, C.; Wang, B.; Woods, R. J. The Amber Biomolecular Simulation Programs. J. Comput. Chem., **2005**, 26, 1668–1688.

[12] Duan, Y.; Wu, C.; Chowdhury, S.; Lee, M. C.; Xiong, G.; Zhang, W.; Yang, R.; Cieplak, P.; Luo, R.; Lee, T.; *et al.* A Point-Charge Force Field for Molecular Mechanics Simulations of Proteins Based on Condensed-Phase Quantum Mechanical Calculations. J. Comput. Chem., **2003**, 24, 1999–2012.

[13] Yanai, T.; Tew, D. P.; Handy, N. C. A New Hybrid Exchange-correlation functional using the Coulomb-Attenuating Method (CAM-B3LYP). Chem. Phys. Lett., **2004**, 393, 51–57.

[14] Frisch, M. J.; Trucks, G. W.; Schlegel, H. B.; Scuseria, G. E.; Robb, M. A.; Cheeseman, J. R.; Scalmani, G.; Barone, V.; Mennucci, B.; Petersson, G. A.; *et al.* Gaussian 09, Revision A.02. Gaussian Inc Wallingford CT, **2009**, 34, Wallingford CT.

[15] Wang, J.; Wolf, R. M.; Caldwell, J. W.; Kollman, P. A.; Case, D. A. Development and Testing of a General Amber Force Field. J. Comput. Chem., **2004**, 25, 1157–1174.

[16] Phillips, J. C.; Braun, R.; Wang, W.; Gumbart, J.; Tajkhorshid, E.; Villa, E.; Chipot, C.; Skeel, R. D.; Kalé, L.; Schulten, K. Scalable Molecular Dynamics with NAMD. J. Comput. Chem., **2005**, 26, 1781–1802.

[17] Essmann, U.; Perera, L.; Berkowitz, M. L.; Darden, T.; Lee, H.; Pedersen, L. G. A Smooth Particle Mesh Ewald Method. J. Chem. Phys., **1995**, 103, 8577–8593.

[18] Stewart, J. J. P. Optimization of Parameters for Semiempirical Methods V: Modification of NDDO Approximations and Application to 70 Elements. J. Mol. Model., **2007**, 13, 1173–1213.

[19] Dubey, K. D.; Ojha, R. P. Binding Free Energy Calculation with QM/MM Hybrid Methods for Abl-Kinase Inhibitor. J. Biol. Phys., **2011**, 37, 69–78.

[20] Nunthaboot, N.; Tanaka, F.; Kokpol, S.; Chosrowjan, H.; Taniguchi, S.; Mataga, N. Quantum Mechanical Study of Photoinduced Charge Transfer in FMN Binding Protein. J. Phys. Chem. B, **2008**, 112, 15837–15843.

[21] Xiong, Y.-Z.; Chen, P.-Y. ONIOM DFT/PM3 Calculation on the Interaction between STI-571 and Abelson Tyrosine Kinase. J. Mol. Model. 2008, 14, 1083–1086.

[22] Pinto da Silva, L.; Vieira, J.; Esteves da Silva, J. C. G. Comparative Theoretical Study of the Binding of Luciferyl-Adenylate and Dehydroluciferyl-Adenylate to Firefly Luciferase. Chem. Phys. Lett., **2012**, 543, 137–141.

[23] Araújo, P. M. M.; Pinto da Silva, L.; Esteves da Silva, J. C. G. Comparative Theoretical Study of the Binding of Potential Cancer-Treatment Drugs to Checkpoint Kinase 1. Chem. Phys. Lett., **2014**, 591, 273–276.

Chapter 5 – Conclusions and Future perspectives

5.1. – Conclusion

As a final remark a comparison between the proposed objectives at the beginning of this work and the obtained results shall be made.

Initially, the focus of this work was Checkpoint kinase 1. The studies targeting this enzyme are in the chapter 4 of this document in two published papers. The first document reports our observations studying the binding mode of two molecules to Chk1, Compound 39 and Compound 40. Within this work it was successfully observed the major characteristics in the formation of those enzyme-inhibitor complex, the most relevant residues for those bindings and it was concluded that Compound 39 has the best inhibitory potential of the two. The second publication consists of our attempts to improve the binding potential of Compound 39-like molecules to Chk1. We created 10 novel molecules in a two-phased study based in the knowledge obtained in the previously referred publication. The obtained result was an improvement around 20% in the binding energy of Modified molecules 8 and 9 (MD8 and MD9) to Checkpoint kinase 1, when compared to Compound 39 in the same conditions. After a general look it is safe to say that the objectives proposed in the study of Chk1 were accomplished. We successfully understood the binding of potential inhibitors to this kinase and it was also possible to create compounds with improved binding energy to the enzyme.

The study of MK2 naturally emerged after entering in contact with research that reports second G2/M checkpoint event in the p53-deficient tumors cells, as stated in the introduction of this document. Similarly to the Chk1 work, in the study of MK2 the objective was also to understand the binding mode of potential inhibitors to this enzyme. However this task was expected to be more challenging than Chk1 due to the absence of high resolution crystallography structures. In order to understand the binding mode of potential inhibitors to MK2 another enzyme, MK3, was added to the study. MK3 belongs to the same family of kinases and has a high degree of similarity to MK2. With the inclusion of MK3 in the study, which has crystallography structures with better resolution, the understanding of MK2's ATP binding site could possibly be enrich. Our studies in MK2 and MK3 resulted in the work presented in the Chapter 4, were it is described the most relevant residues for the binding of two different molecules, P4O and 05B, to these two kinases. In this report special attention was given to the role of water molecules in the ATP binding sites. Within this chapter the binding mode of potential inhibitors to MK2 and MK3 was defined as previously proposed in the objectives, the description of the central role of some water molecules, the differences between MK2 and MK3 and also the core similarities between the most relevant residues for both protein kinases was observed.

5.2. - Future perspectives

The work here reported can be seen as a starting point, a gathering of data which can be used for future studies targeting the inhibition of Chk1 or MK2.

The information about the key features of Chk1 binding site here obtained can be used in any project targeting this enzyme. In the second published work (topic 3.2.) presented in Chapter 3 we tried to perform the suggestions of improvement that resulted from our first work (topic 3.1.). Although we achieved some improvement the possibility of best solutions for those questions still exist. The study of more molecules with known Chk1 inhibitor potential would be a good source of information for further improvement. The inhibitory potential of the molecules proposed by us (topic 3.2.) needs to be verified experimentally, if those results show to be promising those molecules may enter in more advanced testing.

The data obtained for MK2 and MK3 showed impressive similarities, which indicates that compound with high specificity for only one of this kinases will be hard to obtain. The usage of MK3 as MK2 model already happens and in the absence of structures with better resolution for MK2 this appears to be a reasonable solution. Further studies should consider the possibility to use induced mutagenesis of MK3 to create an ATP binding site without differences from MK2, either computational or experimental.

Since Chk1 and MK2 have been reported with a central function in p53-deficient tumor cells would be interesting to study compound with inhibitory potential for both of them. One molecule with the ability to successful inhibit Chk1 and MK2 would be extremely competitive in the field of cancer treatment for chemosensitization and radiosensitization.

Appendix 1

Comparative Theoretical Study of the Binding of Potential Cancer-Treatment Drugs to Checkpoint Kinase 1

Pedro M.M. Araújo, Luís Pinto da Silva and Joaquim C.G. Esteves da Silva*

Centro de Investigação em Química, Departamento de Química e Bioquímica, Faculdade de Ciências da Universidade do Porto, R. Campo Alegre 687, 4169-007 Porto, Portugal.
*Corresponding Author: Joaquim C.G. Esteves da Silva; Email: jcsilva@fc.up.pt; Tel.: +351 226082869; Fax: +351 22608259;

Table 1: Cartesian coordinates of Checkpoint kinase 1 complexed with compound 39.

Table2: Cartesian coordinates of Checkpoint kinase 1 complexed with compound 40.

Table1: Cartesian coordinates of Checkpoint kinase 1 complexed with compound 39			
N	**2.10900**	**-8.08600**	**-11.99600**
H	**1.09900**	**-8.12300**	**-11.95500**
C	**2.80200**	**-7.32400**	**-10.94600**
H	**3.86900**	**-7.26100**	**-11.17100**
C	**2.20700**	**-5.89600**	**-10.93900**
H	**1.17800**	**-5.96000**	**-10.58600**
H	**2.76500**	**-5.29300**	**-10.22100**
C	**2.20700**	**-5.16300**	**-12.30500**
H	**1.63200**	**-5.74300**	**-13.02700**
C	**1.52100**	**-3.79700**	**-12.17700**
H	**1.48400**	**-3.30600**	**-13.14900**
H	**0.50100**	**-3.92100**	**-11.81800**
H	**2.07400**	**-3.16700**	**-11.48600**
C	**3.62600**	**-4.96700**	**-12.85900**
H	**3.58300**	**-4.42400**	**-13.80400**
H	**4.23200**	**-4.40200**	**-12.14900**
H	**4.09600**	**-5.93200**	**-13.04400**
C	**2.70400**	**-7.99800**	**-9.55700**
O	**3.36700**	**-7.56700**	**-8.61300**
H	**2.38900**	**-7.72300**	**-12.90700**
N	**1.89400**	**-9.06100**	**-9.44100**
H	**1.42000**	**-9.35600**	**-10.28500**
C	**1.63100**	**-9.83800**	**-8.21700**
H	**2.44500**	**-10.54700**	**-8.07400**
H	**1.61900**	**-9.17900**	**-7.34800**
C	**0.31000**	**-10.61800**	**-8.26000**
O	**-0.65900**	**-10.16600**	**-8.87400**
H	**0.23200**	**-11.52500**	**-7.77300**
N	**-5.91800**	**-12.50200**	**-3.51100**
H	**-4.91000**	**-12.54000**	**-3.49500**
C	**-6.53800**	**-11.26000**	**-4.01600**
H	**-7.51900**	**-11.14800**	**-3.55000**
C	**-5.68000**	**-10.07000**	**-3.54900**
H	**-6.13800**	**-9.14600**	**-3.90000**
H	**-5.72900**	**-10.04000**	**-2.45900**
C	**-4.21500**	**-10.06200**	**-3.96500**
C	**-3.84200**	**-9.83300**	**-5.30600**
H	**-4.59600**	**-9.68000**	**-6.06400**
C	**-2.48200**	**-9.77600**	**-5.66600**
H	**-2.19400**	**-9.59800**	**-6.69000**
C	**-1.48100**	**-9.92700**	**-4.68300**
O	**-0.16700**	**-9.83200**	**-5.02400**
H	**0.40400**	**-9.91700**	**-4.25800**
C	**-1.85000**	**-10.15700**	**-3.34000**
H	**-1.08900**	**-10.25900**	**-2.58000**
C	**-3.21200**	**-10.22800**	**-2.98700**

H	-3.48700	-10.37800	-1.95200
C	-6.80300	-11.22200	-5.54300
O	-7.17900	-10.17500	-6.07200
H	-6.27000	-13.29100	-4.05300
H	-6.66500	-12.07000	-6.11400
N	-2.79800	-8.72800	-10.05500
H	-2.01200	-9.27100	-9.69500
C	-2.54600	-7.31300	-10.40600
H	-3.50400	-6.83400	-10.59600
C	-1.86500	-6.55000	-9.24400
H	-0.90700	-7.02800	-9.02900
C	-1.60600	-5.06700	-9.56200
H	-1.10900	-4.59200	-8.71600
H	-0.96000	-4.97000	-10.43100
H	-2.54700	-4.55200	-9.75800
C	-2.73600	-6.60600	-7.97700
H	-2.21800	-6.10700	-7.16400
H	-3.69100	-6.10800	-8.15300
H	-2.92200	-7.63500	-7.67700
C	-1.69200	-7.23500	-11.68300
O	-0.73600	-7.99100	-11.83300
H	-3.18400	-9.20600	-10.86900
H	-1.92300	-6.54600	-12.41500
N	-6.53700	-4.72600	-11.49000
H	-7.36400	-4.17600	-11.71000
C	-6.71700	-5.90300	-10.61000
H	-5.78800	-6.47400	-10.58000
C	-7.01600	-5.40700	-9.17900
H	-6.23800	-4.69300	-8.90100
H	-7.97100	-4.87900	-9.17200
C	-7.04600	-6.52200	-8.11500
H	-7.86200	-7.21400	-8.33000
H	-6.10300	-7.07000	-8.14500
C	-7.24200	-5.92900	-6.70700
H	-6.46000	-5.19000	-6.52500
H	-8.20800	-5.42200	-6.65800
C	-7.17800	-7.00100	-5.60700
H	-8.00700	-7.70400	-5.73900
H	-6.24300	-7.55700	-5.70900
N	-7.24600	-6.38300	-4.25800
H	-6.49800	-5.70900	-4.13000
H	-8.12100	-5.86700	-4.12700
H	-7.18000	-7.05300	-3.49900
C	-7.81300	-6.84200	-11.17300
O	-8.88600	-6.38800	-11.57100
H	-5.83200	-4.11300	-11.08100
H	-7.64200	-7.85900	-11.21500
N	-14.52400	-4.20800	-2.22700

H	-14.48800	-5.20500	-2.38600
C	-13.37200	-3.40400	-2.66400
H	-13.03900	-2.78500	-1.82900
C	-12.21700	-4.34500	-3.04500
H	-12.02800	-5.01200	-2.20300
H	-12.51700	-4.94100	-3.90500
C	-10.92300	-3.59600	-3.38800
H	-11.10000	-2.96800	-4.26100
H	-10.64600	-2.95600	-2.55000
C	-9.75400	-4.52900	-3.70700
O	-9.82500	-5.74100	-3.42100
O	-8.74200	-4.04500	-4.25800
C	-13.74400	-2.46500	-3.82400
O	-13.39000	-1.28900	-3.79400
H	-15.36900	-3.83600	-2.66100
H	-14.28900	-2.82200	-4.62500
N	-4.04600	5.45800	-4.52800
H	-3.75300	4.78800	-3.80700
C	-4.33200	4.93400	-5.88900
H	-3.68500	5.47200	-6.58400
C	-3.99300	3.42300	-6.01200
H	-4.42700	2.90700	-5.15400
C	-4.51800	2.73600	-7.28700
H	-4.29300	1.67100	-7.24100
H	-5.59900	2.83600	-7.37100
H	-4.04900	3.15900	-8.17200
C	-2.46800	3.22100	-5.97500
H	-2.23700	2.16000	-6.06100
H	-2.00000	3.75100	-6.80600
H	-2.05200	3.59500	-5.04100
C	-5.79200	5.18400	-6.30700
O	-6.72500	4.73400	-5.63900
H	-4.86500	5.96500	-4.19200
H	-5.99200	5.73500	-7.15600
N	-7.02600	0.89600	-12.65400
H	-6.40800	0.39100	-13.28300
C	-6.37700	1.62500	-11.55100
H	-7.11200	2.23900	-11.03200
C	-5.79400	0.58100	-10.56900
H	-5.10700	-0.05500	-11.12800
H	-5.21000	1.09800	-9.80600
C	-6.81400	-0.33200	-9.85300
H	-7.46100	-0.80800	-10.58800
C	-6.06800	-1.44400	-9.10500
H	-6.78300	-2.10100	-8.60800
H	-5.48000	-2.03600	-9.80700
H	-5.40500	-1.00600	-8.35900
C	-7.68800	0.45100	-8.86400

H	-8.37600	-0.22700	-8.35900
H	-7.06200	0.94300	-8.11900
H	-8.27000	1.20100	-9.39200
C	-5.26200	2.58300	-12.02300
O	-4.71600	2.44200	-13.11700
H	-7.71100	0.24700	-12.26700
H	-4.96800	3.35800	-11.40800
N	-1.67000	3.82300	-12.47600
H	-2.02700	4.38200	-13.23300
C	-0.32700	3.24400	-12.62500
H	-0.33500	2.24600	-12.18500
C	-0.01000	3.10200	-14.12500
H	-0.67700	2.35300	-14.55200
H	-0.23000	4.05200	-14.61500
C	1.42200	2.70700	-14.45500
C	1.97700	1.52700	-13.92200
H	1.37600	0.88400	-13.29600
C	3.31400	1.18000	-14.20100
H	3.74000	0.27700	-13.78900
C	4.10100	2.00300	-15.03500
O	5.39500	1.66600	-15.29300
H	5.83300	2.27200	-15.90900
C	3.54100	3.17700	-15.58600
H	4.13600	3.81300	-16.22500
C	2.20900	3.52900	-15.28700
H	1.79000	4.43800	-15.69500
C	0.76300	4.05500	-11.89200
O	0.84700	5.27500	-12.03300
H	-2.33200	3.07200	-12.28100
N	1.63500	3.35200	-11.16200
H	1.48100	2.35400	-11.08900
C	2.72400	3.90900	-10.35100
H	2.65700	5.00000	-10.31400
C	2.53100	3.36000	-8.92900
H	2.52100	2.26900	-8.96300
H	3.36100	3.68100	-8.30000
S	0.96900	3.97400	-8.23000
H	0.83600	3.07800	-7.24600
C	4.10600	3.55500	-10.94500
O	4.70600	2.53300	-10.61100
N	4.62800	4.37900	-11.85400
H	4.10700	5.22500	-12.08500
C	5.85900	4.06100	-12.61300
H	5.74500	3.05800	-13.02300
C	6.04000	5.01100	-13.81000
H	6.80300	4.60200	-14.47400
H	5.10100	5.05900	-14.36100
O	6.41500	6.32800	-13.43300

H	7.38600	6.34800	-13.25400
C	7.16100	4.00400	-11.79400
O	8.13600	3.40600	-12.25600
H	7.21800	4.46000	-10.87000
N	7.18300	2.32100	-8.92100
H	6.41600	2.66500	-9.48900
C	7.06000	0.96000	-8.37300
H	6.22500	0.46100	-8.86000
H	7.97600	0.40500	-8.58000
C	6.79500	0.88700	-6.86800
O	6.31100	1.83800	-6.26200
H	7.34400	2.97300	-8.15300
N	7.08700	-0.27300	-6.27800
H	7.48900	-0.99600	-6.85000
C	6.91000	-0.56200	-4.84400
H	5.94100	-0.18100	-4.52500
C	6.92400	-2.08600	-4.61300
H	7.83200	-2.49900	-5.05500
H	6.94300	-2.28400	-3.54000
C	5.69400	-2.78800	-5.21600
H	4.81100	-2.50600	-4.64300
H	5.55400	-2.45800	-6.24500
C	5.81100	-4.31400	-5.21600
O	6.56100	-4.89900	-4.40700
O	5.14300	-4.97500	-6.04400
C	7.97500	0.11800	-3.96000
O	9.13900	0.24600	-4.34800
H	7.70900	0.47200	-3.02800
N	5.20100	-3.05400	1.15300
H	5.29800	-3.53300	2.05100
C	4.70300	-3.85800	0.02300
H	5.43700	-3.81300	-0.78300
C	4.54500	-5.33100	0.44400
H	3.72700	-5.42700	1.16100
H	4.26900	-5.89400	-0.44700
C	5.80800	-5.99200	1.01300
H	5.81600	-7.02800	0.67400
H	6.69600	-5.50600	0.60900
C	5.85500	-5.98900	2.54300
O	5.66100	-4.91600	3.15200
O	6.07900	-7.08000	3.12700
C	3.35800	-3.37800	-0.56200
O	3.03200	-3.71400	-1.69800
H	4.59700	-2.24100	1.27400
N	2.56100	-2.61400	0.19400
H	2.89100	-2.36700	1.11800
C	1.27200	-2.04600	-0.24600
H	0.95000	-2.54700	-1.16100

C	0.21900	-2.33800	0.84300
H	0.55900	-1.92400	1.79300
H	-0.71900	-1.84800	0.58100
C	-0.08900	-3.82600	1.02700
O	0.12500	-4.66600	0.16100
N	-0.61300	-4.20600	2.17400
H	-0.79100	-3.54000	2.91700
H	-0.92200	-5.16200	2.27600
C	1.36500	-0.53400	-0.59800
O	0.34800	0.12500	-0.84400
H	2.28800	-0.07400	-0.62700
N	3.26300	2.49800	-3.06800
H	2.43700	3.03100	-2.82300
C	3.77200	2.67000	-4.43800
H	4.62100	2.00800	-4.59500
C	2.64200	2.28400	-5.41200
H	1.85100	3.02300	-5.31600
H	3.03200	2.33700	-6.42700
C	2.00600	0.89400	-5.21700
H	1.64200	0.78600	-4.19400
C	0.80000	0.77700	-6.15000
H	0.31000	-0.18200	-5.98600
H	0.08600	1.57000	-5.93400
H	1.12300	0.85900	-7.18600
C	3.00500	-0.22800	-5.51200
H	2.49600	-1.18800	-5.46500
H	3.44300	-0.10100	-6.50300
H	3.79100	-0.22100	-4.76100
C	4.26400	4.10700	-4.71100
O	4.05300	4.99100	-3.88100
H	4.00800	2.71600	-2.40600
H	4.76700	4.32600	-5.58500
N	-2.19100	1.78000	-1.71200
H	-1.57500	1.43200	-0.99000
C	-2.90200	0.74900	-2.49800
H	-3.79200	1.18300	-2.95600
C	-1.99500	0.24700	-3.63500
H	-2.59700	-0.31600	-4.34800
H	-1.57500	1.11000	-4.15200
O	-0.93300	-0.58100	-3.18700
H	-0.61800	-0.26600	-2.32300
C	-3.39700	-0.44100	-1.64700
O	-2.99500	-0.58600	-0.49200
H	-2.87300	2.41300	-1.29400
N	-4.28800	-1.25500	-2.22900
H	-4.57700	-1.02000	-3.17400
C	-4.98700	-2.41800	-1.65700
H	-5.52900	-2.87800	-2.48500

C	-4.02200	-3.50400	-1.13200
H	-3.24400	-3.67000	-1.88000
H	-3.53900	-3.16400	-0.21500
C	-4.72400	-4.84600	-0.85700
O	-5.97600	-4.92200	-0.92100
O	-4.01900	-5.85400	-0.61800
C	-6.04500	-2.02600	-0.60700
O	-5.73300	-1.75500	0.55300
H	-7.03900	-1.99000	-0.88300
N	2.40000	-5.15700	-5.26300
C	1.55100	-6.04000	-6.06600
C	0.29900	-6.33600	-5.24200
N	-0.42500	-5.09700	-4.91100
C	0.43500	-4.11100	-4.23900
C	1.73800	-3.87200	-5.00400
C	-1.79500	-5.09700	-4.69400
C	-2.37400	-6.11600	-3.95000
C	-3.73900	-6.14700	-3.76700
N	-4.55400	-5.22600	-4.30600
C	-3.99700	-4.22700	-5.01800
C	-2.62800	-4.12600	-5.25500
N	-2.07100	-3.13800	-6.14800
C	-2.62000	-2.03000	-6.71400
C	-1.71600	-1.40900	-7.71100
C	-2.08400	-0.29600	-8.42400
N	-0.44100	-1.86500	-8.01300
C	0.15800	-1.08200	-8.92000
S	-0.83400	0.23500	-9.48700
N	1.48300	-1.28400	-9.28800
C	2.20900	-0.53600	-10.15800
C	2.28500	-2.37500	-8.68400
C	3.63300	-2.18300	-9.32700
C	3.58000	-1.11000	-10.18000
C	4.70000	-0.70500	-10.90400
C	5.89200	-1.41900	-10.74100
C	5.93600	-2.51700	-9.87400
C	4.80200	-2.91500	-9.15300
O	7.06200	-1.05100	-11.37700
C	7.19100	0.17400	-12.14300
O	-3.73000	-1.60800	-6.42900
O	1.82100	0.42100	-10.79900
H	3.28100	-4.97700	-5.76700
H	2.08500	-6.97200	-6.26800
H	1.28700	-5.56100	-7.01400
H	0.60900	-6.82400	-4.31600
H	-0.34600	-7.01500	-5.80300
H	0.69100	-4.47900	-3.24500
H	-0.08700	-3.15800	-4.12500

H	**2.39900**	**-3.23600**	**-4.41100**
H	**1.51700**	**-3.37600**	**-5.95100**
H	**-1.76200**	**-6.88400**	**-3.49100**
H	**-4.21300**	**-6.93800**	**-3.19200**
H	**-4.71100**	**-3.52700**	**-5.44400**
H	**-1.12500**	**-3.35100**	**-6.42800**
H	**-3.00600**	**0.27200**	**-8.40500**
H	**1.85200**	**-3.35000**	**-8.92800**
H	**2.34400**	**-2.24500**	**-7.60200**
H	**4.64300**	**0.15800**	**-11.55800**
H	**6.87000**	**-3.06000**	**-9.76800**
H	**4.83200**	**-3.77000**	**-8.47400**
H	**8.22100**	**0.26800**	**-12.49600**
H	**6.94800**	**1.03100**	**-11.50900**
H	**6.51600**	**0.14500**	**-13.00400**

Table2: Cartesian coordinates of Checkpoint kinase 1 complexed with compound 40

N	**3.90400**	**-7.66700**	**-10.43700**
H	**2.90300**	**-7.69500**	**-10.56300**
C	**4.43500**	**-6.78600**	**-9.38500**
H	**5.45300**	**-6.48500**	**-9.64000**
C	**3.53300**	**-5.53500**	**-9.31300**
H	**2.50700**	**-5.85200**	**-9.12000**
H	**3.85000**	**-4.92900**	**-8.46400**
C	**3.55900**	**-4.65100**	**-10.58000**
H	**3.37300**	**-5.26900**	**-11.45900**
C	**2.43900**	**-3.60300**	**-10.50500**
H	**2.51400**	**-2.90200**	**-11.33400**
H	**1.47100**	**-4.09700**	**-10.56000**
H	**2.50600**	**-3.05200**	**-9.57100**
C	**4.91700**	**-3.95300**	**-10.75700**
H	**4.88400**	**-3.28200**	**-11.61500**
H	**5.16300**	**-3.37600**	**-9.86600**
H	**5.69900**	**-4.69200**	**-10.93000**
C	**4.53500**	**-7.49700**	**-8.02100**
O	**5.46900**	**-7.24600**	**-7.25300**
H	**4.34100**	**-7.42000**	**-11.32500**
N	**3.59700**	**-8.41700**	**-7.75600**
H	**2.85400**	**-8.51100**	**-8.43400**
C	**3.58400**	**-9.34200**	**-6.61300**
H	**4.54700**	**-9.84900**	**-6.55300**
H	**3.46800**	**-8.77600**	**-5.68800**
C	**2.46700**	**-10.39100**	**-6.67200**
O	**1.40500**	**-10.14500**	**-7.24900**

H	2.60500	-11.31100	-6.22500
N	-3.64600	-12.59800	-0.94400
H	-2.78300	-12.16800	-0.64300
C	-4.61600	-11.73100	-1.64000
H	-5.57800	-11.80500	-1.13100
C	-4.10200	-10.28500	-1.50600
H	-4.79900	-9.60500	-1.99100
H	-4.08500	-10.01700	-0.44800
C	-2.71400	-10.07500	-2.09100
C	-2.53300	-9.89400	-3.47800
H	-3.38700	-9.85100	-4.13800
C	-1.23300	-9.79400	-4.01300
H	-1.08200	-9.66900	-5.07200
C	-0.11100	-9.86600	-3.16100
O	1.14300	-9.75200	-3.66700
H	1.79900	-9.85100	-2.96300
C	-0.29300	-10.02800	-1.77200
H	0.56500	-10.06500	-1.11500
C	-1.59200	-10.13300	-1.24300
H	-1.72600	-10.26100	-0.18000
C	-4.87600	-12.06000	-3.13200
O	-5.69700	-11.39000	-3.76200
H	-3.42800	-13.39700	-1.54000
H	-4.36800	-12.83100	-3.59300
N	-1.05000	-9.05000	-8.12200
H	-0.15300	-9.45800	-7.85200
C	-1.03500	-7.71600	-8.75200
H	-2.03300	-7.49600	-9.12400
C	-0.63700	-6.59000	-7.76400
H	0.40100	-6.74100	-7.45800
C	-0.75500	-5.20600	-8.42700
H	-0.48100	-4.42800	-7.71600
H	-0.08500	-5.13500	-9.28100
H	-1.77900	-5.03600	-8.76500
C	-1.51400	-6.58400	-6.50000
H	-1.18500	-5.79000	-5.83200
H	-2.55700	-6.41800	-6.76900
H	-1.42500	-7.52900	-5.96700
C	-0.05900	-7.72400	-9.93400
O	1.10500	-8.09600	-9.78200
H	-1.53500	-9.70100	-8.74000
H	-0.38000	-7.41500	-10.86500
N	-5.03800	-5.77100	-9.80700
H	-5.69200	-4.99500	-9.72800
C	-5.20900	-6.92400	-8.90900
H	-4.24100	-7.40000	-8.78200
C	-5.68200	-6.43600	-7.52800
H	-5.06800	-5.59000	-7.21500

H	-6.71300	-6.09600	-7.61000
C	-5.58900	-7.53000	-6.44800
H	-6.00100	-8.46600	-6.82400
H	-4.54000	-7.69200	-6.19600
C	-6.36700	-7.12200	-5.19000
H	-6.06700	-6.11600	-4.89800
H	-7.43400	-7.11800	-5.41600
C	-6.09600	-8.09300	-4.03400
H	-6.35400	-9.11100	-4.34600
H	-5.02600	-8.07100	-3.80600
N	-6.87000	-7.72300	-2.82200
H	-6.64500	-8.28000	-2.00600
H	-6.72200	-6.76100	-2.53300
H	-7.88300	-7.75300	-2.94700
C	-6.17900	-7.95500	-9.52400
O	-7.30700	-7.61000	-9.88000
H	-4.08900	-5.41100	-9.70100
H	-5.88200	-8.93700	-9.63700
N	-13.64200	-5.27000	0.32200
H	-13.68000	-6.28100	0.23400
C	-12.45500	-4.55300	-0.19100
H	-12.01900	-3.98600	0.63400
C	-11.38200	-5.54000	-0.69400
H	-11.14800	-6.24700	0.10300
H	-11.77700	-6.09300	-1.54800
C	-10.08800	-4.80800	-1.10000
H	-10.30500	-4.09900	-1.89900
H	-9.71600	-4.25000	-0.23900
C	-8.98500	-5.74100	-1.60200
O	-9.29500	-6.78000	-2.22200
O	-7.78400	-5.42300	-1.40700
C	-12.83100	-3.54200	-1.29100
O	-12.44700	-2.37500	-1.20900
H	-14.47500	-4.87400	-0.11300
H	-13.40400	-3.84200	-2.09500
N	-3.62500	4.81200	-2.56700
H	-3.42300	4.17700	-1.78400
C	-3.80000	4.21800	-3.91600
H	-3.20000	4.80000	-4.61800
C	-3.33200	2.74200	-3.99200
H	-3.80300	2.18800	-3.17900
C	-3.71600	2.05200	-5.31600
H	-3.40600	1.01100	-5.27800
H	-4.79400	2.05500	-5.46800
H	-3.23300	2.55000	-6.15700
C	-1.80800	2.64700	-3.82600
H	-1.49000	1.61300	-3.95000
H	-1.31000	3.26100	-4.57800

H	-1.51300	2.98500	-2.83300
C	-5.26900	4.29600	-4.34800
O	-6.14200	3.70200	-3.71200
H	-4.45400	5.36100	-2.34000
H	-5.52900	4.85100	-5.17800
N	-6.12600	-0.04300	-10.50800
H	-5.46600	-0.62500	-11.01800
C	-5.55200	0.74400	-9.40800
H	-6.31700	1.37000	-8.95300
C	-5.00700	-0.26100	-8.36500
H	-4.30700	-0.92200	-8.88000
H	-4.43800	0.27600	-7.60600
C	-6.07700	-1.13000	-7.66400
H	-6.82000	-1.46400	-8.38600
C	-5.43500	-2.38600	-7.06300
H	-6.19400	-2.98900	-6.56400
H	-4.98100	-2.98200	-7.85600
H	-4.66800	-2.10400	-6.34400
C	-6.79600	-0.33800	-6.56200
H	-7.58400	-0.95000	-6.12200
H	-6.08800	-0.05600	-5.78200
H	-7.24300	0.56100	-6.97900
C	-4.42300	1.67600	-9.89500
O	-3.75000	1.38900	-10.88600
H	-6.87900	-0.62800	-10.14500
H	-4.22900	2.55100	-9.38400
N	-0.83200	3.12900	-10.35900
H	-1.10300	3.71700	-11.13900
C	0.52200	2.55600	-10.37600
H	0.44900	1.53700	-9.99800
C	0.98600	2.47700	-11.84200
H	0.29200	1.83700	-12.38400
H	0.90700	3.47800	-12.26900
C	2.39000	1.95500	-12.11600
C	2.90700	0.82800	-11.44100
H	2.30400	0.30300	-10.71500
C	4.21400	0.37500	-11.71500
H	4.62000	-0.47600	-11.18800
C	4.99600	1.02200	-12.69900
O	6.26400	0.60000	-12.96000
H	6.69000	1.13500	-13.65000
C	4.46400	2.12100	-13.40400
H	5.05800	2.61600	-14.15800
C	3.17100	2.58900	-13.10300
H	2.77600	3.44600	-13.63100
C	1.53000	3.30800	-9.47000
O	1.52400	4.54100	-9.36900
H	-1.50900	2.37200	-10.26600

N	2.42300	2.53300	-8.83600
H	2.31700	1.53700	-8.94700
C	3.47300	2.97800	-7.91000
H	3.50600	4.06700	-7.88700
C	3.09200	2.47600	-6.50600
H	2.93500	1.39700	-6.53100
H	3.91100	2.68300	-5.81500
S	1.59000	3.31600	-5.92100
H	1.33400	2.52400	-4.87400
C	4.87900	2.49900	-8.34800
O	5.44400	1.55400	-7.80300
N	5.46500	3.14100	-9.35500
H	4.92200	3.86600	-9.82000
C	6.77400	2.77800	-9.94800
H	6.74000	1.72000	-10.20900
C	7.00200	3.54900	-11.26200
H	7.86700	3.12900	-11.77900
H	6.13200	3.41400	-11.90000
O	7.20100	4.94200	-11.07200
H	8.09400	5.08800	-10.68800
C	8.01100	2.92400	-9.03400
O	9.12800	2.64200	-9.47300
H	7.90300	3.25500	-8.06300
N	7.75700	1.19700	-6.00400
H	7.02800	1.48600	-6.65000
C	7.60800	-0.12200	-5.36300
H	6.86500	-0.70200	-5.90900
H	8.56100	-0.64900	-5.40400
C	7.15500	-0.08400	-3.89900
O	6.59300	0.90000	-3.43300
H	7.85600	1.90700	-5.27900
N	7.40000	-1.17100	-3.16800
H	7.92300	-1.91800	-3.61300
C	7.09300	-1.30400	-1.73100
H	6.10800	-0.88700	-1.52600
C	7.06900	-2.79500	-1.33800
H	8.04400	-3.21400	-1.58400
H	6.92700	-2.87900	-0.26000
C	5.95900	-3.60700	-2.04300
H	4.99100	-3.30300	-1.64200
H	5.96700	-3.38900	-3.11100
C	6.12700	-5.12200	-1.88000
O	7.27800	-5.60100	-1.77100
O	5.12800	-5.87400	-1.91300
C	8.11300	-0.53800	-0.86200
O	9.31700	-0.56600	-1.13700
H	7.78700	0.00200	-0.04500
N	5.21000	-3.19600	3.83500

H	5.24600	-3.65200	4.74700
C	4.72000	-4.01300	2.71500
H	5.43200	-3.95000	1.89100
C	4.61700	-5.48300	3.14800
H	3.87700	-5.59300	3.94000
H	4.26300	-6.05100	2.28700
C	5.95000	-6.10100	3.58400
H	5.91700	-7.15900	3.31800
H	6.76700	-5.64300	3.02400
C	6.24400	-6.00700	5.08300
O	5.83900	-5.03100	5.75700
O	6.92300	-6.93100	5.58900
C	3.34800	-3.58800	2.16300
O	3.05300	-3.86400	1.00600
H	4.64000	-2.35300	3.90600
N	2.49900	-2.92600	2.95500
H	2.80100	-2.70900	3.89600
C	1.20300	-2.37900	2.50200
H	0.88000	-2.90900	1.60400
C	0.15400	-2.63800	3.59900
H	0.50000	-2.21400	4.54200
H	-0.78200	-2.14900	3.33100
C	-0.15000	-4.12300	3.79400
O	0.07700	-4.96400	2.93800
N	-0.65400	-4.50900	4.94600
H	-0.78700	-3.85000	5.70300
H	-0.87900	-5.48500	5.08800
C	1.29500	-0.88500	2.10200
O	0.29600	-0.25200	1.73900
H	2.20900	-0.40800	2.13900
N	3.28200	1.82000	-0.44800
H	2.40500	2.31500	-0.33500
C	3.93000	1.91800	-1.75700
H	4.76300	1.21800	-1.81500
C	2.88400	1.55000	-2.82300
H	2.00800	2.18200	-2.67000
H	3.28500	1.77500	-3.80900
C	2.45000	0.06900	-2.80200
H	2.27400	-0.25800	-1.77600
C	1.13900	-0.07100	-3.57100
H	0.80300	-1.10700	-3.52900
H	0.38000	0.55700	-3.11100
H	1.27900	0.23700	-4.60500
C	3.50900	-0.83800	-3.44300
H	3.15700	-1.86800	-3.45700
H	3.71600	-0.51700	-4.46500
H	4.42400	-0.79900	-2.86300
C	4.51000	3.31900	-1.99900

O	4.12800	4.28500	-1.33900
H	3.93500	2.13400	0.27000
H	5.23100	3.45300	-2.72600
N	-2.17800	1.18600	0.61600
H	-1.64500	0.89300	1.42500
C	-2.76700	0.08400	-0.17600
H	-3.69200	0.41700	-0.64800
C	-1.78700	-0.31600	-1.29100
H	-2.28000	-0.99700	-1.98400
H	-1.50500	0.58100	-1.84100
O	-0.61600	-0.94700	-0.79200
H	-0.41200	-0.60400	0.09400
C	-3.12500	-1.15100	0.68300
O	-2.86200	-1.16400	1.88600
H	-2.91900	1.82100	0.91200
N	-3.74200	-2.17200	0.07500
H	-3.94500	-2.07000	-0.91600
C	-4.19000	-3.43100	0.69800
H	-4.72000	-3.97800	-0.08300
C	-3.00100	-4.32700	1.11100
H	-2.28800	-4.36900	0.28700
H	-2.49200	-3.88200	1.96700
C	-3.42000	-5.76500	1.46900
O	-4.63500	-6.09000	1.42900
O	-2.53900	-6.57600	1.83900
C	-5.22100	-3.21400	1.82700
O	-4.95300	-3.42900	3.01200
H	-6.16600	-2.87800	1.58200
C	5.33500	-4.29300	-5.80300
C	4.03100	-4.57100	-5.37900
C	2.95600	-3.77600	-5.79200
C	3.22600	-2.67700	-6.62000
C	4.50000	-2.44400	-7.04300
C	5.58400	-3.22100	-6.66200
C	4.43200	-1.33500	-7.91500
N	2.44300	-1.70500	-7.19100
N	3.17000	-0.87400	-8.01700
C	1.10500	-1.50300	-6.87200
S	0.35300	-0.05200	-7.41100
C	-1.00500	-0.51200	-6.44900
C	-0.83000	-1.70400	-5.77300
N	0.40600	-2.28400	-6.04400
C	-1.89300	-2.19700	-4.86400
N	-1.61100	-3.43100	-4.40000
C	-2.39600	-4.28100	-3.55900
C	-3.79200	-4.26100	-3.62300
C	-4.55200	-5.10100	-2.81300
C	-3.92000	-6.02800	-1.99200

C	**-2.53400**	**-6.09700**	**-1.95800**
C	**-1.76200**	**-5.21400**	**-2.72600**
N	**-0.39100**	**-5.25800**	**-2.65100**
C	**0.27900**	**-6.55000**	**-2.64300**
C	**0.28500**	**-4.27100**	**-1.82100**
C	**1.75800**	**-4.16100**	**-2.17700**
N	**2.32100**	**-5.50000**	**-2.04200**
C	**1.74300**	**-6.42000**	**-3.00900**
O	**-2.90500**	**-1.59500**	**-4.54600**
H	**6.15300**	**-4.93200**	**-5.47700**
H	**3.86000**	**-5.42300**	**-4.72600**
H	**1.95900**	**-4.03900**	**-5.46000**
H	**6.58600**	**-3.01500**	**-7.03300**
H	**5.23300**	**-0.85100**	**-8.46200**
H	**-1.85100**	**0.16400**	**-6.46300**
H	**-0.72000**	**-3.81700**	**-4.66700**
H	**-4.29400**	**-3.56800**	**-4.29000**
H	**-5.63700**	**-5.02400**	**-2.81900**
H	**-4.49500**	**-6.68900**	**-1.35400**
H	**-2.05600**	**-6.81800**	**-1.29400**
H	**-0.20500**	**-7.20900**	**-3.36000**
H	**0.21300**	**-6.99100**	**-1.64900**
H	**0.20100**	**-4.56500**	**-0.77500**
H	**-0.17900**	**-3.29200**	**-1.94000**
H	**2.25700**	**-3.47500**	**-1.49200**
H	**1.87500**	**-3.80100**	**-3.19900**
H	**3.34200**	**-5.46000**	**-2.17700**
H	**2.23500**	**-7.39000**	**-2.92700**
H	**1.84900**	**-6.03700**	**-4.02500**

Appendix 2

Modelling of Potential Chk1 Inhibitors Aiming for Cancer Treatment

Pedro M.M. Araújo, Luís Pinto da Silva and Joaquim C.G. Esteves da Silva*

Centro de Investigação em Química, Departamento de Química e Bioquímica, Faculdade de Ciências da Universidade do Porto, R. Campo Alegre 687, 4169-007 Porto, Portugal.
*Corresponding Author: Joaquim C.G. Esteves da Silva; Email: jcsilva@fc.up.pt; Tel.: +351 226082869; Fax: +351 22608259;

Table 1: Cartesian coordinates of Checkpoint kinase 1 complexed with MD8.

Table2: Cartesian coordinates of Checkpoint kinase 1 complexed with MD9.

Table 1: Cartesian coordinates of Checkpoint kinase 1 complexed with MD9			
N	**2.54900**	**-8.13900**	**-11.70000**
H	**1.56400**	**-8.36100**	**-11.62000**
C	**3.11600**	**-7.24900**	**-10.67900**
H	**4.18300**	**-7.10300**	**-10.85900**
C	**2.38300**	**-5.89000**	**-10.77500**
H	**1.34600**	**-6.04600**	**-10.47200**
H	**2.83200**	**-5.20300**	**-10.05700**
C	**2.38400**	**-5.21400**	**-12.16600**
H	**1.98200**	**-5.90400**	**-12.90800**
C	**1.46500**	**-3.98700**	**-12.14400**
H	**1.36800**	**-3.58800**	**-13.15100**
H	**0.47300**	**-4.27200**	**-11.80000**
H	**1.86900**	**-3.22100**	**-11.48400**
C	**3.79300**	**-4.79400**	**-12.60600**
H	**3.74300**	**-4.29900**	**-13.57700**
H	**4.22500**	**-4.10700**	**-11.87800**
H	**4.43400**	**-5.67000**	**-12.69800**
C	**2.98700**	**-7.82600**	**-9.25000**
O	**3.55700**	**-7.26600**	**-8.31600**
H	**2.72500**	**-7.74000**	**-12.62200**
N	**2.24300**	**-8.92800**	**-9.07300**
H	**1.82900**	**-9.33700**	**-9.90100**
C	**1.95400**	**-9.57400**	**-7.78000**
H	**2.77500**	**-10.2490**	**-7.53900**
H	**1.90500**	**-8.82800**	**-6.98500**
C	**0.65100**	**-10.3800**	**-7.77400**
O	**-0.3150**	**-10.009**	**-8.44500**
N	**0.61700**	**-11.4720**	**-7.00500**
H	**1.41700**	**-11.6840**	**-6.43000**
C	**-0.4890**	**-12.443**	**-6.97900**
H	**-1.4170**	**-11.874**	**-6.95400**
C	**-0.4990**	**-13.280**	**-8.27400**
H	**-1.4220**	**-13.860**	**-8.31800**
H	**-0.4980**	**-12.605**	**-9.12700**
C	**0.69300**	**-14.2380**	**-8.41500**
H	**1.62200**	**-13.7060**	**-8.20800**
H	**0.59400**	**-15.0590**	**-7.70400**
C	**0.74700**	**-14.7980**	**-9.83200**
O	**-0.2060**	**-15.487**	**-10.26600**
O	**1.69500**	**-14.4940**	**-10.58300**
C	**-0.5060**	**-13.355**	**-5.73600**
O	**0.48400**	**-13.4730**	**-5.00500**
H	**-1.3650**	**-13.880**	**-5.50900**
N	**-5.1370**	**-12.531**	**-2.73300**
H	**-4.1840**	**-12.586**	**-3.05900**
C	**-5.9310**	**-11.357**	**-3.16500**

H	-6.8710	-11.342	-2.61200
C	-5.1610	-10.076	-2.78000
H	-5.7230	-9.2100	-3.12900
H	-5.1510	-10.016	-1.69100
C	-3.7290	-9.9410	-3.28400
C	-3.4470	-9.8210	-4.66300
H	-4.2480	-9.8300	-5.38600
C	-2.1200	-9.6590	-5.10800
H	-1.9050	-9.5590	-6.16100
C	-1.0640	-9.5950	-4.17400
O	0.21700	-9.40800	-4.59500
H	0.81800	-9.29800	-3.85400
C	-1.3430	-9.6970	-2.79400
H	-0.5420	-9.6210	-2.07200
C	-2.6690	-9.8740	-2.35600
H	-2.8760	-9.9300	-1.29600
C	-6.3400	-11.345	-4.66300
O	-6.8740	-10.345	-5.14600
H	-5.6290	-13.382	-3.00500
H	-6.1650	-12.173	-5.25300
N	-2.4970	-8.7700	-9.73700
H	-1.6550	-9.2420	-9.40300
C	-2.3460	-7.4240	-10.33500
H	-3.3210	-7.0990	-10.68700
C	-1.8480	-6.3670	-9.31700
H	-0.7900	-6.5400	-9.11600
C	-2.0160	-4.9440	-9.88300
H	-1.6260	-4.2150	-9.17300
H	-1.4710	-4.8370	-10.81700
H	-3.0710	-4.7340	-10.06600
C	-2.6050	-6.4320	-7.97900
H	-2.2490	-5.6400	-7.32200
H	-3.6760	-6.3050	-8.14400
H	-2.4260	-7.3860	-7.48300
C	-1.3870	-7.4770	-11.53500
O	-0.3060	-8.0490	-11.43500
H	-2.9690	-9.3760	-10.40800
H	-1.6530	-7.0310	-12.42700
N	-2.6570	0.16300	-14.42700
H	-3.1200	0.94300	-13.96200
C	-2.6320	-1.1140	-13.70000
H	-1.9120	-1.7910	-14.16200
C	-2.1680	-0.8290	-12.26400
H	-2.1640	-1.7480	-11.67600
H	-1.1620	-0.4110	-12.26600
H	-2.8350	-0.1060	-11.79200
C	-4.0090	-1.8170	-13.74200
O	-5.0280	-1.1640	-13.95300

H	-1.7010	0.43300	-14.65700
H	-4.0720	-2.8360	-13.59300
N	-6.1560	-5.0020	-11.45100
H	-6.8050	-4.2180	-11.44500
C	-6.4300	-6.1310	-10.53800
H	-5.5050	-6.6880	-10.39100
C	-6.8540	-5.5800	-9.15800
H	-6.1000	-4.8590	-8.83800
H	-7.8010	-5.0510	-9.25400
C	-6.9850	-6.6540	-8.05900
H	-7.7510	-7.3790	-8.33800
H	-6.0320	-7.1740	-7.95500
C	-7.3630	-6.0170	-6.70800
H	-6.6660	-5.2050	-6.49700
H	-8.3680	-5.5940	-6.77400
C	-7.3160	-7.0240	-5.54600
H	-8.0650	-7.8050	-5.70900
H	-6.3310	-7.4990	-5.52900
N	-7.5590	-6.3470	-4.24500
H	-6.8980	-5.5910	-4.09800
H	-8.4830	-5.9120	-4.21500
H	-7.4770	-6.9660	-3.44500
C	-7.4560	-7.1070	-11.16100
O	-8.5060	-6.6960	-11.65600
H	-5.2160	-4.6520	-11.26800
H	-7.2570	-8.1200	-11.16200
N	-14.660	-3.848	-2.36300
H	-14.627	-4.847	-2.51100
C	-13.499	-3.052	-2.79400
H	-13.159	-2.452	-1.94800
C	-12.347	-3.994	-3.18700
H	-12.124	-4.638	-2.33400
H	-12.662	-4.620	-4.02200
C	-11.070	-3.239	-3.58100
H	-11.246	-2.699	-4.51100
H	-10.827	-2.521	-2.79800
C	-9.8800	-4.1750	-3.79200
O	-10.097	-5.334	-4.20100
O	-8.7220	-3.7500	-3.57000
C	-13.858	-2.077	-3.93200
O	-13.495	-0.907	-3.85900
H	-15.498	-3.477	-2.81100
H	-14.399	-2.405	-4.74800
N	-4.0070	5.56100	-4.60800
H	-3.7670	4.90100	-3.85700
C	-4.2840	5.00100	-5.95600
H	-3.6460	5.53100	-6.66600
C	-3.9320	3.48900	-6.03500

H	-4.3520	2.99500	-5.15800
C	-4.4630	2.75300	-7.28100
H	-4.1990	1.69700	-7.22200
H	-5.5470	2.82000	-7.34000
H	-4.0270	3.17000	-8.18500
C	-2.4040	3.31600	-6.00600
H	-2.1510	2.26000	-6.09000
H	-1.9490	3.85100	-6.84200
H	-1.9940	3.70100	-5.07400
C	-5.7470	5.23500	-6.37500
O	-6.6770	4.90100	-5.64200
H	-4.8080	6.11900	-4.31200
H	-5.9510	5.67900	-7.28400
N	-6.7130	0.64000	-12.59500
H	-6.0880	0.12100	-13.20400
C	-6.0720	1.34800	-11.46700
H	-6.8030	1.99200	-10.97800
C	-5.5870	0.27400	-10.46200
H	-4.9680	-0.4360	-11.01200
H	-4.9490	0.74300	-9.71000
C	-6.6920	-0.5200	-9.72800
H	-7.4420	-0.8600	-10.43800
C	-6.0820	-1.7700	-9.08300
H	-6.8500	-2.3210	-8.54000
H	-5.6650	-2.4180	-9.85500
H	-5.2900	-1.4810	-8.39500
C	-7.3860	0.33100	-8.65600
H	-8.1680	-0.2520	-8.16900
H	-6.6630	0.65100	-7.90500
H	-7.8410	1.20900	-9.10900
C	-4.8930	2.26400	-11.88400
O	-4.2840	2.08400	-12.94000
H	-7.4270	0.00800	-12.23100
N	-4.5550	3.23700	-11.02900
H	-5.1380	3.34200	-10.20700
C	-3.4630	4.21300	-11.22500
H	-3.5670	4.62400	-12.22800
C	-3.6300	5.39000	-10.23800
H	-4.6470	5.76300	-10.34700
H	-3.5150	5.04300	-9.21300
C	-2.6500	6.55500	-10.46400
H	-1.6870	6.31200	-10.01300
H	-2.4960	6.70000	-11.53300
C	-3.1900	7.86100	-9.87300
O	-4.1580	8.41500	-10.44300
O	-2.6750	8.34700	-8.83400
C	-2.0560	3.58700	-11.14500
O	-1.5330	3.30800	-10.06700

N	-1.4150	3.39300	-12.30400
H	-1.8970	3.62100	-13.15900
C	-0.0580	2.83600	-12.39000
H	-0.0560	1.91000	-11.81300
C	0.27600	2.47800	-13.84600
H	-0.5830	0 1.98200	-14.29200
H	0.45800	3.39100	-14.41500
C	1.47600	1.55500	-13.97200
C	1.28100	0.16200	-14.00500
H	0.28100	-0.24200	-13.99400
C	2.38500	-0.70800	-14.04100
H	2.24400	-1.77400	-14.05800
C	3.69400	-0.18900	-14.06700
O	4.75300	-1.04100	-14.09400
H	5.59000	-0.58200	-13.97300
C	3.89500	1.20800	-14.04200
H	4.89800	1.60400	-14.05000
C	2.78500	2.07700	-13.99800
H	2.93700	3.14700	-13.96600
C	1.02600	3.75700	-11.79200
O	1.06500	4.95800	-12.05600
N	1.94900	3.16000	-11.03300
H	1.84000	2.16400	-10.89100
C	3.00900	3.83000	-10.27200
H	2.89200	4.91600	-10.32300
C	2.80600	3.38700	-8.81300
H	2.80300	2.29600	-8.75600
H	3.62800	3.75500	-8.20100
S	1.24300	4.04800	-8.15400
H	0.38900	3.57700	-9.08300
C	4.41800	3.49000	-10.81900
O	4.95900	2.41300	-10.57000
N	5.02500	4.39100	-11.59400
H	4.53300	5.26900	-11.76000
C	6.28400	4.13900	-12.34100
H	6.17200	3.20000	-12.88000
C	6.52900	5.23800	-13.38800
H	7.40600	4.97900	-13.98400
H	5.66700	5.27800	-14.05700
O	6.71900	6.52500	-12.81600
H	7.56900	6.56200	-12.31600
C	7.57200	3.95700	-11.51900
O	8.56400	3.46200	-12.06100
N	7.56600	4.31500	-10.23100
H	6.71500	4.73200	-9.86200
C	8.65000	4.04700	-9.27300
H	9.60900	4.02600	-9.79200
H	8.65800	4.83500	-8.52200

C	8.49800	2.71400	-8.53300
O	9.36400	2.36100	-7.73300
N	7.41100	1.97100	-8.77800
H	6.72500	2.34700	-9.42500
C	7.14700	0.65000	-8.19300
H	6.30400	0.19400	-8.70800
H	8.02900	0.02100	-8.31500
C	6.78700	0.69600	-6.70900
O	6.05600	1.57700	-6.27000
N	7.27300	-0.29200	-5.95800
H	7.89900	-0.94500	-6.39800
C	7.00500	-0.48900	-4.52500
H	6.05200	-0.02900	-4.26600
C	6.90800	-1.99600	-4.22600
H	7.78200	-2.49300	-4.65200
H	6.91300	-2.15600	-3.14600
C	5.62300	-2.61200	-4.80000
H	4.77800	-2.28800	-4.19200
H	5.46900	-2.25800	-5.82000
C	5.63700	-4.13800	-4.83300
O	6.51700	-4.78300	-4.22000
O	4.75200	-4.71600	-5.50200
C	8.08200	0.14400	-3.62700
O	9.27000	0.15800	-3.96200
H	7.80600	0.56500	-2.72600
N	5.33200	-3.20400	1.22100
H	5.38300	-3.64100	2.14400
C	4.80400	-4.04300	0.13300
H	5.58300	-4.18200	-0.61800
C	4.40500	-5.42100	0.69400
H	3.65700	-5.30200	1.47700
H	3.92700	-5.98800	-0.10000
C	5.57800	-6.26300	1.21500
H	5.36800	-7.30700	0.97500
H	6.49600	-5.98600	0.69700
C	5.77700	-6.15500	2.72600
O	5.67300	-5.03800	3.27400
O	6.02500	-7.21600	3.35400
C	3.57300	-3.46100	-0.58900
O	3.40300	-3.71000	-1.78000
H	4.77500	-2.35200	1.28600
N	2.71500	-2.71000	0.11500
H	2.95500	-2.51800	1.07900
C	1.44900	-2.14600	-0.39400
H	1.18400	-2.64400	-1.32800
C	0.34500	-2.44000	0.64200
H	0.64700	-2.04700	1.61300
H	-0.5730	-1.9300	0 0.34900

C	-0.0020	-3.9210	0 0.78800
O	0.20900	-4.74300	-0.09700
N	-0.5660	-4.3110	0 1.91400
H	-0.7610	-3.6530	0 2.66000
H	-0.9350	-5.2510	0 1.95300
C	1.52200	-0.62800	-0.71400
O	0.52100	-0.01600	-1.10400
N	2.69100	0.00000	-0.53000
H	3.48200	-0.57400	-0.26400
C	2.93600	1.43300	-0.75200
H	1.99100	1.95300	-0.91400
C	3.62000	2.01800	0.50200
H	4.53000	1.44600	0.69100
H	3.91400	3.04900	0.29700
C	2.74100	1.99600	1.77400
H	2.36500	0.98900	1.93900
C	3.58200	2.38600	2.99900
H	2.96500	2.35700	3.89700
H	4.40400	1.68200	3.12200
H	3.98700	3.39100	2.87500
C	1.52900	2.93000	1.65400
H	0.97900	2.94600	2.59500
H	1.85700	3.93900	1.41200
H	0.85700	2.57100	0.87600
C	3.77100	1.65000	-2.02600
O	4.82400	1.03800	-2.19700
N	3.27900	2.50900	-2.92200
H	2.42300	2.99900	-2.68800
C	3.77900	2.67300	-4.29500
H	4.62000	2.00100	-4.44900
C	2.64700	2.28700	-5.26700
H	1.84500	3.01400	-5.16400
H	3.03100	2.35200	-6.28300
C	2.03600	0.88600	-5.07700
H	1.65800	0.77700	-4.06000
C	0.85400	0.73600	-6.03400
H	0.38700	-0.23500	-5.88100
H	0.11600	1.51200	-5.83500
H	1.19700	0.82800	-7.06400
C	3.06300	-0.21900	-5.34600
H	2.58500	-1.19400	-5.26200
H	3.48600	-0.11000	-6.34600
H	3.85700	-0.16300	-4.60700
C	4.30400	4.09400	-4.58300
O	4.10900	4.99500	-3.76900
H	4.81800	4.28800	-5.45700
N	-2.3080	1.86300	-1.66500
H	-1.7420	1.50100	-0.91100

C	-2.9710	0.83900	-2.50100
H	-3.8910	1.25200	-2.91800
C	-2.0580	0.46100	-3.68000
H	-2.6680	0.01600	-4.46500
H	-1.6050	1.36800	-4.07900
O	-1.0290	-0.4560	-3.33700
H	-0.6130	-0.1940	-2.49600
C	-3.3810	-0.4260	-1.71300
O	-2.8920	-0.6370	-0.60300
H	-3.0130	2.49400	-1.28400
N	-4.2970	-1.2170	-2.28800
H	-4.6420	-0.9090	-3.19200
C	-5.0400	-2.3600	-1.71700
H	-5.5020	-2.8800	-2.55800
C	-4.1390	-3.3980	-1.00700
H	-3.2740	-3.5980	-1.64200
H	-3.7780	-2.9920	-0.06100
C	-4.8470	-4.7370	-0.71900
O	-6.0990	-4.8100	-0.76500
O	-4.1400	-5.7440	-0.47800
C	-6.1860	-1.8760	-0.80800
O	-5.9520	-1.3160	0.26400
N	-7.4340	-2.1440	-1.21000
H	-7.5600	-2.6360	-2.08900
C	-8.6360	-1.8680	-0.41400
H	-8.3220	-1.6200	0.59700
C	-9.3410	-0.6170	-0.97400
H	-9.5010	-0.7350	-2.04500
H	-10.318	-0.510	-0.50400
C	-8.5490	0.65700	-0.72000
C	-7.6020	1.11000	-1.65800
H	-7.4640	0.57400	-2.58600
C	-6.8140	2.24200	-1.38200
H	-6.0830	2.57600	-2.10600
C	-6.9740	2.93100	-0.16800
H	-6.3620	3.79500	0.04700
C	-7.9260	2.49000	0.76800
H	-8.0450	3.01200	1.70600
C	-8.7120	1.35700	0.49100
H	-9.4320	1.01600	1.21900
C	-9.5280	-3.1170	-0.23900
O	-10.711	-3.009	0.09900
N	-8.9460	-4.3140	-0.40400
H	-7.9700	-4.3110	-0.70000
C	-9.5720	-5.6210	-0.14600
H	-10.632	-5.581	-0.39700
H	-9.0850	-6.3710	-0.76800
C	-9.4590	-6.1010	1.30700

O	-10.269	-6.922	1.73300
H	-8.7120	-5.7390	1.92000
N	2.06000	-4.98300	-4.51100
C	1.36400	-5.90800	-5.42000
C	-0.0430	-6.1870	-4.86800
N	-0.7980	-4.9470	-4.61100
C	-0.0600	-3.9160	-3.85800
C	1.35500	-3.69000	-4.41600
C	-2.1700	-4.9830	-4.49500
C	-2.7750	-5.9970	-3.76200
C	-4.1480	-6.0300	-3.65000
N	-4.9370	-5.1200	-4.24900
C	-4.3500	-4.1310	-4.96000
C	-2.9690	-4.0220	-5.12000
O	-2.3690	-3.0840	-5.96000
C	-2.8520	-1.9440	-6.51100
C	-1.8720	-1.3960	-7.48500
N	-2.1860	-0.2740	-8.16900
C	-0.5790	-1.9350	-7.79000
C	0.04600	-1.13700	-8.69500
S	-1.0110	0.17200	-9.11500
N	1.36900	-1.35700	-9.07300
C	2.07500	-0.62000	-9.97300
C	2.19300	-2.43400	-8.46400
C	3.52500	-2.23600	-9.13700
C	3.44200	-1.18500	-10.01200
C	4.52900	-0.78900	-10.78000
C	5.72800	-1.50500	-10.66100
C	5.81300	-2.57500	-9.75000
C	4.70700	-2.94800	-8.97500
C	6.91000	-1.12300	-11.50000
O	6.90900	-0.23000	-12.32800
O	-3.9400	-1.4690	-6.22700
O	1.66700	0.32000	-10.62700
H	3.02300	-4.82500	-4.86200
H	1.92300	-6.84600	-5.49000
H	1.29300	-5.46900	-6.42000
H	0.05600	-6.74200	-3.93400
H	-0.5860	-6.8120	-5.58100
H	0.01900	-4.22500	-2.81400
H	-0.6030	-2.9680	-3.88700
H	1.28800	-3.23400	-5.40700
H	1.90400	-3.01200	-3.75800
H	-2.1850	-6.7480	-3.24900
H	-4.6480	-6.8100	-3.08100
H	-5.0410	-3.4410	-5.43900
H	-0.1900	-2.8230	-7.30300
H	1.76900	-3.41700	-8.69000

H	**2.27000**	**-2.29400**	**-7.38200**
H	**4.44400**	**0.06000**	**-11.45500**
H	**6.74300**	**-3.13300**	**-9.64700**
H	**4.76300**	**-3.77700**	**-8.26800**
H	**7.82600**	**-1.73000**	**-11.32800**

Table 2:Cartesian coordinates of Checkpoint kinase 1 complexed with MD8			
N	**2.92500**	**-8.41300**	**-11.89700**
H	**1.95500**	**-8.67500**	**-11.76500**
C	**3.52900**	**-7.53100**	**-10.88500**
H	**4.60100**	**-7.44000**	**-11.06800**
C	**2.86200**	**-6.14000**	**-11.01600**
H	**1.80200**	**-6.25100**	**-10.78100**
H	**3.29500**	**-5.47400**	**-10.26800**
C	**2.98500**	**-5.46000**	**-12.40000**
H	**2.60300**	**-6.12700**	**-13.17300**
C	**2.12900**	**-4.18800**	**-12.43300**
H	**2.18900**	**-3.73500**	**-13.42000**
H	**1.08800**	**-4.43300**	**-12.23500**
H	**2.48000**	**-3.47500**	**-11.68900**
C	**4.43800**	**-5.09600**	**-12.74000**
H	**4.47600**	**-4.60100**	**-13.71100**
H	**4.84400**	**-4.42600**	**-11.98200**
H	**5.05100**	**-5.99500**	**-12.79000**
C	**3.38400**	**-8.07500**	**-9.44100**
O	**3.91500**	**-7.47300**	**-8.50600**
H	**3.02900**	**-7.98200**	**-12.81500**
N	**2.67700**	**-9.19900**	**-9.24900**
H	**2.30100**	**-9.64800**	**-10.07500**
C	**2.39400**	**-9.83600**	**-7.94600**
H	**3.17400**	**-10.5700**	**-7.74800**
H	**2.42500**	**-9.09900**	**-7.14300**
C	**1.04500**	**-10.5650**	**-7.88700**
O	**0.10800**	**-10.2050**	**-8.60200**
N	**0.94200**	**-11.5800**	**-7.02300**
H	**1.71700**	**-11.7750**	**-6.41000**
C	**-0.19900**	**-12.510**	**-6.95700**
H	**-1.11000**	**-11.920**	**-7.03400**
C	**-0.15900**	**-13.467**	**-8.16400**
H	**-1.10700**	**-14.002**	**-8.23700**
H	**-0.04600**	**-12.879**	**-9.07400**
C	**0.98000**	**-14.4930**	**-8.08900**
H	**1.89400**	**-14.0140**	**-7.73300**
H	**0.71400**	**-15.2940**	**-7.39800**

C	1.23700	-15.0710	-9.47100
O	0.36300	-15.7800	-10.02200
O	2.26200	-14.7290	-10.09500
C	-0.29900	-13.311	-5.64200
O	0.64500	-13.3690	-4.84600
H	-1.17500	-13.810	-5.42200
N	-5.01500	-12.322	-3.04200
H	-4.01000	-12.364	-3.12300
C	-5.69300	-11.142	-3.61700
H	-6.67400	-11.040	-3.15000
C	-4.88300	-9.8880	-3.23500
H	-5.36200	-9.0100	-3.66600
H	-4.95200	-9.7740	-2.15300
C	-3.41100	-9.8660	-3.62400
C	-3.01900	-9.7360	-4.97300
H	-3.76400	-9.6680	-5.75200
C	-1.65300	-9.6660	-5.31200
H	-1.35200	-9.5560	-6.34200
C	-0.66900	-9.7120	-4.30200
O	0.65000	-9.61000	-4.62200
H	1.20300	-9.59600	-3.83800
C	-1.05800	-9.8360	-2.95000
H	-0.31200	-9.8490	-2.17000
C	-2.42500	-9.9150	-2.61800
H	-2.71600	-9.9830	-1.57900
C	-5.97400	-11.215	-5.14100
O	-6.33700	-10.206	-5.74700
H	-5.41500	-13.166	-3.45300
H	-5.85700	-12.107	-5.64600
N	-2.05200	-8.9880	-9.94500
H	-1.24400	-9.4650	-9.54400
C	-1.85700	-7.6200	-10.47200
H	-2.82800	-7.2120	-10.74000
C	-1.23800	-6.6720	-9.41600
H	-0.22900	-7.0140	-9.17900
C	-1.15200	-5.2250	-9.93300
H	-0.72400	-4.5840	-9.16300
H	-0.51200	-5.1710	-10.81000
H	-2.14600	-4.8570	-10.19400
C	-2.06300	-6.6570	-8.11600
H	-1.61600	-5.9610	-7.40800
H	-3.08800	-6.3480	-8.32300
H	-2.07200	-7.6460	-7.65800
C	-0.97300	-7.6570	-11.72900
O	0.07500	-8.29800	-11.72800
H	-2.44500	-9.5720	-10.68300
H	-1.26100	-7.1420	-12.57600
N	-2.31500	0.10100	-14.53500

H	-2.81400	0.85700	-14.06800
C	-2.27000	-1.1930	-13.83600
H	-1.54800	-1.8530	-14.31800
C	-1.79500	-0.9310	-12.40100
H	-1.77700	-1.8600	-11.83000
H	-0.79200	-0.5050	-12.40700
H	-2.46200	-0.2220	-11.90900
C	-3.63800	-1.9100	-13.87800
O	-4.65900	-1.2740	-14.12700
H	-1.36200	0.40500	-14.73300
H	-3.69400	-2.9240	-13.69700
N	-5.79400	-5.1250	-11.51600
H	-6.47200	-4.3660	-11.53100
C	-6.03200	-6.2520	-10.58400
H	-5.10400	-6.8140	-10.46800
C	-6.40600	-5.6850	-9.19500
H	-5.63600	-4.9690	-8.90500
H	-7.35200	-5.1490	-9.26700
C	-6.51400	-6.7490	-8.08200
H	-7.31100	-7.4530	-8.32300
H	-5.57100	-7.2940	-8.02000
C	-6.81100	-6.1000	-6.71600
H	-6.05300	-5.3430	-6.51400
H	-7.78700	-5.6100	-6.74900
C	-6.80400	-7.1310	-5.57400
H	-7.61200	-7.8520	-5.73200
H	-5.85800	-7.6790	-5.59900
N	-6.96300	-6.4770	-4.24800
H	-6.25600	-5.7680	-4.09300
H	-7.86800	-6.0090	-4.16200
H	-6.90200	-7.1260	-3.46900
C	-7.08800	-7.2350	-11.14700
O	-8.15600	-6.8280	-11.60200
H	-4.87000	-4.7360	-11.33100
H	-6.89200	-8.2480	-11.14000
N	-14.2910	-4.285	-2.47700
H	-14.2360	-5.290	-2.57300
C	-13.1270	-3.486	-2.89600
H	-12.8560	-2.812	-2.08100
C	-11.9270	-4.412	-3.15100
H	-11.7220	-4.972	-2.23800
H	-12.1910	-5.115	-3.93900
C	-10.6590	-3.647	-3.56000
H	-10.8160	-3.195	-4.53900
H	-10.4730	-2.856	-2.83500
C	-9.42600	-4.5460	-3.65000
O	-9.58000	-5.7480	-3.94300
O	-8.29000	-4.0480	-3.47500

C	-13.4500	-2.617	-4.12300
O	-13.1020	-1.440	-4.13800
H	-15.1150	-3.952	-2.97700
H	-13.9550	-3.020	-4.92700
N	-3.72700	5.20400	-4.82400
H	-3.49900	4.54000	-4.07200
C	-3.98800	4.65800	-6.18000
H	-3.34800	5.20000	-6.88000
C	-3.62100	3.15100	-6.26800
H	-4.07000	2.64000	-5.41600
C	-4.10500	2.44600	-7.54800
H	-3.82800	1.39200	-7.51300
H	-5.18800	2.50000	-7.63400
H	-3.64900	2.89900	-8.42500
C	-2.09500	2.97900	-6.18500
H	-1.84000	1.92300	-6.26500
H	-1.61000	3.52000	-6.99900
H	-1.71800	3.35600	-5.23500
C	-5.45200	4.88400	-6.60200
O	-6.37900	4.46200	-5.91100
H	-4.52900	5.76400	-4.53600
H	-5.65800	5.39500	-7.47400
N	-6.38200	0.49000	-12.80100
H	-5.74300	-0.0200	-13.40400
C	-5.76200	1.19500	-11.66100
H	-6.50700	1.82400	-11.17900
C	-5.27100	0.12300	-10.65700
H	-4.62800	-0.5690	-11.20100
H	-4.65800	0.59900	-9.89100
C	-6.37000	-0.7000	-9.94900
H	-7.08200	-1.0730	-10.68000
C	-5.73800	-1.9170	-9.26200
H	-6.50900	-2.4990	-8.75600
H	-5.25100	-2.5490	-10.00500
H	-4.99900	-1.5870	-8.53400
C	-7.13500	0.13200	-8.91200
H	-7.90900	-0.4780	-8.44500
H	-6.45200	0.49000	-8.14200
H	-7.60900	0.98400	-9.39300
C	-4.59100	2.13100	-12.05800
O	-3.98400	1.98000	-13.11900
H	-7.09500	-0.1500	-12.45100
N	-4.25900	3.09000	-11.18700
H	-4.83100	3.16600	-10.35400
C	-3.18500	4.08700	-11.38000
H	-3.30500	4.50500	-12.37800
C	-3.36600	5.24900	-10.38000
H	-4.39300	5.59800	-10.47000

H	-3.22600	4.89500	-9.36000
C	-2.42100	6.43900	-10.61900
H	-1.44500	6.22100	-10.18300
H	-2.28700	6.58800	-11.69100
C	-2.98600	7.73100	-10.02000
O	-3.93300	8.29600	-10.61400
O	-2.50600	8.19500	-8.95500
C	-1.76600	3.49000	-11.31000
O	-1.26900	3.12600	-10.24600
N	-1.08600	3.41900	-12.46000
H	-1.54100	3.72700	-13.30400
C	0.27400	2.87100	-12.56000
H	0.26500	1.91000	-12.04400
C	0.62000	2.60500	-14.03200
H	-0.24500	2.16100	-14.51800
H	0.83000	3.55000	-14.53500
C	1.78900	1.65600	-14.21100
C	1.55200	0.26900	-14.24800
H	0.54300	-0.10500	-14.19200
C	2.62700	-0.63200	-14.34300
H	2.44900	-1.69400	-14.36100
C	3.94700	-0.14800	-14.42900
O	4.98100	-1.02600	-14.51600
H	5.83300	-0.58500	-14.44600
C	4.19000	1.24400	-14.40000
H	5.20300	1.61200	-14.45500
C	3.11000	2.14400	-14.29000
H	3.29200	3.20900	-14.25100
C	1.35700	3.74200	-11.88700
O	1.34300	4.96900	-11.97900
N	2.33100	3.07800	-11.25600
H	2.24200	2.07000	-11.23500
C	3.39400	3.67100	-10.43500
H	3.33200	4.76200	-10.45300
C	3.12800	3.19000	-8.99800
H	3.09600	2.09900	-8.97500
H	3.94100	3.51800	-8.35200
S	1.56400	3.86400	-8.35400
H	0.71500	3.40900	-9.29500
C	4.80800	3.28100	-10.93700
O	5.33300	2.22000	-10.60500
N	5.43900	4.12100	-11.76000
H	4.95900	4.99000	-11.99000
C	6.71400	3.81800	-12.46400
H	6.59400	2.87000	-12.98600
C	7.00800	4.89200	-13.52600
H	7.93200	4.64100	-14.04900
H	6.19600	4.88500	-14.25400

O	7.11600	6.20500	-12.98900
H	7.92700	6.28800	-12.43400
C	7.97700	3.61700	-11.60500
O	8.97200	3.08500	-12.11000
N	7.94500	3.99600	-10.32200
H	7.09600	4.44000	-9.98300
C	9.00300	3.72500	-9.33800
H	9.97200	3.69100	-9.83500
H	9.00200	4.52100	-8.59400
C	8.82700	2.40100	-8.58600
O	9.69100	2.03900	-7.78800
N	7.72600	1.67400	-8.81900
H	7.04400	2.05600	-9.46800
C	7.43500	0.36900	-8.20500
H	6.58500	-0.08500	-8.71200
H	8.30600	-0.27700	-8.31000
C	7.07900	0.45500	-6.72000
O	6.41700	1.39400	-6.29000
N	7.48800	-0.55800	-5.95400
H	8.06600	-1.26100	-6.38300
C	7.25000	-0.68200	-4.50500
H	6.29300	-0.22500	-4.25800
C	7.18400	-2.17100	-4.11000
H	8.05900	-2.68200	-4.51500
H	7.21200	-2.25700	-3.02200
C	5.90500	-2.85700	-4.61500
H	5.05700	-2.50600	-4.02700
H	5.73400	-2.58700	-5.65900
C	5.97900	-4.38100	-4.52100
O	6.54800	-4.93900	-3.55900
O	5.46800	-5.07300	-5.43400
C	8.32000	0.03400	-3.66200
O	9.50000	0.07600	-4.02000
H	8.04400	0.48900	-2.77800
N	5.52500	-3.09600	0.97700
H	5.60300	-3.57300	1.87800
C	5.01900	-3.89600	-0.15200
H	5.72300	-3.80700	-0.98200
C	4.93400	-5.38300	0.23900
H	4.10500	-5.53500	0.93200
H	4.71100	-5.94500	-0.66800
C	6.21500	-5.98100	0.84000
H	6.30200	-7.00600	0.47900
H	7.08800	-5.43100	0.48600
C	6.19500	-6.00700	2.37100
O	5.97100	-4.94600	2.98900
O	6.39100	-7.10700	2.94700
C	3.63600	-3.45700	-0.68100

O	3.25300	-3.84700	-1.78000
H	4.93800	-2.27000	1.08800
N	2.86500	-2.67300	0.08300
H	3.23500	-2.39200	0.98200
C	1.56900	-2.09700	-0.33000
H	1.22700	-2.58400	-1.24500
C	0.53000	-2.38100	0.77400
H	0.91000	-2.01900	1.73000
H	-0.38800	-1.8360	0 0.55500
C	0.14600	-3.85400	0.91400
O	0.32400	-4.68300	0.03000
N	-0.40400	-4.2350	0 2.04700
H	-0.54800	-3.5750	0 2.80200
H	-0.74000	-5.1830	0 2.13800
C	1.66000	-0.58100	-0.66100
O	0.65000	0.06200	-0.97100
N	2.86600	0.00200	-0.59500
H	3.65400	-0.59700	-0.38300
C	3.16100	1.41600	-0.87100
H	2.23300	1.96400	-1.04200
C	3.88300	2.01800	0.35300
H	4.77500	1.41900	0.54900
H	4.21200	3.02900	0.10800
C	3.02700	2.07300	1.63900
H	2.61800	1.08700	1.84800
C	3.90100	2.48100	2.83400
H	3.29700	2.51100	3.74200
H	4.69900	1.75200	2.97400
H	4.33900	3.46400	2.66300
C	1.84700	3.04300	1.50200
H	1.31300	3.11200	2.45000
H	2.20500	4.03000	1.21500
H	1.15200	2.67600	0.74900
C	3.99400	1.55600	-2.15800
O	5.03500	0.91900	-2.30900
N	3.51400	2.38600	-3.08600
H	2.66300	2.89000	-2.86800
C	4.02400	2.51800	-4.45800
H	4.87600	1.85500	-4.58600
C	2.90000	2.09100	-5.42100
H	2.06400	2.77500	-5.29300
H	3.26000	2.19200	-6.44300
C	2.37100	0.65600	-5.24000
H	2.07800	0.49000	-4.20300
C	1.12700	0.48000	-6.10900
H	0.71900	-0.51900	-5.95900
H	0.37100	1.20900	-5.82100
H	1.38300	0.63000	-7.15700

C	3.42600	-0.38300	-5.63400
H	3.00200	-1.38200	-5.56600
H	3.77200	-0.20600	-6.65300
H	4.26600	-0.32200	-4.95000
C	4.52800	3.94000	-4.77400
O	4.30800	4.85500	-3.98300
H	5.04800	4.12300	-5.64600
N	-2.01300	1.58300	-1.78600
H	-1.43100	1.25400	-1.02800
C	-2.68500	0.52600	-2.57000
H	-3.59800	0.92500	-3.01600
C	-1.77100	0.06700	-3.71800
H	-2.35500	-0.5270	-4.41900
H	-1.40200	0.94800	-4.24200
O	-0.66400	-0.7080	-3.28000
H	-0.32800	-0.3430	-2.44400
C	-3.11500	-0.6860	-1.71300
O	-2.66200	-0.8280	-0.57600
H	-2.71400	2.22500	-1.41700
N	-4.01400	-1.5120	-2.26400
H	-4.32500	-1.2640	-3.19900
C	-4.77100	-2.6170	-1.64400
H	-5.22400	-3.1770	-2.46400
C	-3.88500	-3.6200	-0.87000
H	-2.99500	-3.8290	-1.46700
H	-3.56300	-3.1830	0.07600
C	-4.59600	-4.9550	-0.57600
O	-5.85000	-5.0000	-0.51300
O	-3.89700	-5.9870	-0.45400
C	-5.92600	-2.0850	-0.77500
O	-5.70700	-1.4700	0.27000
N	-7.16600	-2.3770	-1.17700
H	-7.27900	-2.9120	-2.03300
C	-8.38200	-2.0660	-0.41500
H	-8.08700	-1.7840	0.59300
C	-9.06400	-0.8370	-1.04200
H	-9.19600	-0.9940	-2.11200
H	-10.0510	-0.703	-0.60000
C	-8.26300	0.43500	-0.81200
C	-7.32100	0.87200	-1.76300
H	-7.19300	0.32800	-2.68800
C	-6.52300	2.00100	-1.50300
H	-5.79400	2.32300	-2.23400
C	-6.66600	2.69900	-0.29100
H	-6.04500	3.55900	-0.08700
C	-7.61100	2.27200	0.65800
H	-7.71400	2.79700	1.59500
C	-8.40800	1.14300	0.39700

H	-9.11800	0.80700	1.13700
C	-9.28300	-3.3030	-0.21700
O	-10.4770	-3.179	0.07200
N	-8.69800	-4.5050	-0.31600
H	-7.71100	-4.5120	-0.57200
C	-9.32900	-5.8020	-0.02300
H	-10.3790	-5.780	-0.31200
H	-8.81200	-6.5760	-0.59100
C	-9.25900	-6.2020	1.45600
O	-10.1520	-6.902	1.93200
H	-8.47200	-5.8880	2.04500
N	2.63900	-5.19800	-5.08000
C	1.81600	-6.09600	-5.90600
C	0.52500	-6.38900	-5.12800
N	-0.19900	-5.1510	-4.79800
C	0.63300	-4.15800	-4.09900
C	1.96700	-3.91000	-4.82000
C	-1.56400	-5.1650	-4.57900
C	-2.12700	-6.1400	-3.76600
C	-3.49100	-6.1590	-3.56300
N	-4.31500	-5.2710	-4.14700
C	-3.76800	-4.3140	-4.92500
C	-2.40100	-4.2270	-5.18800
N	-1.84100	-3.2810	-6.12400
C	-2.36900	-2.1850	-6.72100
C	-1.41500	-1.6080	-7.70300
N	-1.78700	-0.5000	-8.37700
C	-0.10300	-2.0880	-8.03400
C	0.46600	-1.26400	-8.95200
S	-0.64700	0.01000	-9.33100
N	1.78000	-1.43700	-9.38600
C	2.42000	-0.67400	-10.31300
C	2.66900	-2.48400	-8.81500
C	3.96900	-2.22300	-9.52900
C	3.80600	-1.17700	-10.39800
C	4.84600	-0.72700	-11.19900
C	6.08600	-1.36800	-11.11400
C	6.25500	-2.44000	-10.21500
C	5.19100	-2.87500	-9.41100
C	7.21800	-0.90600	-11.98200
O	7.13100	-0.01500	-12.80900
O	-3.48200	-1.7670	0 -6.45400
O	1.95300	0.24500	-10.95700
H	3.57000	-5.03300	-5.49800
H	2.35500	-7.03000	-6.08700
H	1.58300	-5.62800	-6.86800
H	0.79200	-6.89600	-4.19700
H	-0.11100	-7.0540	-5.71600

H	**0.85100**	**-4.52400**	**-3.09300**
H	**0.09700**	**-3.20900**	**-4.00000**
H	**1.78000**	**-3.39500**	**-5.76600**
H	**2.60500**	**-3.27700**	**-4.19900**
H	**-1.50700**	**-6.8750**	**-3.26600**
H	**-3.95900**	**-6.9130**	**-2.93400**
H	**-4.48700**	**-3.6350**	**-5.37700**
H	**-0.89100**	**-3.4960**	**-6.38100**
H	**0.34000**	**-2.96300**	**-7.57200**
H	**2.27800**	**-3.48000**	**-9.04200**
H	**2.77200**	**-2.35000**	**-7.73500**
H	**4.69500**	**0.11700**	**-11.86600**
H	**7.21600**	**-2.94700**	**-10.14700**
H	**5.31300**	**-3.70600**	**-8.71700**
H	**8.17700**	**-1.45100**	**-11.83800**

Appendix 3

Theoretical Analysis of the Binding of Potential Inhibitors to Protein Kinases MK2 and MK3

Pedro M.M. Araújo, Luís Pinto da Silva and Joaquim C.G. Esteves da Silva*

Centro de Investigação em Química, Departamento de Química e Bioquímica, Faculdade de Ciências da Universidade do Porto, R. Campo Alegre 687, 4169-007 Porto, Portugal.
*Corresponding Author: Joaquim C.G. Esteves da Silva; Email: jcsilva@fc.up.pt; Tel.: +351 226082869; Fax: +351 22608259;

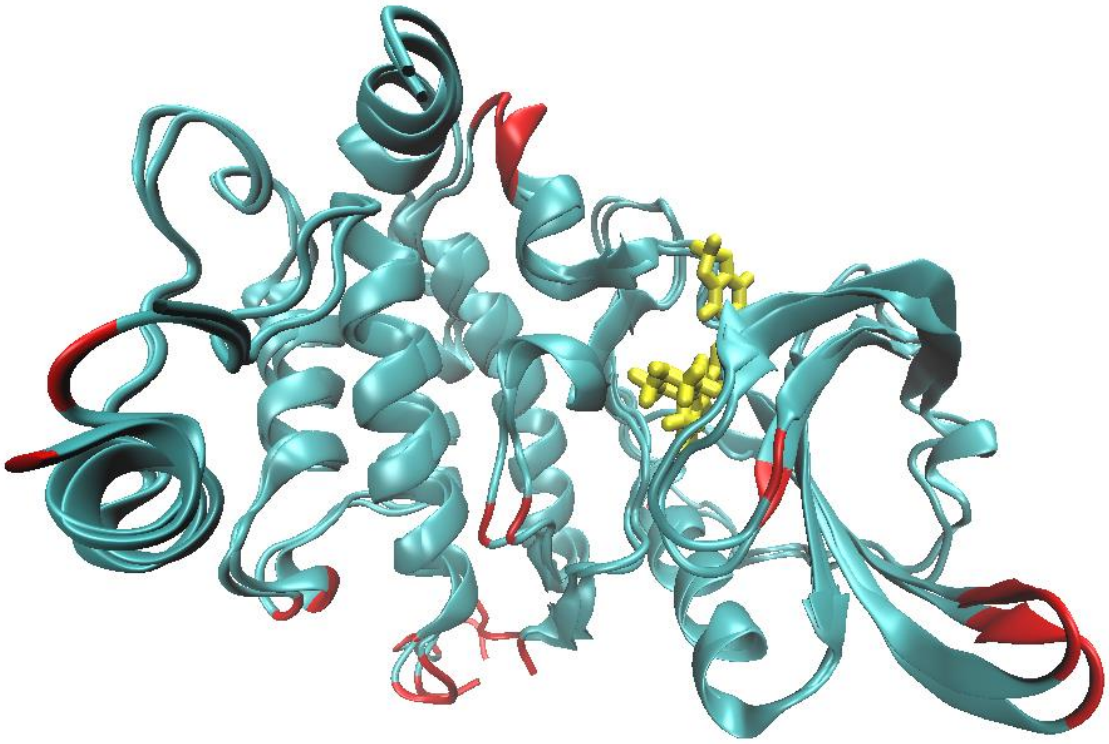

Figure 1: Three dimensional representation of ligand 05B bond to MK2. Yellow for 05B; blue for MK2 residues with RMSD values inferior to 3Å; red for MK2 residues with RMSD values superior to 3Å.

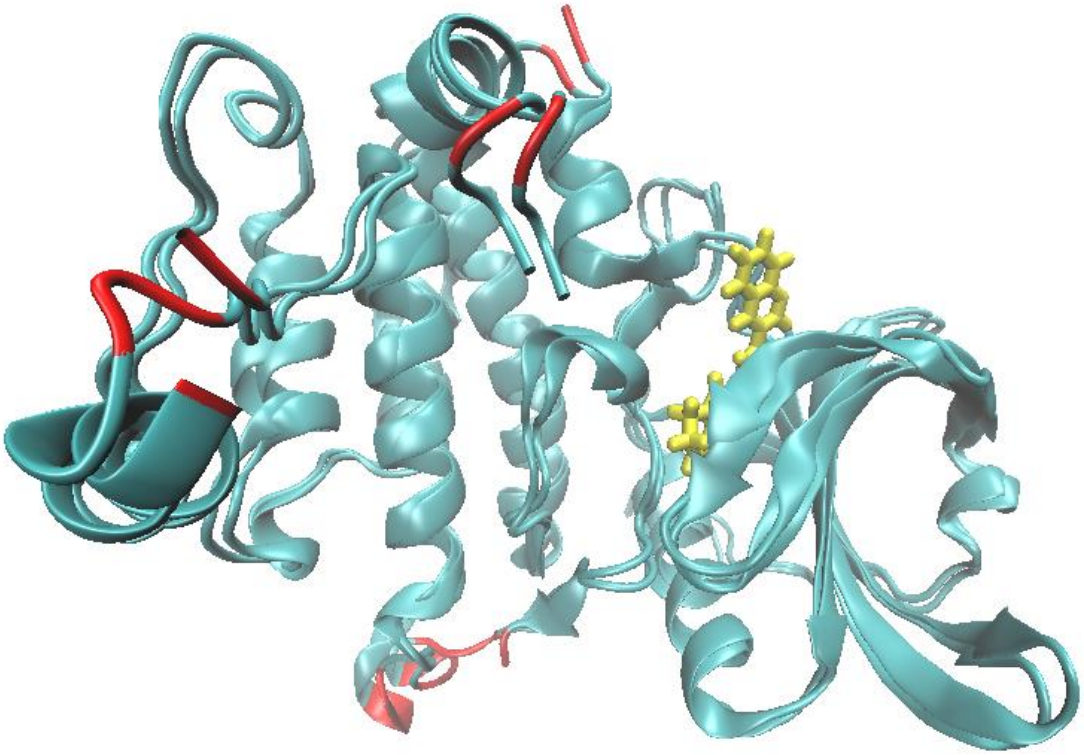

Figure 2: Three dimensional representation of ligand P4O bond to MK2. Yellow for P4O; blue for MK2 residues with RMSD values inferior to 3Å; red for MK2 residues with RMSD values superior to 3Å.

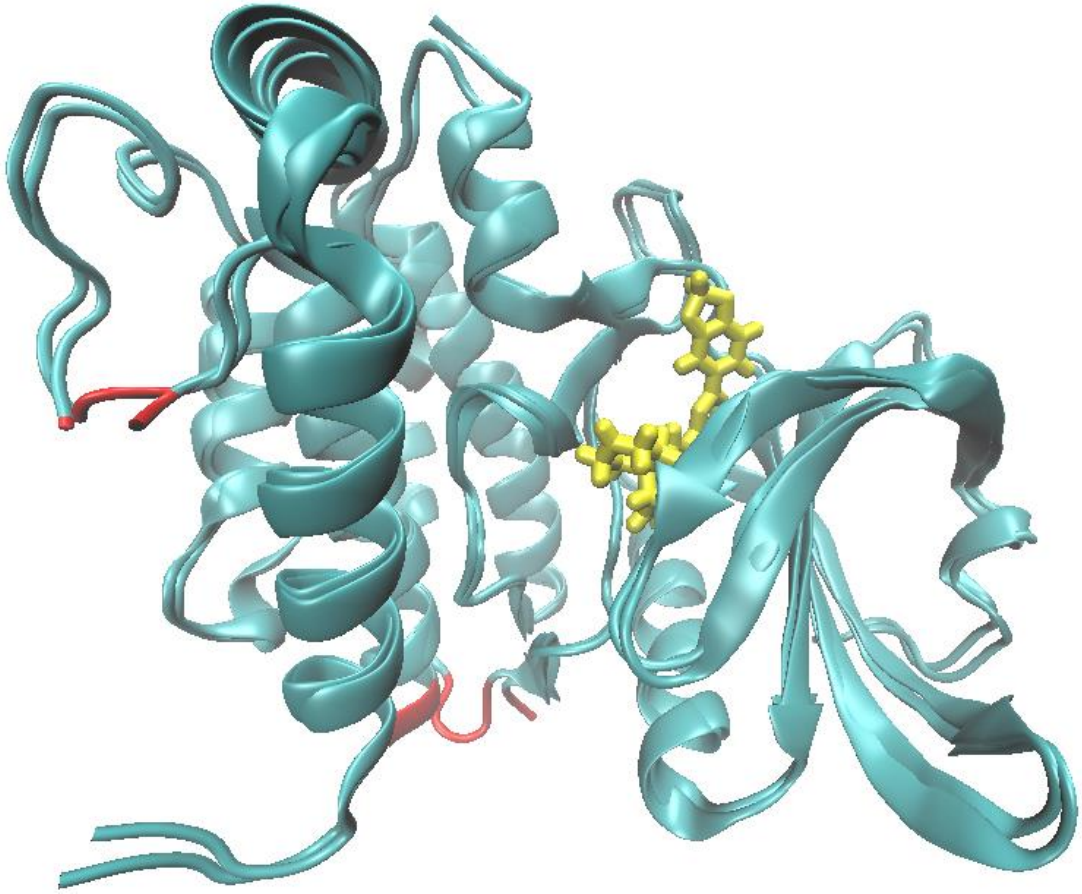

Figure 3: Three dimensional representation of ligand 05B bond to MK3. Yellow for 05B; blue for MK3 residues with RMSD values inferior to 3Å; red for MK3 residues with RMSD values superior to 3Å.

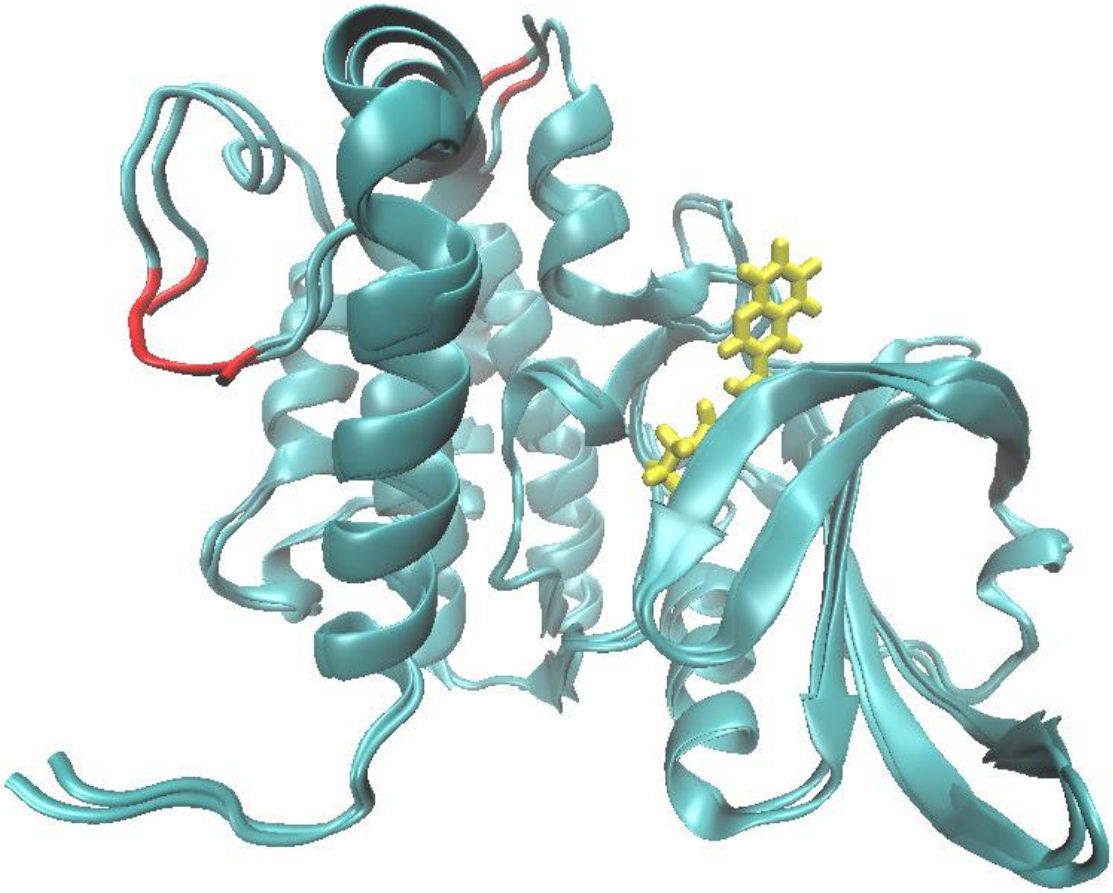

Figure 4: Three dimensional representation of ligand P4O bond to MK3. Yellow for 05B; blue for MK3 residues with RMSD values inferior to 3Å; red for MK3 residues with RMSD values superior to 3Å.

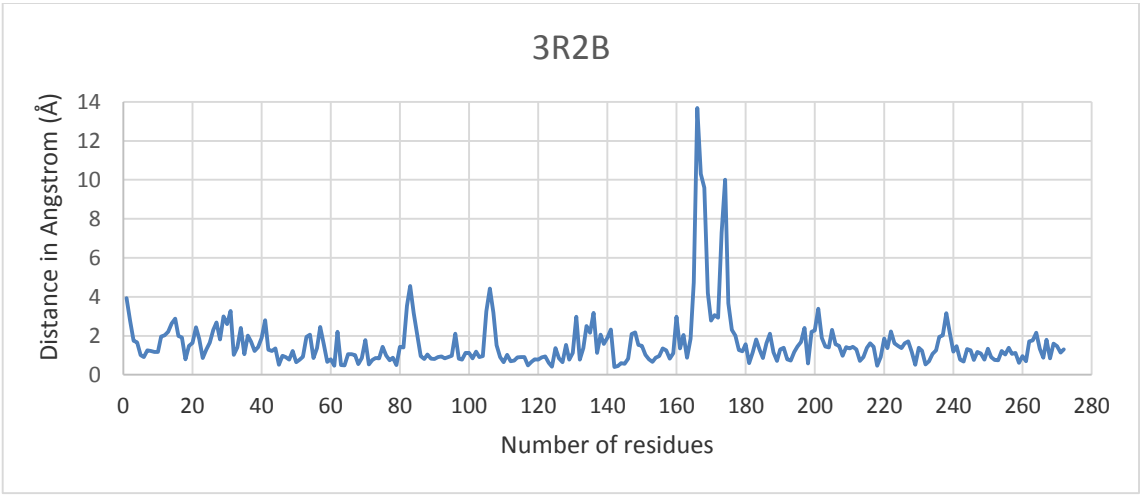

Graphic 1: RMSD values for the 3R2B structure (05B bond to MK2). Note that the residues numeration is altered, residue number 1 corresponds to the first residue in the structure and so on.

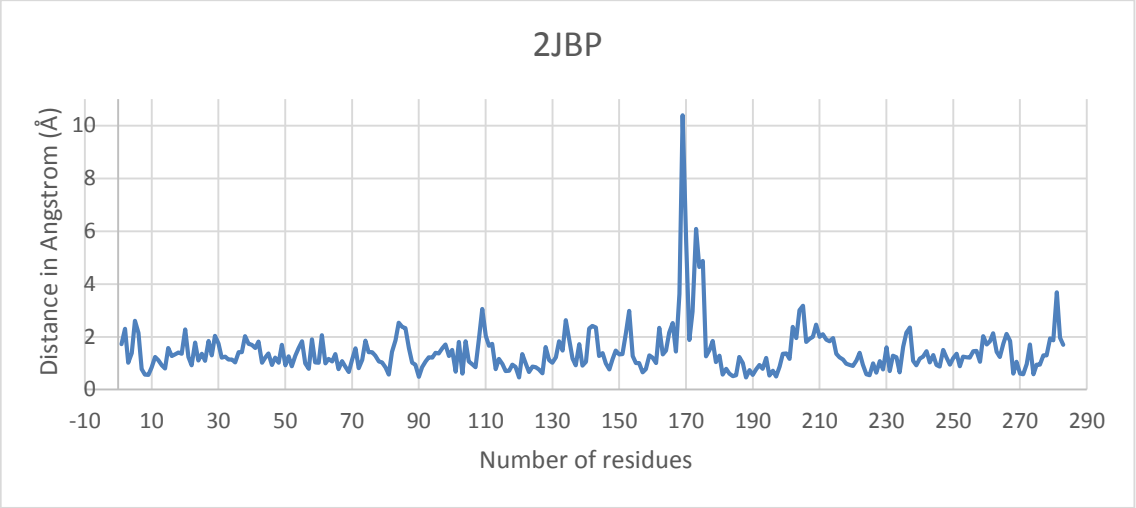

Graphic 2: RMSD values for the 2JBP structure (P4O bond to MK2). Note that the residues numeration is altered, residue number 1 corresponds to the first residue in the structure and so on.

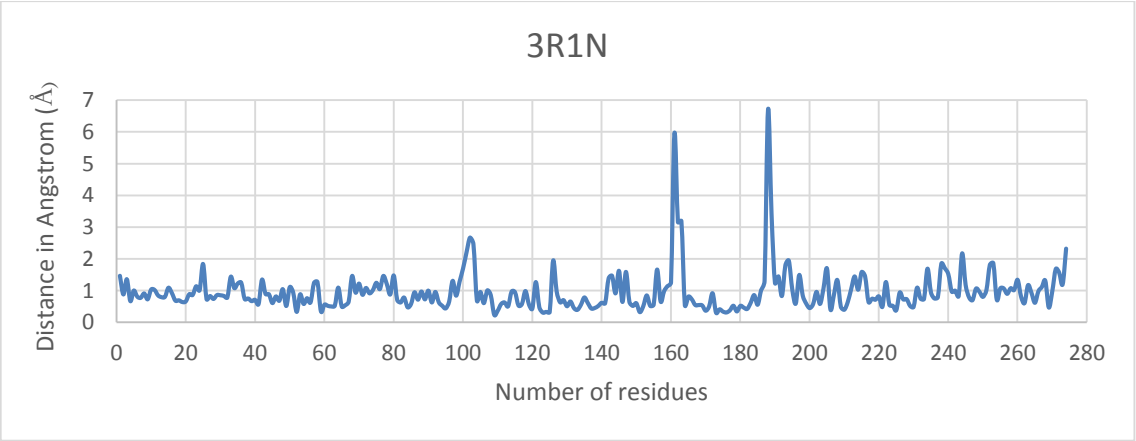

Graphic 3: RMSD values for the 3R1N structure (05B bond to MK3). Note that the residues numeration is altered, residue number 1 corresponds to the first residue in the structure and so on.

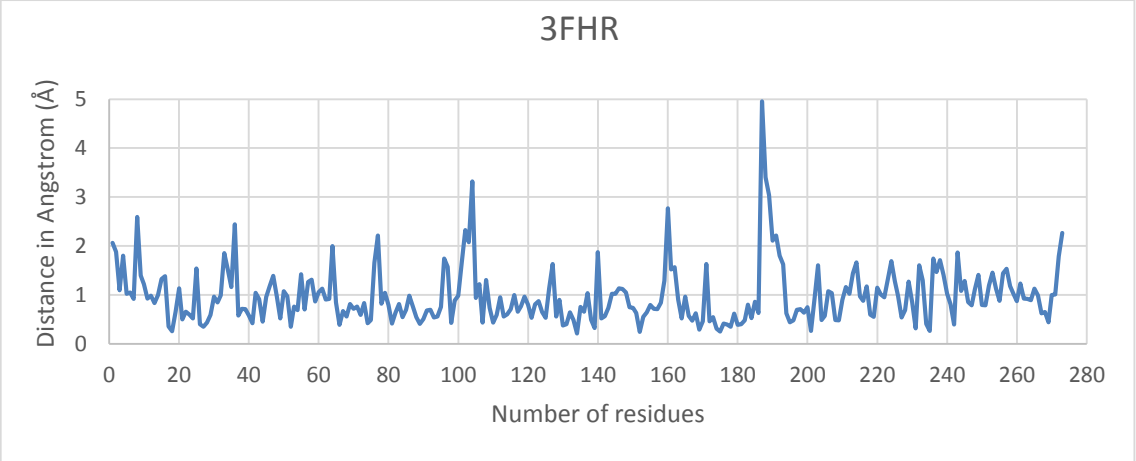

Graphic 4: RMSD values for the 3FHR structure (P4O bond to MK3). Note that the residues numeration is altered, residue number 1 corresponds to the first residue in the structure and so on.

Table 1: Cartesian coordinates of MK3 bound to 05B.

Table 2: Cartesian coordinates of MK3 bound to 05B without binding site water molecules.
Table 3: Cartesian coordinates of MK2 bound to 05B.
Table 4: Cartesian coordinates of MK3 bound to P4O.
Table 5: Cartesian coordinates of MK3 bound to P4O without binding site water molecules.
Table 6: Cartesian coordinates of MK2 bound to P40.
Table 7: Cartesian coordinates of MK2 bound to P4O without binding site water molecules.

Table 1: Cartesian coordinates of MK3 bound to 05B.			
N	**7.58900**	**8.50800**	**-4.70700**
H	**7.93200**	**8.23800**	**-3.79000**
C	**8.23500**	**7.89100**	**-5.88200**
H	**7.93200**	**8.41100**	**-6.79000**
C	**9.76700**	**8.06200**	**-5.72900**
H	**10.0950**	**7.4630**	**-4.87700**
H	**10.2470**	**7.6550**	**-6.62000**
C	**10.2940**	**9.4990**	**-5.51400**
H	**9.86200**	**9.91300**	**-4.60200**
C	**11.8170**	**9.4590**	**-5.33100**
H	**12.1940**	**10.465**	**-5.14400**
H	**12.0720**	**8.8290**	**-4.47700**
H	**12.2950**	**9.0580**	**-6.22600**
C	**9.94100**	**10.4280**	**-6.68400**
H	**10.3840**	**11.411**	**-6.52100**
H	**10.3210**	**10.014**	**-7.61800**
H	**8.86200**	**10.5470**	**-6.74900**
C	**7.87100**	**6.39900**	**-6.08500**
O	**8.39200**	**5.53000**	**-5.38100**
H	**6.58600**	**8.32900**	**-4.75000**
H	**7.19000**	**6.13100**	**-6.81200**
N	**-8.5040**	**19.474**	**-3.21700**
H	**-8.9560**	**19.376**	**-2.32100**
C	**-7.1130**	**18.995**	**-3.27700**
H	**-6.5250**	**19.640**	**-3.93400**
C	**-6.5860**	**19.106**	**-1.83300**
H	**-6.7790**	**20.119**	**-1.47600**
H	**-7.1690**	**18.426**	**-1.20900**
C	**-5.0940**	**18.806**	**-1.61500**
H	**-4.8600**	**17.800**	**-1.96400**
H	**-4.4840**	**19.528**	**-2.15900**
C	**-4.8180**	**18.910**	**-0.10500**
H	**-5.0630**	**19.921**	**0.22900**
H	**-5.4740**	**18.209**	**0.41800**
C	**-3.3730**	**18.602**	**0.29900**
H	**-3.1000**	**17.609**	**-0.06800**

H	**-2.7000**	**19.332**	**-0.16300**
N	**-3.2550**	**18.653**	**1.77800**
H	**-2.3050**	**18.512**	**2.09900**
H	**-3.5500**	**19.565**	**2.11700**
H	**-3.8670**	**17.964**	**2.22200**
C	**-7.0270**	**17.539**	**-3.80300**
O	**-7.7800**	**16.670**	**-3.35400**
H	**-9.0560**	**18.992**	**-3.92600**
H	**-6.3380**	**17.295**	**-4.53100**
N	**0.03800**	**11.4470**	**-10.29000**
H	**-0.9030**	**11.142**	**-10.52700**
C	**1.17100**	**10.6200**	**-10.73700**
H	**2.05600**	**10.9050**	**-10.17200**
C	**0.86200**	**9.14600**	**-10.41400**
H	**0.51800**	**9.09300**	**-9.38100**
H	**0.05400**	**8.79600**	**-11.05800**
C	**2.07600**	**8.21100**	**-10.56000**
H	**2.41400**	**8.19400**	**-11.59500**
H	**2.89200**	**8.57700**	**-9.93700**
C	**1.69600**	**6.78800**	**-10.12100**
H	**1.22400**	**6.83300**	**-9.13700**
H	**0.97500**	**6.37300**	**-10.82900**
C	**2.91900**	**5.86700**	**-10.04000**
H	**3.39500**	**5.81400**	**-11.02300**
H	**3.63700**	**6.28200**	**-9.32700**
N	**2.51900**	**4.50500**	**-9.61600**
H	**3.30900**	**3.87300**	**-9.53000**
H	**2.02600**	**4.50500**	**-8.73000**
H	**1.89900**	**4.08800**	**-10.30800**
C	**1.48200**	**10.8450**	**-12.23000**
O	**0.60100**	**10.6990**	**-13.08000**
H	**0.17100**	**12.3980**	**-10.63400**
H	**2.43400**	**11.1200**	**-12.52000**
N	**-5.6790**	**11.389**	**-8.57200**
H	**-4.9810**	**12.086**	**-8.33200**
C	**-6.1820**	**10.532**	**-7.47800**
H	**-7.0090**	**9.9200**	**-7.83200**
C	**-5.0510**	**9.6020**	**-7.00200**
H	**-4.2360**	**10.219**	**-6.63200**
H	**-5.4070**	**8.9860**	**-6.17400**
C	**-4.5170**	**8.6710**	**-8.09800**
H	**-5.2950**	**7.9470**	**-8.34300**
H	**-4.3000**	**9.2460**	**-8.99800**
S	**-3.0110**	**7.7690**	**-7.65300**

C	-1.8270	9.1400	-7.70200
H	-0.8240	8.7570	-7.52000
H	-1.8660	9.6210	-8.68100
H	-2.0670	9.8710	-6.93100
C	-6.6990	11.339	-6.27700
O	-6.3170	12.498	-6.08800
H	-5.3110	10.795	-9.31500
H	-7.3710	10.909	-5.62300
N	-4.6600	11.280	-0.29800
H	-4.2620	11.022	-1.19600
C	-4.3830	10.381	0.85000
H	-5.3370	10.140	1.31700
C	-3.7850	9.0540	0.34700
H	-2.8020	9.2400	-0.07900
H	-3.6450	8.3940	1.20000
C	-4.6550	8.3320	-0.69500
H	-4.8040	8.9880	-1.55300
H	-4.1130	7.4580	-1.05600
S	-6.2840	7.7950	-0.11800
C	-5.7670	6.4500	0.96500
H	-6.6340	5.9790	1.42400
H	-5.2180	5.7070	0.39000
H	-5.1120	6.8340	1.74100
C	-3.5250	11.004	1.98000
O	-2.5410	10.427	2.44400
H	-5.6700	11.383	-0.40100
N	-3.9100	12.189	2.46000
H	-4.7520	12.582	2.05100
C	-3.1990	12.960	3.50200
H	-2.1430	12.953	3.23700
C	-3.6400	14.439	3.47400
H	-3.0470	14.997	4.20000
H	-3.4180	14.845	2.48700
C	-5.1290	14.662	3.77400
H	-5.7330	14.220	2.98200
H	-5.3770	14.166	4.71200
C	-5.4800	16.147	3.89000
O	-6.2180	16.504	4.84200
O	-5.0570	16.954	3.03000
C	-3.2490	12.355	4.92700
O	-2.7530	12.953	5.88000
H	-3.7030	11.441	5.07800
N	4.49900	0.94200	2.40800
H	5.34500	0.42500	2.16400

C	4.26100	2.25500	1.76400
H	4.05500	2.97900	2.55100
C	5.48400	2.76900	0.98400
H	5.47000	2.34500	-0.02200
H	5.37300	3.84900	0.88300
C	6.85500	2.49000	1.60100
H	7.54000	3.28400	1.30000
H	6.79600	2.48300	2.69100
C	7.38900	1.16400	1.07300
O	7.96600	1.17300	-0.03500
O	7.17300	0.12700	1.73900
C	3.05500	2.27800	0.80700
O	2.46700	3.33100	0.57800
H	3.69000	0.34400	2.23900
N	2.66800	1.12700	0.24800
H	3.15500	0.28600	0.51700
C	1.56000	1.01100	-0.71300
H	1.59200	1.87300	-1.38100
C	1.77900	-0.2580	-1.56200
H	1.88100	-1.1210	-0.90400
H	0.90500	-0.4270	-2.18800
C	2.99200	-0.1930	-2.49200
O	3.64500	0.82500	-2.67500
N	3.36500	-1.3060	-3.08500
H	4.13800	-1.3030	-3.73900
H	2.93700	-2.1930	-2.85800
C	0.15900	1.02900	-0.04400
O	-0.8600	0.9150	-0.72900
H	0.08000	1.13700	0.97900
N	-2.6140	1.0420	-3.05800
H	-1.8940	0.6490	-2.46000
C	-2.1320	1.8430	-4.20800
H	-2.9060	1.8600	-4.97500
C	-1.9090	3.2960	-3.74500
H	-2.5010	3.4500	-2.84100
C	-0.4770	3.7020	-3.40000
H	-0.4870	4.6950	-2.95300
H	-0.0570	2.9960	-2.68500
H	0.14200	3.73500	-4.29300
O	-2.4190	4.1810	-4.70900
H	-1.9480	4.1010	-5.55700
C	-0.8940	1.2070	-4.85600
O	-0.3830	0.2050	-4.36900
H	-3.2110	0.2900	-3.40100

N	**-0.4440**	**1.7770**	**-5.97100**
H	**-0.9770**	**2.5720**	**-6.29900**
C	**0.77500**	**1.46400**	**-6.74200**
H	**0.84900**	**2.25400**	**-7.49000**
C	**2.05900**	**1.55800**	**-5.87700**
H	**1.94900**	**2.38700**	**-5.17700**
H	**2.17800**	**0.64700**	**-5.28900**
C	**3.33700**	**1.81800**	**-6.69700**
O	**4.44700**	**1.41900**	**-6.27300**
O	**3.27000**	**2.52100**	**-7.73500**
C	**0.64900**	**0.15200**	**-7.54300**
O	**1.27700**	**-0.8610**	**-7.23400**
H	**0.02100**	**0.12200**	**-8.36100**
O	**-0.9980**	**3.1230**	**-9.72300**
H	**-0.3270**	**3.2360**	**-10.44400**
H	**-1.8170**	**3.2660**	**-10.23100**
O	**-1.3800**	**4.1450**	**-7.24300**
H	**-0.4920**	**4.5690**	**-7.25400**
H	**-1.3880**	**3.7780**	**-8.16200**
C	**2.20500**	**6.61400**	**-4.09800**
C	**1.82700**	**5.35500**	**-6.26800**
N	**3.08500**	**4.90900**	**-6.20100**
C	**4.06400**	**5.31500**	**-5.17300**
C	**3.49500**	**5.88700**	**-3.80700**
C	**3.17400**	**4.76500**	**-2.80000**
C	**4.43600**	**4.05400**	**-2.32400**
N	**5.37100**	**5.04100**	**-1.76600**
O	**1.15200**	**5.00000**	**-7.20700**
C	**1.43400**	**6.29000**	**-5.19200**
N	**1.52400**	**7.53300**	**-3.32100**
C	**0.31500**	**7.75400**	**-3.94100**
C	**0.20800**	**6.99600**	**-5.08000**
C	**-0.6690**	**8.6820**	**-3.43600**
N	**-0.3180**	**9.4460**	**-2.40900**
C	**-1.2120**	**10.336**	**-1.98900**
N	**-2.4340**	**10.515**	**-2.50100**
C	**-2.7920**	**9.7290**	**-3.51500**
C	**-1.9110**	**8.8060**	**-4.01200**
C	**-0.8150**	**11.192**	**-0.80500**
C	**-1.5160**	**12.400**	**-0.54200**
C	**0.25100**	**10.8110**	**0.06500**
C	**0.54700**	**11.6330**	**1.14000**
C	**-1.1690**	**13.215**	**0.53900**
C	**-0.1360**	**12.799**	**1.36400**

O	**1.52300**	**11.4550**	**2.07800**
O	**0.36400**	**13.4510**	**2.45400**
C	**1.45800**	**12.6200**	**2.95200**
C	**5.76500**	**6.09100**	**-2.71200**
C	**4.51200**	**6.84600**	**-3.15600**
H	**3.31600**	**4.13600**	**-6.81700**
H	**4.65700**	**6.10200**	**-5.64700**
H	**4.73700**	**4.47300**	**-5.00500**
H	**2.50100**	**4.03600**	**-3.25200**
H	**2.66300**	**5.18300**	**-1.93000**
H	**4.91200**	**3.52300**	**-3.14900**
H	**4.16900**	**3.32700**	**-1.55700**
H	**6.21200**	**4.53100**	**-1.48500**
H	**1.82700**	**7.94800**	**-2.44500**
H	**-0.6220**	**6.9330**	**-5.78100**
H	**-3.7850**	**9.8600**	**-3.93900**
H	**-2.2110**	**8.1650**	**-4.82900**
H	**-2.3240**	**12.730**	**-1.19400**
H	**0.83300**	**9.90000**	**-0.06900**
H	**-1.6810**	**14.150**	**0.73700**
H	**2.40900**	**13.1750**	**2.90400**
H	**1.24900**	**12.3030**	**3.98600**
H	**6.27000**	**5.64600**	**-3.57300**
H	**6.45500**	**6.78200**	**-2.22100**
H	**4.77200**	**7.63500**	**-3.86000**
H	**4.06400**	**7.32200**	**-2.28300**
H	**4.06400**	**7.32200**	**-2.28300**

Table 2: Cartesian coordinates of MK3 bound to 05B without binding site water molecules.

N	**6.86500**	**8.62100**	**-5.24900**
H	**7.03200**	**8.07200**	**-4.41800**
C	**7.19600**	**7.98200**	**-6.53600**
H	**6.80100**	**8.56300**	**-7.36700**
C	**8.73200**	**7.88300**	**-6.67100**
H	**9.10400**	**7.25700**	**-5.85700**
H	**8.96300**	**7.36500**	**-7.60400**
C	**9.51400**	**9.21400**	**-6.64700**
H	**9.28900**	**9.75100**	**-5.72500**
C	**11.02000**	**8.92300**	**-6.66600**
H	**11.58100**	**9.85700**	**-6.63500**
H	**11.29300**	**8.32400**	**-5.79600**
H	**11.28400**	**8.37600**	**-7.57200**

C	9.15400	10.11400	-7.83700
H	9.76800	11.01600	-7.81700
H	9.32700	9.58400	-8.77500
H	8.11100	10.41100	-7.77500
C	6.56800	6.58000	-6.62800
O	6.75100	5.77700	-5.71700
H	5.88800	8.91300	-5.26400
H	5.99800	6.31700	-7.44700
N	-9.49200	19.1380	-3.39600
H	-10.0180	18.811	-2.59900
C	-8.06200	18.7820	-3.42700
H	-7.54700	19.4030	-4.16400
C	-7.46700	19.0820	-2.03700
H	-7.68800	20.1170	-1.77300
H	-7.94700	18.4340	-1.30100
C	-5.94400	18.8700	-1.97700
H	-5.69900	17.8550	-2.29200
H	-5.45100	19.5710	-2.65100
C	-5.42000	19.0640	-0.54800
H	-5.64600	20.0720	-0.19700
H	-5.91300	18.3410	0.10600
C	-3.90600	18.8320	-0.51300
H	-3.68000	17.9240	-1.08000
H	-3.39200	19.6650	-1.00300
N	-3.40700	18.6670	0.87300
H	-2.41900	18.4580	0.86200
H	-3.53500	19.5060	1.43100
H	-3.91400	17.9130	1.34300
C	-7.83400	17.3050	-3.81600
O	-8.42800	16.4010	-3.21600
H	-9.93800	18.8020	-4.25000
H	-7.18200	17.0710	-4.58100
N	-0.61300	11.3490	-10.30900
H	-1.55700	11.0700	-10.56600
C	0.51000	10.55000	-10.82500
H	1.39000	10.77200	-10.22500
C	0.18700	9.05600	-10.64200
H	-0.34200	8.92800	-9.69800
H	-0.47300	8.72600	-11.44400
C	1.43300	8.15600	-10.60100
H	1.97300	8.21800	-11.54500
H	2.09300	8.48600	-9.79900
C	1.00500	6.70400	-10.34400
H	0.38500	6.66600	-9.44500

H	0.40500	6.35800	-11.18900
C	2.19700	5.75900	-10.15600
H	2.81600	5.78900	-11.05800
H	2.78800	6.09200	-9.30100
N	1.70400	4.37700	-9.94700
H	2.43700	3.69200	-9.79900
H	1.07600	4.32700	-9.15300
H	1.22300	4.07700	-10.79700
C	0.82700	10.92000	-12.29200
O	-0.05200	10.8600	-13.15500
H	-0.47400	12.3230	-10.57900
H	1.78000	11.21900	-12.55100
N	-6.19600	11.3100	-8.46900
H	-5.49500	12.0140	-8.26800
C	-6.60700	10.4430	-7.34900
H	-7.42100	9.78900	-7.65900
C	-5.40500	9.58300	-6.91800
H	-4.61700	10.2520	-6.57500
H	-5.69300	8.94900	-6.07700
C	-4.85000	8.67900	-8.02600
H	-5.60000	7.92000	-8.25700
H	-4.68000	9.26300	-8.93200
S	-3.29300	7.85300	-7.60200
C	-2.19000	9.29000	-7.61400
H	-1.15900	8.95800	-7.49400
H	-2.29700	9.81800	-8.56300
H	-2.43900	9.96500	-6.79700
C	-7.07900	11.2480	-6.12700
O	-6.76400	12.4310	-5.98600
H	-5.86800	10.7260	-9.23800
H	-7.66900	10.7910	-5.41400
N	-4.48200	11.3580	-0.25300
H	-4.03000	11.1010	-1.12300
C	-4.21600	10.4960	0.92600
H	-5.17200	10.2750	1.39500
C	-3.60700	9.15300	0.48000
H	-2.65400	9.33400	-0.01000
H	-3.40100	8.54600	1.36000
C	-4.51900	8.35800	-0.46900
H	-4.77200	8.98100	-1.32800
H	-3.96400	7.50000	-0.84900
S	-6.06200	7.75700	0.26100
C	-5.39000	6.46200	1.32200
H	-6.19600	5.97000	1.86600

H	-4.86600	5.72800	0.71200
H	-4.68800	6.89100	2.03200
C	-3.37100	11.1720	2.02900
O	-2.29900	10.7070	2.41800
H	-5.48900	11.4090	-0.40600
N	-3.86500	12.2940	2.54800
H	-4.78600	12.5690	2.21500
C	-3.18000	13.1800	3.50800
H	-2.12200	13.1670	3.24900
C	-3.65000	14.6310	3.28400
H	-3.08600	15.3030	3.93100
H	-3.39800	14.8820	2.25400
C	-5.15600	14.8650	3.50200
H	-5.72600	14.0860	3.00300
H	-5.37200	14.8140	4.57000
C	-5.65400	16.2020	2.95000
O	-6.72600	16.6530	3.42300
O	-5.02800	16.7540	2.01400
C	-3.22400	12.7070	4.98200
O	-3.24000	13.5130	5.91300
H	-3.24000	11.6960	5.18800
N	4.47400	-0.11000	2.70800
H	5.15100	-0.86200	2.55600
C	4.68200	1.14400	1.96900
H	4.91700	1.92700	2.68800
C	5.86500	1.01300	0.98700
H	5.58300	0.36200	0.16000
H	6.04900	2.00400	0.56900
C	7.18200	0.51200	1.60000
H	8.01300	0.99500	1.08300
H	7.22400	0.80300	2.64700
C	7.34600	-1.00300	1.47700
O	8.11300	-1.43800	0.59100
O	6.66300	-1.72200	2.23800
C	3.44500	1.59800	1.17600
O	3.12600	2.78400	1.15400
H	3.53800	-0.46200	2.50500
N	2.73600	0.65900	0.53900
H	3.01900	-0.30100	0.65900
C	1.60000	0.94000	-0.35100
H	1.79400	1.87700	-0.87500
C	1.51100	-0.18600	-1.40300
H	1.36700	-1.13900	-0.89400
H	0.64400	-0.01200	-2.04000

C	2.71900	-0.30200	-2.33200
O	3.58200	0.56000	-2.42100
N	2.82800	-1.40900	-3.03600
H	3.59200	-1.51000	-3.69500
H	2.20000	-2.18100	-2.89000
C	0.25100	1.11900	0.39400
O	-0.78500	1.30600	-0.25000
H	0.22000	1.08200	1.42500
N	-2.56400	1.16900	-2.90500
H	-1.79800	0.78900	-2.36400
C	-2.20600	1.94200	-4.11800
H	-3.08400	2.02300	-4.75800
C	-1.82700	3.37100	-3.71300
H	-2.52800	3.71900	-2.95300
C	-0.41300	3.49900	-3.16200
H	-0.25800	4.51000	-2.78700
H	-0.26800	2.79700	-2.34400
H	0.31100	3.28600	-3.94800
O	-1.93000	4.20600	-4.83400
H	-1.39900	4.98900	-4.65800
C	-1.13700	1.26700	-4.98900
O	-0.56300	0.25200	-4.60300
H	-3.19300	0.41000	-3.16900
N	-0.92400	1.86200	-6.16300
H	-1.41600	2.73900	-6.25800
C	-0.11800	1.43100	-7.32500
H	-0.24600	2.23100	-8.05600
C	1.39800	1.37300	-7.01400
H	1.61000	2.00100	-6.14800
H	1.67800	0.35000	-6.75400
C	2.26400	1.86000	-8.19500
O	3.23400	2.63000	-7.99100
O	1.93900	1.56700	-9.36500
C	-0.63000	0.15000	-8.03000
O	-1.22400	-0.7380	-7.42200
H	-0.46700	0.03900	-9.04300
C	1.88200	6.28200	-3.92400
C	1.50100	5.09900	-6.15000
N	2.68500	4.50600	-5.98100
C	3.68800	4.89000	-4.96900
C	3.17400	5.54900	-3.62800
C	2.91200	4.48700	-2.53700
C	4.20600	3.86300	-2.01500
N	5.08600	4.93600	-1.54100

O	0.87700	4.85400	-7.16100
C	1.13700	6.04200	-5.06200
N	1.25700	7.25400	-3.16900
C	0.10400	7.59500	-3.83400
C	-0.01800	6.86800	-4.99400
C	-0.78500	8.63500	-3.36900
N	-0.38000	9.39300	-2.35300
C	-1.19400	10.3820	-1.98300
N	-2.39400	10.6350	-2.51800
C	-2.80600	9.85400	-3.51200
C	-2.00000	8.85000	-3.97300
C	-0.75200	11.2690	-0.83200
C	-1.45700	12.4790	-0.58200
C	0.33800	10.92500	0.02800
C	0.63500	11.77300	1.08900
C	-1.11400	13.3150	0.48100
C	-0.07700	12.9250	1.30600
O	1.62900	11.64000	2.02500
O	0.40100	13.59700	2.39300
C	1.43900	12.74900	2.96200
C	5.47300	5.86600	-2.60000
C	4.20600	6.56700	-3.08500
H	2.92700	3.78900	-6.65800
H	4.29300	5.63900	-5.47600
H	4.32600	4.02600	-4.77500
H	2.28900	3.69100	-2.93500
H	2.38600	4.94000	-1.69700
H	4.70600	3.29000	-2.80000
H	3.97800	3.18600	-1.19100
H	5.91500	4.51100	-1.13500
H	1.57100	7.64900	-2.28900
H	-0.79200	6.92600	-5.75900
H	-3.77800	10.0590	-3.95700
H	-2.33900	8.22400	-4.78600
H	-2.27600	12.7960	-1.22700
H	0.92400	10.01700	-0.09600
H	-1.64500	14.2420	0.67200
H	2.37300	13.32000	3.08600
H	1.09800	12.35600	3.93400
H	5.95900	5.32100	-3.41000
H	6.17000	6.60700	-2.19900
H	4.45100	7.29400	-3.85900
H	3.78000	7.11000	-2.24000

Table 3: Cartesian coordinates of MK2 bound to 05B.			
N	**2.53000**	**6.02200**	**-22.38800**
H	**1.67100**	**5.56700**	**-22.65900**
C	**2.40000**	**7.30900**	**-21.70000**
H	**3.19800**	**7.96300**	**-22.05700**
C	**1.06800**	**7.98400**	**-22.14100**
H	**1.07400**	**9.00100**	**-21.74400**
H	**1.10800**	**8.09100**	**-23.22700**
C	**-0.31200**	**7.35600**	**-21.79100**
H	**-0.45800**	**7.36300**	**-20.71300**
C	**-1.42200**	**8.23100**	**-22.39200**
H	**-2.39900**	**7.85600**	**-22.08800**
H	**-1.31900**	**9.25800**	**-22.03900**
H	**-1.36100**	**8.22100**	**-23.48100**
C	**-0.51100**	**5.91100**	**-22.27600**
H	**-1.54600**	**5.60700**	**-22.11900**
H	**-0.27700**	**5.83400**	**-23.33800**
H	**0.12100**	**5.23300**	**-21.70300**
C	**2.67400**	**7.19300**	**-20.18200**
O	**3.76400**	**6.77700**	**-19.79400**
H	**3.11700**	**6.14400**	**-23.21400**
H	**1.94800**	**7.46300**	**-19.50000**
N	**15.80000**	**-7.0290**	**-18.43500**
H	**15.20200**	**-7.7360**	**-18.03800**
C	**15.14800**	**-5.9590**	**-19.21100**
H	**15.74200**	**-5.7540**	**-20.10200**
C	**13.81000**	**-6.5600**	**-19.69000**
H	**14.04400**	**-7.4600**	**-20.26200**
H	**13.22900**	**-6.8750**	**-18.82300**
C	**12.93700**	**-5.6620**	**-20.58000**
H	**12.57300**	**-4.8160**	**-20.00000**
H	**13.52500**	**-5.2810**	**-21.41400**
C	**11.74700**	**-6.4640**	**-21.13900**
H	**12.00300**	**-6.8090**	**-22.14300**
H	**11.55200**	**-7.3390**	**-20.51500**
C	**10.47100**	**-5.6200**	**-21.18000**
H	**10.13800**	**-5.4520**	**-20.15300**
H	**10.69500**	**-4.6510**	**-21.63000**
N	**9.40700**	**-6.29600**	**-21.96000**
H	**9.27300**	**-7.25300**	**-21.62600**
H	**8.52500**	**-5.81600**	**-21.86200**
H	**9.65600**	**-6.29200**	**-22.94400**
C	**15.09600**	**-4.6030**	**-18.45200**
O	**16.08500**	**-3.8730**	**-18.46400**

H	**16.35400**	**-6.6070**	**-17.69000**
H	**14.24300**	**-4.3200**	**-17.94500**
N	**10.96700**	**5.67300**	**-16.96100**
H	**11.36500**	**5.40200**	**-16.06500**
C	**10.08800**	**6.86400**	**-17.01700**
H	**9.45600**	**6.76900**	**-17.89900**
C	**9.14200**	**6.92500**	**-15.79000**
H	**8.67000**	**5.95200**	**-15.66200**
H	**9.72100**	**7.14100**	**-14.89400**
C	**8.02400**	**7.98200**	**-15.94200**
H	**8.47400**	**8.94400**	**-16.17800**
H	**7.38700**	**7.70000**	**-16.78100**
C	**7.14400**	**8.16000**	**-14.68600**
H	**6.65700**	**7.21300**	**-14.43900**
H	**7.76700**	**8.46900**	**-13.84500**
C	**6.07400**	**9.23300**	**-14.96400**
H	**6.56000**	**10.12800**	**-15.36000**
H	**5.39800**	**8.85000**	**-15.73500**
N	**5.26500**	**9.61300**	**-13.77500**
H	**4.50500**	**10.22500**	**-14.06100**
H	**4.79800**	**8.82000**	**-13.33800**
H	**5.76800**	**10.15000**	**-13.06700**
C	**10.91400**	**8.15900**	**-17.18200**
O	**11.85600**	**8.40700**	**-16.42300**
H	**11.72600**	**5.79600**	**-17.63100**
H	**10.67600**	**8.82400**	**-17.93500**
N	**12.86600**	**1.59100**	**-13.61500**
H	**12.99500**	**1.57700**	**-14.62600**
C	**11.71200**	**0.85200**	**-13.07200**
H	**11.62800**	**1.03600**	**-12.00100**
C	**10.41900**	**1.35300**	**-13.73900**
H	**10.37900**	**0.99500**	**-14.76900**
H	**9.56600**	**0.93900**	**-13.19900**
C	**10.30800**	**2.88400**	**-13.76500**
H	**10.54200**	**3.28900**	**-12.78200**
H	**11.05200**	**3.27000**	**-14.46500**
S	**8.69400**	**3.49700**	**-14.28900**
C	**7.84500**	**3.47100**	**-12.69300**
H	**6.80000**	**3.75300**	**-12.83200**
H	**7.89500**	**2.47400**	**-12.26100**
H	**8.31100**	**4.18800**	**-12.01800**
C	**11.84200**	**-0.6640**	**-13.28200**
O	**12.11800**	**-1.1150**	**-14.39600**
H	**12.81500**	**2.56000**	**-13.30200**

H	11.69800	-1.3070	-12.48800
N	8.05200	-5.82000	-15.70400
H	8.19800	-5.16000	-16.45100
C	6.67700	-6.32900	-15.53200
H	6.66300	-7.02700	-14.69600
C	5.75100	-5.13600	-15.18300
H	5.66100	-4.51200	-16.07000
H	4.75300	-5.51400	-14.95700
C	6.21800	-4.24800	-14.00700
H	7.23100	-3.90400	-14.20000
C	5.34700	-2.99400	-13.89700
H	5.86000	-2.26200	-13.27800
H	5.19000	-2.55700	-14.88200
H	4.39000	-3.23900	-13.44300
C	6.19500	-4.98800	-12.66000
H	6.50900	-4.30800	-11.86800
H	5.18900	-5.35200	-12.44800
H	6.88400	-5.82900	-12.67900
C	6.17800	-7.15800	-16.74200
O	5.10000	-6.92700	-17.29000
H	8.36500	-5.40400	-14.82700
N	6.96100	-8.15900	-17.15700
H	7.82700	-8.29300	-16.65400
C	6.65300	-9.11500	-18.24600
H	6.27700	-8.53800	-19.09200
C	7.95500	-9.79600	-18.70700
H	8.44300	-10.2690	-17.85200
H	7.72400	-10.5760	-19.43500
C	8.90900	-8.80200	-19.37300
O	8.80900	-8.60400	-20.60700
O	9.73700	-8.20200	-18.65700
C	5.52600	-10.1350	-17.92000
O	5.47500	-11.2360	-18.47500
H	4.80500	-9.88600	-17.22500
N	-4.46000	1.17800	-16.02800
H	-5.30400	1.73100	-16.18400
C	-3.18300	1.85300	-16.30400
H	-2.63900	1.27200	-17.05000
C	-3.44700	3.26500	-16.87100
H	-3.81300	3.91800	-16.07700
H	-2.48800	3.66800	-17.19700
C	-4.41200	3.33400	-18.07100
H	-4.10700	4.17600	-18.69400
H	-4.31800	2.42800	-18.67200

C	-5.88300	3.54600	-17.68500
O	-6.61200	4.16200	-18.49200
O	-6.29000	3.09700	-16.58900
C	-2.28300	1.98300	-15.05900
O	-1.07200	2.17100	-15.16500
H	-4.45700	0.83800	-15.06600
N	-2.86400	1.87000	-13.86200
H	-3.85200	1.65700	-13.83800
C	-2.12700	1.84000	-12.60400
H	-1.23200	2.43500	-12.74600
C	-2.95600	2.53600	-11.50200
H	-4.00600	2.58500	-11.78300
H	-2.89400	1.96800	-10.57500
C	-2.45400	3.94700	-11.21800
O	-3.15300	4.92900	-11.41100
N	-1.23000	4.08500	-10.74600
H	-0.85100	5.01400	-10.59800
H	-0.64300	3.28000	-10.62000
C	-1.64600	0.42900	-12.18500
O	-0.91000	0.34100	-11.20500
H	-1.93400	-0.4100	-12.71200
N	1.77800	1.17300	-10.32300
H	0.84100	1.06200	-10.69700
C	2.75200	1.86400	-11.21100
H	3.72800	1.40900	-11.06700
C	2.40400	1.67300	-12.69800
H	3.08900	2.26700	-13.30800
C	2.49200	0.21600	-13.14200
H	2.25600	0.15400	-14.20300
H	3.50300	-0.15600	-12.98600
H	1.78800	-0.39900	-12.58000
O	1.08300	2.09200	-12.92300
H	0.85500	1.96100	-13.85500
C	2.98300	3.34600	-10.89800
O	3.98600	3.66700	-10.27100
H	1.72700	1.66800	-9.43300
N	2.11500	4.23500	-11.38600
H	1.37100	3.83800	-11.94100
C	2.34500	5.69000	-11.50900
H	3.42100	5.86100	-11.42200
C	1.91200	6.13700	-12.92100
H	2.03800	5.30100	-13.60800
H	0.84900	6.38000	-12.91400
C	2.70100	7.33600	-13.46900

O	2.71300	7.52000	-14.71000
O	3.28100	8.10400	-12.66800
C	1.64300	6.55600	-10.43400
O	0.52200	6.26600	-10.00700
H	2.12300	7.39300	-10.06700
C	3.95400	2.31400	-16.89300
C	4.28300	4.13800	-15.14200
N	3.40400	4.89500	-15.80800
C	2.78100	4.54400	-17.09900
C	2.81500	3.03100	-17.57300
C	1.52300	2.28200	-17.18900
C	0.30600	2.77900	-17.96800
N	0.60000	2.70200	-19.40000
O	4.77400	4.58900	-14.13300
C	4.57100	2.82400	-15.77000
N	4.49900	1.08000	-17.19300
C	5.50100	0.85600	-16.27900
C	5.55700	1.88400	-15.37100
C	6.40000	-0.27200	-16.35800
N	6.14500	-1.20600	-17.27000
C	7.01000	-2.21500	-17.34300
N	8.11800	-2.34900	-16.60900
C	8.37000	-1.41500	-15.70000
C	7.51100	-0.35800	-15.55000
C	6.70100	-3.34100	-18.31000
C	7.71300	-4.29300	-18.60000
C	5.40600	-3.52100	-18.88400
C	5.18400	-4.64600	-19.66800
C	7.45000	-5.41300	-19.38800
C	6.17700	-5.55800	-19.91000
O	4.02900	-5.01600	-20.29800
O	5.73800	-6.55400	-20.73100
C	4.31300	-6.30700	-20.91900
C	1.75600	3.49300	-19.82100
C	2.98700	2.94700	-19.10600
H	3.22100	5.81100	-15.40900
H	3.30700	5.14900	-17.83900
H	1.75200	4.90200	-17.06500
H	1.34400	2.38500	-16.11900
H	1.64300	1.22000	-17.40000
H	0.05300	3.80600	-17.69200
H	-0.55000	2.13800	-17.74900
H	-0.22400	2.95700	-19.93800
H	4.24200	0.46200	-17.95600

H	**6.23300**	**2.01600**	**-14.53300**
H	**9.29900**	**-1.50000**	**-15.13700**
H	**7.72900**	**0.41400**	**-14.83000**
H	**8.71400**	**-4.18100**	**-18.18800**
H	**4.57900**	**-2.83600**	**-18.71100**
H	**8.18600**	**-6.19500**	**-19.53300**
H	**4.06400**	**-6.28100**	**-21.99200**
H	**3.73800**	**-7.09600**	**-20.40800**
H	**1.59900**	**4.54800**	**-19.58300**
H	**1.88600**	**3.39100**	**-20.89900**
H	**3.87100**	**3.50300**	**-19.41600**
H	**3.12300**	**1.90800**	**-19.41200**

Table 4: Cartesian coordinates of MK3 bound to P4O.			
N	**-3.23900**	**12.82300**	**1.99900**
H	**-3.10100**	**12.78900**	**3.00200**
C	**-2.39100**	**11.97300**	**1.15000**
H	**-2.45900**	**12.29600**	**0.10900**
C	**-0.93100**	**12.13500**	**1.62000**
H	**-0.84600**	**11.74600**	**2.63500**
H	**-0.30400**	**11.51700**	**0.97900**
C	**-0.37200**	**13.57600**	**1.60000**
H	**-0.93600**	**14.19300**	**2.30200**
C	**1.08900**	**13.54900**	**2.06800**
H	**1.51800**	**14.54900**	**2.01500**
H	**1.13600**	**13.19800**	**3.09800**
H	**1.67500**	**12.88400**	**1.43700**
C	**-0.45900**	**14.22600**	**0.21000**
H	**0.04300**	**15.19400**	**0.22000**
H	**0.01600**	**13.58700**	**-0.53300**
H	**-1.50100**	**14.38400**	**-0.06600**
C	**-2.79700**	**10.48500**	**1.13700**
O	**-2.58500**	**9.81000**	**0.13000**
H	**-4.21700**	**12.61700**	**1.79600**
H	**-3.24200**	**10.05900**	**1.96500**
N	**0.77000**	**11.01000**	**9.82700**
H	**1.67000**	**10.70900**	**10.19500**
C	**-0.41400**	**10.16900**	**10.07200**
H	**-1.19500**	**10.46300**	**9.37500**
C	**-0.06000**	**8.70800**	**9.75900**
H	**0.49400**	**8.67300**	**8.81900**
H	**0.57900**	**8.31400**	**10.54600**

C	-1.30900	7.82300	9.63000
H	-1.85900	7.83000	10.56800
H	-1.96100	8.21500	8.85000
C	-0.89400	6.38900	9.28000
H	-0.27000	6.40600	8.38400
H	-0.30200	5.97800	10.10100
C	-2.10600	5.48600	9.02800
H	-2.72600	5.45200	9.92800
H	-2.70400	5.89900	8.21100
N	-1.65300	4.12100	8.68400
H	-2.42700	3.47700	8.54600
H	-1.09200	4.12600	7.83900
H	-1.09400	3.73500	9.44500
C	-0.98700	10.36000	11.49300
O	-0.31400	10.08500	12.48900
H	0.57700	11.95200	10.16800
H	-1.94600	10.72300	11.61100
N	7.62300	11.97000	2.27500
H	8.49200	12.45800	2.11800
C	6.54700	12.13200	1.29400
H	5.60200	11.84900	1.76200
C	6.45300	13.61600	0.92600
H	6.60000	14.22200	1.81700
H	7.21900	13.87600	0.19000
S	4.79400	13.95500	0.28100
H	4.12500	13.77600	1.43000
C	6.75000	11.19400	0.08400
O	7.82700	11.15600	-0.51600
H	7.82100	10.97500	2.38200
N	5.71000	10.44400	-0.28800
H	4.86200	10.51500	0.26100
C	5.69400	9.53600	-1.45100
H	6.71700	9.27400	-1.72000
C	4.97200	8.22800	-1.09500
H	3.96100	8.44500	-0.75800
H	4.89900	7.61000	-1.98800
C	5.72000	7.44800	0.00000
H	5.76800	8.06400	0.90000
H	5.14100	6.56000	0.25400
S	7.41000	6.93600	-0.42000
C	7.00700	5.62900	-1.59700
H	7.92000	5.18300	-1.99000
H	6.41100	4.86400	-1.10500
H	6.42400	6.04000	-2.41600

C	5.11500	10.24600	-2.68100
O	4.04500	9.92300	-3.19600
N	5.83600	11.27400	-3.12800
H	6.74300	11.41600	-2.69600
C	5.40500	12.24300	-4.14700
H	4.41800	12.60500	-3.86900
C	6.36200	13.44600	-4.15900
H	7.35700	13.11700	-4.46200
H	5.99500	14.16500	-4.89100
C	6.45300	14.15300	-2.80100
H	5.47700	14.56900	-2.55100
H	6.73800	13.43600	-2.03300
C	7.48400	15.27500	-2.81500
O	8.50000	15.17800	-2.09200
O	7.27700	16.28400	-3.53400
C	5.26700	11.65800	-5.56600
O	4.79700	12.34300	-6.47900
H	5.56900	10.68900	-5.75400
N	-3.60200	0.44900	-2.94400
H	-4.41000	-0.16100	-2.80000
C	-3.57200	1.70500	-2.17800
H	-3.47800	2.53200	-2.88300
C	-4.89700	1.88800	-1.41500
H	-4.95100	1.16600	-0.60000
H	-4.88900	2.88100	-0.96500
C	-6.15800	1.77700	-2.28700
H	-6.88600	2.50900	-1.93200
H	-5.91900	2.02300	-3.32200
C	-6.79000	0.38700	-2.20600
O	-6.15400	-0.60800	-2.62100
O	-7.91500	0.27300	-1.67900
C	-2.40200	1.82400	-1.17700
O	-2.04800	2.94000	-0.80200
H	-3.52200	0.66500	-3.93800
N	-1.80200	0.70500	-0.74500
H	-2.10800	-0.16900	-1.14900
C	-0.70200	0.65700	0.24200
H	-0.72600	1.57000	0.83900
C	-0.94400	-0.53900	1.19500
H	-1.06700	-1.44800	0.60600
H	-0.06800	-0.67600	1.82800
C	-2.14300	-0.38500	2.13800
O	-2.62900	0.69500	2.43500
N	-2.67300	-1.46900	2.66100

H	-2.37100	-2.39300	2.38200
H	-3.45500	-1.39300	3.30000
C	0.71800	0.60300	-0.39900
O	1.71900	0.49400	0.31400
H	0.82100	0.65900	-1.42400
N	7.87200	11.24800	-9.39500
H	7.87300	12.21900	-9.09700
C	7.50500	10.95200	-10.79700
H	6.97700	9.99900	-10.82500
C	6.52800	12.03000	-11.31600
H	6.78300	13.01100	-10.91100
H	6.62600	12.09700	-12.40100
C	5.05200	11.68900	-11.03500
H	4.44300	12.13300	-11.81800
H	4.91000	10.60900	-11.08700
C	4.51600	12.21800	-9.70500
H	5.21700	11.97200	-8.91600
H	4.41000	13.30200	-9.76300
C	3.15600	11.57200	-9.42300
H	2.51100	11.72400	-10.29400
H	3.29500	10.49400	-9.30900
N	2.50600	12.13800	-8.21700
H	1.72900	11.54800	-7.92900
H	3.17100	12.22600	-7.45300
H	2.10400	13.04500	-8.43900
C	8.69200	10.73100	-11.77200
O	8.46300	10.34000	-12.91400
H	8.78900	10.84500	-9.20400
H	9.66100	10.91000	-11.46500
N	3.80500	0.28200	2.89800
H	3.01000	-0.06800	2.37400
C	3.52500	0.87800	4.22300
H	4.31600	0.57200	4.90600
C	3.59000	2.40500	4.13800
H	4.40300	2.67200	3.46700
C	2.32100	3.08400	3.62300
H	2.50100	4.15500	3.52700
H	2.06200	2.68200	2.64400
H	1.48900	2.92400	4.30700
O	3.92000	2.86700	5.42000
H	3.22600	3.49300	5.72100
C	2.22600	0.39100	4.86000
O	1.45000	-0.31300	4.22200
H	4.30400	0.96400	2.32700

N	2.04100	0.77600	6.12300
H	2.77700	1.38100	6.46100
C	0.86900	0.61900	7.00800
H	0.93800	1.42700	7.74000
C	-0.46000	0.82800	6.25500
H	-0.31800	1.60900	5.50500
H	-0.74600	-0.08800	5.73600
C	-1.60400	1.25900	7.17500
O	-2.38800	2.14000	6.75500
O	-1.73000	0.74100	8.31000
C	0.87300	-0.70600	7.80200
O	0.77500	-1.79500	7.23800
H	0.96000	-0.67700	8.83000
N	-1.79500	3.97600	4.68600
C	-2.18300	3.59500	3.32900
C	-0.93000	5.60600	2.64200
C	-0.32200	5.64100	3.85900
C	-0.82800	4.85100	4.99200
C	-2.15400	4.80200	2.39200
O	-0.47200	4.92100	6.15000
C	0.74300	6.59300	3.79100
C	0.67200	7.14400	2.53200
N	-0.35700	6.54000	1.82700
C	1.47600	8.25300	2.02600
C	2.55900	8.76100	2.71800
C	3.28100	9.81600	2.20500
N	2.96400	10.37300	1.02900
C	1.91500	9.89500	0.34900
C	1.15300	8.85100	0.82500
C	1.60500	10.54600	-0.94700
C	2.13000	11.79900	-1.27900
C	1.80500	12.36300	-2.50300
C	0.79300	9.90900	-1.88300
N	0.46800	10.43600	-3.07400
C	0.98200	11.64200	-3.37300
C	0.65300	12.20100	-4.60200
C	1.12200	13.46200	-4.96700
C	1.94100	14.17200	-4.09100
C	2.28300	13.63100	-2.85300
H	-2.11900	3.39600	5.45000
H	-3.18400	3.15200	3.33700
H	-1.46800	2.84800	2.97000
H	-2.18300	4.46300	1.35500
H	-3.03200	5.41400	2.57400

H	**1.41100**	**6.86200**	**4.60900**
H	**-0.67700**	**6.76300**	**0.88300**
H	**2.85800**	**8.32800**	**3.66300**
H	**4.13900**	**10.23100**	**2.73200**
H	**0.28500**	**8.51100**	**0.29300**
H	**2.76800**	**12.34900**	**-0.59600**
H	**-0.00100**	**11.64500**	**-5.26500**
H	**0.83500**	**13.90100**	**-5.92300**
H	**2.30500**	**15.15800**	**-4.37400**
H	**2.91900**	**14.19300**	**-2.16900**
H	**0.36900**	**8.92500**	**-1.70300**
O	**1.56500**	**3.98700**	**9.23600**
H	**2.41100**	**3.72700**	**9.64600**
H	**0.93600**	**3.69900**	**9.95000**
O	**2.08200**	**4.36300**	**6.64800**
H	**1.94800**	**4.24000**	**7.61900**
H	**1.17700**	**4.64400**	**6.39600**

Table 5: Cartesian coordinates of MK3 bound to P4O without binding site water molecules.

N	**-2.52300**	**14.22500**	**2.68800**
H	**-2.35000**	**14.30000**	**3.68200**
C	**-1.77700**	**13.20500**	**1.93800**
H	**-1.67800**	**13.51000**	**0.89400**
C	**-0.37100**	**13.10400**	**2.55700**
H	**-0.46200**	**12.73200**	**3.57700**
H	**0.19400**	**12.36800**	**1.98900**
C	**0.43400**	**14.42200**	**2.58800**
H	**-0.04900**	**15.11300**	**3.27600**
C	**1.84000**	**14.12700**	**3.12400**
H	**2.41900**	**15.04900**	**3.17600**
H	**1.76900**	**13.70400**	**4.12600**
H	**2.35000**	**13.41900**	**2.47200**
C	**0.51200**	**15.09800**	**1.21100**
H	**1.25600**	**15.89300**	**1.21600**
H	**0.78400**	**14.36900**	**0.45600**
H	**-0.45400**	**15.53100**	**0.95300**
C	**-2.46100**	**11.82700**	**1.90000**
O	**-2.27700**	**11.08400**	**0.93400**
H	**-3.52100**	**14.07900**	**2.53800**
H	**-3.06900**	**11.52700**	**2.67800**
N	**1.73500**	**11.64500**	**10.34000**

H	2.65800	11.36900	10.66700
C	0.58800	10.79200	10.68700
H	-0.23300	11.04100	10.01600
C	0.94400	9.32100	10.41800
H	1.39900	9.25000	9.42900
H	1.66800	8.98000	11.16000
C	-0.29600	8.41200	10.44400
H	-0.76800	8.47300	11.42100
H	-1.01400	8.75000	9.69800
C	0.09500	6.95700	10.15200
H	0.58800	6.90800	9.17900
H	0.79900	6.61900	10.91700
C	-1.12100	6.02100	10.14600
H	-1.60300	6.06700	11.12700
H	-1.82700	6.35400	9.38100
N	-0.68000	4.62900	9.88800
H	-1.42300	3.93900	9.91200
H	-0.19900	4.55300	8.99900
H	-0.06200	4.35100	10.65200
C	0.10000	11.06000	12.12800
O	0.83200	10.86400	13.10200
H	1.76600	11.75500	9.32600
H	-0.85900	11.41000	12.27900
N	7.79100	12.20900	2.51900
H	8.60700	12.79900	2.46600
C	6.59900	12.60900	1.76500
H	5.71600	12.24200	2.29000
C	6.54600	14.14200	1.75700
H	6.75000	14.53300	2.75600
H	7.29600	14.53600	1.06500
S	4.88800	14.65200	1.23400
H	4.20600	14.17300	2.28300
C	6.57300	11.98900	0.35100
O	7.44200	12.26400	-0.47600
H	8.05200	11.26300	2.24200
N	5.56700	11.15900	0.06000
H	4.88500	10.97800	0.78400
C	5.46700	10.37100	-1.18500
H	6.47300	10.07700	-1.47800
C	4.68000	9.07300	-0.92600
H	3.66200	9.31600	-0.63300
H	4.62400	8.50100	-1.85200
C	5.32800	8.20100	0.16400
H	5.37300	8.76600	1.09600

H	4.69100	7.33600	0.34800
S	7.00100	7.61400	-0.20300
C	6.57700	6.36500	-1.42900
H	7.48000	5.88200	-1.80100
H	5.92500	5.61600	-0.98000
H	6.04700	6.82500	-2.25600
C	4.91200	11.18300	-2.36900
O	3.81600	10.92500	-2.86300
N	5.69400	12.16900	-2.82300
H	6.58100	12.28300	-2.33800
C	5.33800	13.20300	-3.82200
H	4.51200	13.78800	-3.42800
C	6.53200	14.16300	-4.01300
H	7.39300	13.58900	-4.34300
H	6.30700	14.86700	-4.81500
C	6.93700	14.96000	-2.76200
H	6.55300	14.48800	-1.85700
H	8.02600	14.97300	-2.69700
C	6.43300	16.39700	-2.82600
O	7.26200	17.33400	-2.78900
O	5.20100	16.59700	-2.91000
C	4.88000	12.67700	-5.20300
O	4.48300	13.46300	-6.06500
H	4.90700	11.66500	-5.40300
N	-3.94000	1.29200	-2.24800
H	-4.72600	0.63700	-2.22400
C	-3.98100	2.42400	-1.30300
H	-4.11400	3.34300	-1.87400
C	-5.17100	2.27500	-0.33000
H	-4.96900	1.45700	0.36000
H	-5.21600	3.18900	0.26400
C	-6.55900	2.07000	-0.96400
H	-7.30300	2.53000	-0.31300
H	-6.60300	2.58000	-1.92600
C	-6.91800	0.59100	-1.13400
O	-6.36100	-0.03300	-2.06300
O	-7.71400	0.07900	-0.31200
C	-2.69600	2.58600	-0.46200
O	-2.36300	3.69200	-0.04100
H	-3.84100	1.65500	-3.19600
N	-1.97000	1.48700	-0.22800
H	-2.27900	0.63000	-0.66600
C	-0.76900	1.42000	0.61200
H	-0.72100	2.31800	1.23000

C	-0.91100	0.20500	1.55600
H	-0.99900	-0.70300	0.95900
H	-0.01200	0.11700	2.16500
C	-2.09800	0.27700	2.52100
O	-2.75800	1.28700	2.70500
N	-2.42400	-0.82400	3.16200
H	-2.00900	-1.70800	2.92300
H	-3.18000	-0.79400	3.83900
C	0.55300	1.37200	-0.20400
O	1.61800	1.12600	0.36800
H	0.54000	1.54500	-1.22100
N	7.44700	12.26000	-8.87200
H	7.48500	13.21500	-8.52700
C	7.21600	12.06300	-10.31700
H	6.47500	11.27600	-10.45200
C	6.66100	13.37700	-10.91600
H	6.82000	14.21100	-10.23200
H	7.20600	13.61600	-11.83100
C	5.17200	13.29800	-11.28300
H	4.90600	14.20700	-11.82200
H	5.01300	12.45000	-11.95000
C	4.25300	13.16900	-10.06200
H	4.49800	12.26300	-9.51400
H	4.39700	14.03400	-9.41200
C	2.79400	13.09700	-10.52600
H	2.57800	13.96800	-11.15500
H	2.65500	12.19800	-11.13200
N	1.85700	13.07200	-9.38000
H	0.91300	12.88700	-9.72100
H	2.08600	12.32300	-8.73400
H	1.87300	13.97000	-8.90100
C	8.44700	11.57400	-11.11700
O	8.28300	11.09300	-12.23500
H	8.30700	11.78000	-8.60700
H	9.39500	11.65100	-10.71600
N	3.51500	1.15200	3.08800
H	2.74800	0.73200	2.57800
C	3.14900	1.97000	4.26700
H	4.00200	2.02200	4.94000
C	2.84900	3.40400	3.81900
H	3.64900	3.73500	3.15600
C	1.52400	3.55300	3.07900
H	1.42600	4.57200	2.71100
H	1.50300	2.88000	2.22700

H	0.69300	3.31700	3.74100
O	2.82500	4.24500	4.94200
H	2.31800	5.02700	4.70300
C	2.00800	1.36100	5.09200
O	1.34800	0.42400	4.65400
H	4.07000	1.72000	2.44800
N	1.83700	1.91000	6.29300
H	2.39600	2.73900	6.43200
C	0.98700	1.48700	7.42500
H	1.08900	2.29100	8.15400
C	-0.51600	1.40200	7.06500
H	-0.69800	1.95800	6.14800
H	-0.78700	0.36300	6.87100
C	-1.41600	1.96300	8.18500
O	-2.45100	2.60900	7.89500
O	-1.04900	1.84700	9.37400
C	1.46300	0.20800	8.15300
O	2.06800	-0.68700	7.56600
H	1.26700	0.10300	9.16100
N	-1.63100	4.32700	5.72200
C	-2.16800	3.97700	4.40500
C	-0.89800	5.97400	3.63700
C	-0.21100	5.99100	4.81400
C	-0.62800	5.18200	5.97000
C	-2.12600	5.16100	3.43400
O	-0.16900	5.22400	7.09400
C	0.86000	6.93000	4.68400
C	0.73100	7.47600	3.42700
N	-0.34800	6.89000	2.78100
C	1.54900	8.55200	2.87200
C	2.73900	8.93400	3.46100
C	3.48800	9.95200	2.91300
N	3.08000	10.60700	1.82200
C	1.92500	10.26200	1.24300
C	1.14200	9.23400	1.74000
C	1.53900	11.04400	0.03800
C	2.24400	12.19600	-0.34100
C	1.83700	12.89700	-1.46600
C	0.46200	10.65600	-0.75800
N	0.05800	11.31600	-1.85300
C	0.75400	12.41400	-2.20200
C	0.33600	13.11200	-3.32800
C	0.98200	14.28400	-3.72400
C	2.05300	14.76400	-2.97600

C	**2.48900**	**14.07600**	**-1.84600**
H	**-1.91700**	**3.74200**	**6.49700**
H	**-3.19700**	**3.61800**	**4.51100**
H	**-1.56500**	**3.15900**	**4.00200**
H	**-2.18300**	**4.78200**	**2.41000**
H	**-3.00300**	**5.78300**	**3.60300**
H	**1.56900**	**7.19600**	**5.46800**
H	**-0.67500**	**7.06500**	**1.84300**
H	**3.11000**	**8.42600**	**4.34200**
H	**4.43800**	**10.25800**	**3.34600**
H	**0.19700**	**8.98600**	**1.29600**
H	**3.08900**	**12.57200**	**0.22900**
H	**-0.50700**	**12.72900**	**-3.88900**
H	**0.65100**	**14.83000**	**-4.60800**
H	**2.56000**	**15.67900**	**-3.28000**
H	**3.33500**	**14.46200**	**-1.27700**
H	**-0.13400**	**9.77600**	**-0.53400**

Table 6: Cartesian coordinates of MK2 bound to P40.			
N	**7.73200**	**-17.35900**	**9.29300**
H	**8.27800**	**-16.96000**	**8.54000**
C	**7.07600**	**-16.42200**	**10.22700**
H	**6.69500**	**-16.97100**	**11.09100**
C	**8.12900**	**-15.40500**	**10.72000**
H	**8.41300**	**-14.77300**	**9.88200**
H	**7.65900**	**-14.76400**	**11.46700**
C	**9.41400**	**-15.99900**	**11.33500**
H	**9.92900**	**-16.58700**	**10.57800**
C	**10.35200**	**-14.85700**	**11.75100**
H	**11.27700**	**-15.26500**	**12.15400**
H	**10.59100**	**-14.24300**	**10.88300**
H	**9.87800**	**-14.23400**	**12.50800**
C	**9.12200**	**-16.90300**	**12.54100**
H	**10.05600**	**-17.29900**	**12.93500**
H	**8.61000**	**-16.33800**	**13.32000**
H	**8.50300**	**-17.74700**	**12.24200**
C	**5.84700**	**-15.68400**	**9.64300**
O	**5.18500**	**-14.94000**	**10.36300**
H	**8.32200**	**-17.99700**	**9.82600**
H	**5.58500**	**-15.81600**	**8.65400**
N	**12.03800**	**-11.01500**	**5.34400**
H	**12.42600**	**-10.12700**	**5.65200**

C	11.04400	-11.02400	4.26100
H	10.42800	-11.91500	4.37600
C	10.10600	-9.81300	4.39400
H	9.77800	-9.73000	5.43100
H	10.63900	-8.90300	4.11800
C	8.86900	-9.98900	3.50000
H	9.18400	-10.12200	2.46800
H	8.32500	-10.88300	3.80700
C	7.93800	-8.77800	3.58900
H	7.70400	-8.58300	4.63700
H	8.43500	-7.89900	3.17200
C	6.63800	-9.04600	2.82100
H	6.86300	-9.23600	1.76900
H	6.15700	-9.93500	3.23900
N	5.73000	-7.88800	2.93800
H	4.79200	-8.07400	2.59100
H	5.62000	-7.61600	3.91100
H	6.08400	-7.06500	2.44300
C	11.71700	-11.11600	2.87800
O	12.44300	-10.21100	2.45700
H	12.80700	-11.63300	5.08500
H	11.55800	-11.95100	2.29200
N	12.04500	-9.44000	15.31300
H	12.89100	-9.32800	15.84800
C	11.21300	-10.62100	15.60100
H	10.82800	-11.01400	14.65700
C	12.14100	-11.67300	16.22700
H	13.05300	-11.77500	15.63200
H	12.41500	-11.36000	17.23800
S	11.29000	-13.27300	16.29500
H	11.85000	-13.79400	15.18600
C	9.98900	-10.30400	16.50200
O	10.15100	-9.79600	17.61600
H	11.47500	-8.60100	15.41800
N	8.77400	-10.61900	16.02900
H	8.72600	-11.00200	15.09600
C	7.49000	-10.29700	16.68300
H	7.66800	-9.54600	17.44800
C	6.53800	-9.68900	15.62300
H	6.26700	-10.47800	14.92100
H	5.61900	-9.37900	16.12300
C	7.07600	-8.49300	14.80400
H	7.97800	-8.79300	14.27200
C	6.02600	-8.07800	13.76600

H	6.41900	-7.28400	13.13400
H	5.76700	-8.93000	13.13600
H	5.13200	-7.71500	14.27200
C	7.41000	-7.27800	15.67700
H	7.79300	-6.47100	15.05400
H	6.51100	-6.92900	16.18500
H	8.17600	-7.53900	16.40800
C	6.85800	-11.50400	17.42300
O	5.86000	-12.06600	16.97900
N	7.42600	-11.91400	18.56600
H	8.19300	-11.35900	18.92500
C	7.11800	-13.20900	19.21900
H	7.16600	-13.95600	18.42600
C	8.23400	-13.59400	20.22200
H	8.06600	-14.62300	20.54400
H	9.18700	-13.58600	19.69000
C	8.36300	-12.71000	21.47400
O	9.21200	-11.79100	21.47100
O	7.64100	-12.93200	22.47700
C	5.69200	-13.37400	19.81100
O	5.35800	-14.45200	20.31100
H	5.02600	-12.58600	19.78700
N	-3.33000	-10.78500	9.89600
H	-4.02100	-11.03200	9.18400
C	-1.96500	-11.27500	9.66800
H	-1.68800	-11.91900	10.50300
C	-1.92800	-12.11400	8.37500
H	-2.07900	-11.46900	7.51100
H	-0.92200	-12.52800	8.29000
C	-2.91900	-13.29600	8.31800
H	-2.45700	-14.07700	7.71300
H	-3.06000	-13.69900	9.32100
C	-4.29100	-12.98000	7.69700
O	-4.76200	-11.82700	7.81100
O	-4.88800	-13.91200	7.09700
C	-0.90900	-10.15300	9.58300
O	0.26500	-10.39300	9.85900
H	-3.65500	-11.11400	10.80500
N	-1.32000	-8.92500	9.24200
H	-2.30800	-8.80000	9.07200
C	-0.47200	-7.72400	9.21400
H	0.56100	-8.02700	9.04700
C	-0.91600	-6.81900	8.04600
H	-1.97300	-6.57800	8.15500

H	-0.36300	-5.88300	8.10300
C	-0.68400	-7.36400	6.64000
O	-0.20100	-8.45800	6.39200
N	-1.06400	-6.59600	5.64400
H	-1.60400	-5.76100	5.81800
H	-0.88600	-6.85300	4.68300
C	-0.49500	-6.91600	10.53900
O	0.21500	-5.91600	10.65700
H	-1.10200	-7.21500	11.31800
N	5.38400	-11.62300	23.78700
H	6.22600	-12.15300	23.56400
C	4.67900	-11.95700	25.03900
H	3.60600	-11.92100	24.86000
C	5.03200	-13.39300	25.48900
H	6.10000	-13.58100	25.37400
H	4.81100	-13.47300	26.55500
C	4.22000	-14.50400	24.80400
H	4.16500	-15.35100	25.49000
H	3.20200	-14.15500	24.62300
C	4.83900	-15.00500	23.49600
H	4.94200	-14.17500	22.79800
H	5.82800	-15.42100	23.70100
C	3.93000	-16.08700	22.89800
H	3.69900	-16.82800	23.67100
H	2.99200	-15.62500	22.57900
N	4.56800	-16.76800	21.74900
H	3.89100	-17.37100	21.28700
H	4.91600	-16.08300	21.08300
H	5.34400	-17.34500	22.07100
C	4.93000	-10.96000	26.20200
O	4.14000	-10.94500	27.14900
H	4.72900	-11.70200	23.00900
H	5.74100	-10.32300	26.18300
N	2.48500	-4.01700	8.85900
H	1.50800	-4.27200	8.80200
C	3.35600	-4.61500	7.81600
H	4.30500	-4.08500	7.77000
C	3.65200	-6.08800	8.14900
H	4.46000	-6.43800	7.50600
C	4.05000	-6.35100	9.60100
H	4.41300	-7.37400	9.69400
H	4.83300	-5.66200	9.90100
H	3.18800	-6.23000	10.26000
O	2.49700	-6.84900	7.91300

H	2.30700	-6.84100	6.96900
C	2.72800	-4.53600	6.41500
O	1.61000	-4.05600	6.25800
H	2.57000	-3.00100	8.82600
N	3.44200	-5.04900	5.41000
H	4.41500	-5.25200	5.61500
C	2.96500	-5.44300	4.06000
H	3.81300	-5.96300	3.62000
C	1.79600	-6.45700	4.15600
H	1.78000	-6.88300	5.15900
H	0.85400	-5.93200	4.00100
C	1.89500	-7.64100	3.18100
O	3.03300	-8.09300	2.91200
O	0.86000	-8.20700	2.76600
C	2.71300	-4.26300	3.08800
O	1.76000	-4.23900	2.30700
H	3.36900	-3.46600	3.09500
N	3.51600	-9.23900	5.58000
C	2.59000	-10.30600	5.97300
C	3.90400	-10.37800	8.06900
C	4.84500	-9.56400	7.52200
C	4.62400	-8.87300	6.24400
C	2.53900	-10.48500	7.49100
O	5.35600	-8.06100	5.72100
C	5.96600	-9.53300	8.40600
C	5.66300	-10.40100	9.43300
N	4.39600	-10.92600	9.22400
C	6.52200	-10.71100	10.57600
C	7.68200	-9.99800	10.81600
C	8.46700	-10.29200	11.90900
N	8.15100	-11.27400	12.75500
C	7.03900	-11.97800	12.53400
C	6.20800	-11.72800	11.45800
C	6.73100	-13.02100	13.53700
C	5.43400	-13.51800	13.72000
C	5.21200	-14.44500	14.72700
C	7.74200	-13.50100	14.36700
N	7.55100	-14.41400	15.32600
C	6.29300	-14.85200	15.51500
C	6.07200	-15.77300	16.53200
C	4.79500	-16.27600	16.78200
C	3.72700	-15.86600	15.98900
C	3.92700	-14.95300	14.95500
H	3.33800	-8.76300	4.70500

H	**2.95000**	**-11.23700**	**5.53200**
H	**1.59100**	**-10.09900**	**5.57900**
H	**1.91900**	**-9.69000**	**7.91200**
H	**2.06000**	**-11.42900**	**7.75200**
H	**6.87300**	**-8.95300**	**8.25500**
H	**3.87100**	**-11.52100**	**9.84900**
H	**7.97100**	**-9.18300**	**10.16900**
H	**9.37300**	**-9.73200**	**12.12200**
H	**5.34100**	**-12.34300**	**11.28500**
H	**4.59200**	**-13.18100**	**13.12000**
H	**6.92000**	**-16.08000**	**17.13100**
H	**4.63200**	**-16.98900**	**17.58900**
H	**2.73100**	**-16.26500**	**16.17500**
H	**3.08900**	**-14.64300**	**14.33100**
H	**8.77100**	**-13.15600**	**14.26900**
O	**6.26400**	**-4.37800**	**5.15500**
H	**6.23900**	**-4.72700**	**4.22300**
H	**7.19300**	**-4.09600**	**5.20000**

Table 7: Cartesian coordinates of MK2 bound to P4O without binding site water molecules.

N	**7.97100**	**-16.52700**	**-2.70300**
H	**8.58700**	**-16.19400**	**-3.43600**
C	**7.24200**	**-15.50500**	**-1.92900**
H	**6.84900**	**-15.95400**	**-1.01500**
C	**8.24200**	**-14.39600**	**-1.54500**
H	**8.54200**	**-13.87500**	**-2.44900**
H	**7.73000**	**-13.67700**	**-0.90300**
C	**9.51500**	**-14.87400**	**-0.82100**
H	**10.08400**	**-15.52300**	**-1.48400**
C	**10.38700**	**-13.65300**	**-0.51600**
H	**11.26900**	**-13.95100**	**0.04800**
H	**10.70700**	**-13.19000**	**-1.44600**
H	**9.82600**	**-12.92000**	**0.05400**
C	**9.17700**	**-15.65800**	**0.45300**
H	**10.08000**	**-15.85700**	**1.02400**
H	**8.48000**	**-15.08800**	**1.06100**
H	**8.72200**	**-16.61400**	**0.19600**
C	**6.01200**	**-14.93200**	**-2.66900**
O	**5.49200**	**-13.87500**	**-2.31300**
H	**8.50600**	**-17.11100**	**-2.06000**
H	**5.62000**	**-15.44400**	**-3.47500**

N	**12.34900**	**-10.02400**	**-6.65300**
H	**12.75200**	**-9.12300**	**-6.40600**
C	**11.41200**	**-10.09300**	**-7.78900**
H	**10.78800**	**-10.97900**	**-7.66200**
C	**10.47900**	**-8.87100**	**-7.72700**
H	**10.08200**	**-8.81000**	**-6.71200**
H	**11.05100**	**-7.96400**	**-7.92300**
C	**9.29300**	**-8.94600**	**-8.70500**
H	**9.65200**	**-8.86000**	**-9.73200**
H	**8.78900**	**-9.90600**	**-8.58800**
C	**8.29600**	**-7.81500**	**-8.40900**
H	**8.02800**	**-7.84600**	**-7.35100**
H	**8.76600**	**-6.85200**	**-8.62300**
C	**7.01500**	**-7.94700**	**-9.24100**
H	**7.26500**	**-7.81600**	**-10.30000**
H	**6.59500**	**-8.94500**	**-9.09300**
N	**6.03200**	**-6.91200**	**-8.84100**
H	**5.13300**	**-7.00300**	**-9.30900**
H	**5.87100**	**-6.90700**	**-7.83900**
H	**6.35900**	**-5.98800**	**-9.12900**
C	**12.14500**	**-10.24700**	**-9.14200**
O	**12.98000**	**-9.41700**	**-9.51800**
H	**13.10700**	**-10.68700**	**-6.81500**
H	**11.93300**	**-11.05900**	**-9.74300**
N	**12.37400**	**-7.84200**	**3.59400**
H	**13.26700**	**-7.75800**	**4.05300**
C	**11.58300**	**-9.04800**	**3.86700**
H	**11.28700**	**-9.48600**	**2.91100**
C	**12.51400**	**-10.03500**	**4.58300**
H	**13.43800**	**-10.17700**	**4.01600**
H	**12.76000**	**-9.65000**	**5.57600**
S	**11.65800**	**-11.62000**	**4.75000**
H	**11.95500**	**-12.11100**	**3.53000**
C	**10.28200**	**-8.79400**	**4.67000**
O	**10.31700**	**-8.29400**	**5.79700**
H	**11.81100**	**-7.02100**	**3.81600**
N	**9.13400**	**-9.20700**	**4.11700**
H	**9.17600**	**-9.54800**	**3.16500**
C	**7.79700**	**-9.08000**	**4.72400**
H	**7.87200**	**-8.45300**	**5.61200**
C	**6.85000**	**-8.36000**	**3.73300**
H	**6.65400**	**-9.02400**	**2.89100**
H	**5.89900**	**-8.18500**	**4.23900**
C	**7.36100**	**-7.00900**	**3.18300**

H	8.26900	-7.17700	2.60500
C	6.31500	-6.39700	2.24300
H	6.70100	-5.47500	1.81400
H	6.08700	-7.09200	1.43500
H	5.40600	-6.16200	2.79600
C	7.67400	-5.99800	4.29500
H	8.01200	-5.06400	3.84800
H	6.78400	-5.81400	4.89800
H	8.47400	-6.37200	4.93200
C	7.23100	-10.42000	5.25300
O	6.08900	-10.78100	4.97900
N	8.01700	-11.16500	6.04300
H	8.97000	-10.85800	6.17200
C	7.61800	-12.48200	6.59200
H	7.17200	-13.03100	5.76500
C	8.86500	-13.28700	7.02100
H	8.56200	-14.32300	7.17600
H	9.57600	-13.29200	6.19300
C	9.58100	-12.81000	8.29200
O	10.81700	-12.61900	8.24800
O	8.94400	-12.71700	9.36600
C	6.50000	-12.47500	7.66600
O	6.19800	-13.51300	8.25900
H	6.00600	-11.59600	7.88600
N	-3.24700	-9.31000	-1.03000
H	-4.11700	-9.37700	-1.56200
C	-2.06500	-9.98200	-1.59800
H	-1.69100	-10.69900	-0.86700
C	-2.45200	-10.74800	-2.87800
H	-2.57000	-10.04300	-3.70300
H	-1.61900	-11.40600	-3.13000
C	-3.72500	-11.60600	-2.76700
H	-3.58600	-12.50400	-3.37100
H	-3.88400	-11.92300	-1.73500
C	-4.95400	-10.85800	-3.28800
O	-5.39500	-9.89300	-2.62300
O	-5.41700	-11.21600	-4.39500
C	-0.92000	-9.00500	-1.92400
O	0.25400	-9.37400	-1.91600
H	-3.02700	-8.32600	-0.87700
N	-1.26200	-7.73700	-2.17100
H	-2.24800	-7.51300	-2.16400
C	-0.32700	-6.62700	-2.33500
H	0.60000	-7.02000	-2.74600

C	-0.92000	-5.63800	-3.35800
H	-1.90500	-5.30600	-3.03500
H	-0.27800	-4.75900	-3.41700
C	-1.03400	-6.22600	-4.76000
O	-2.00000	-6.88700	-5.12000
N	-0.05100	-5.99000	-5.60400
H	0.73300	-5.40700	-5.32400
H	-0.14900	-6.33400	-6.54000
C	0.03100	-5.92400	-0.99900
O	0.76700	-4.94100	-1.02300
H	-0.34300	-6.27700	-0.10400
N	7.27300	-11.23000	12.06700
H	8.14100	-11.71000	11.86000
C	6.45200	-11.75200	13.18000
H	5.44700	-11.96600	12.81400
C	7.08000	-13.06800	13.69200
H	8.16800	-12.98200	13.71000
H	6.75500	-13.22600	14.72300
C	6.67200	-14.33000	12.91600
H	7.06000	-15.19300	13.45900
H	5.58300	-14.40500	12.89900
C	7.20400	-14.38700	11.48000
H	6.75100	-13.59200	10.88700
H	8.28700	-14.26000	11.49100
C	6.85700	-15.74000	10.85700
H	7.31000	-16.53800	11.45500
H	5.77100	-15.88000	10.88800
N	7.33400	-15.82200	9.45800
H	7.14400	-16.74800	9.09000
H	6.87900	-15.11400	8.88800
H	8.33800	-15.66500	9.39600
C	6.25400	-10.77400	14.36400
O	5.25500	-10.89700	15.08000
H	6.70300	-11.20100	11.22200
H	6.94600	-10.03100	14.55200
N	2.92600	-3.50100	-2.36300
H	1.96200	-3.81300	-2.33900
C	3.79300	-4.16700	-3.36500
H	4.73700	-3.63100	-3.41900
C	4.10200	-5.61800	-2.96300
H	4.89900	-5.99600	-3.60600
C	4.52300	-5.80200	-1.50600
H	4.87900	-6.82000	-1.35200
H	5.32200	-5.10800	-1.26500

H	3.67900	-5.61800	-0.83800
O	2.95500	-6.40000	-3.14300
H	3.09800	-7.24500	-2.70700
C	3.19600	-4.14100	-4.78200
O	1.99300	-3.96300	-4.96000
H	2.94800	-2.49300	-2.51800
N	4.07900	-4.31500	-5.77000
H	5.01700	-4.50500	-5.46800
C	3.88000	-4.24100	-7.23900
H	4.78600	-4.65900	-7.67700
C	2.71200	-5.11700	-7.74100
H	2.67200	-6.02900	-7.14300
H	1.76700	-4.58800	-7.60800
C	2.87900	-5.51100	-9.21900
O	3.32800	-6.66100	-9.45200
O	2.59300	-4.68800	-10.11900
C	3.76200	-2.80300	-7.79200
O	2.95700	-1.99900	-7.32700
H	4.37400	-2.51100	-8.57000
N	3.60100	-8.40200	-5.86100
C	2.56900	-9.16900	-5.15100
C	4.42800	-9.81900	-3.62400
C	5.20200	-8.83600	-4.16300
C	4.84000	-8.14800	-5.41200
C	3.17400	-10.28000	-4.27900
O	5.53200	-7.38000	-6.05200
C	6.33300	-8.65700	-3.30900
C	6.18500	-9.56200	-2.28000
N	5.04600	-10.32100	-2.50600
C	7.06500	-9.68200	-1.11500
C	8.03000	-8.72500	-0.84900
C	8.83500	-8.83000	0.26400
N	8.73300	-9.86400	1.10200
C	7.80800	-10.79300	0.86200
C	6.95200	-10.73400	-0.22300
C	7.78500	-11.92600	1.80600
C	6.61200	-12.63000	2.09600
C	6.68800	-13.71500	2.95800
C	8.96800	-12.31900	2.42700
N	9.06400	-13.38300	3.23300
C	7.93400	-14.06700	3.48700
C	8.02400	-15.18000	4.31200
C	6.89000	-15.92000	4.64900
C	5.65000	-15.54300	4.13900

C	**5.54100**	**-14.44700**	**3.28500**
H	**3.31300**	**-7.86600**	**-6.66000**
H	**1.87000**	**-9.60200**	**-5.87400**
H	**2.00500**	**-8.47900**	**-4.51400**
H	**2.43700**	**-10.58900**	**-3.53400**
H	**3.39300**	**-11.14400**	**-4.90600**
H	**7.13000**	**-7.93300**	**-3.46100**
H	**4.71100**	**-11.10000**	**-1.95400**
H	**8.14900**	**-7.86900**	**-1.49700**
H	**9.59500**	**-8.08400**	**0.49000**
H	**6.24100**	**-11.52500**	**-0.40000**
H	**5.65200**	**-12.35000**	**1.66600**
H	**8.99700**	**-15.45100**	**4.70300**
H	**6.97000**	**-16.78200**	**5.31100**
H	**4.76100**	**-16.11000**	**4.41000**
H	**4.56600**	**-14.16100**	**2.88700**
H	**9.90900**	**-11.80300**	**2.23200**